MRL-TR-65-3

ANALYSIS OF MARKOV CHAIN MODELS OF ADAPTIVE PROCESSES

K. R. KAPLAN, PhD
J. SKLANSKY, DSc ENG

RADIO CORPORATION OF AMERICA

JANUARY 1965

BIOPHYSICS LABORATORY
AEROSPACE MEDICAL RESEARCH LABORATORIES
AEROSPACE MEDICAL DIVISION
AIR FORCE SYSTEMS COMMAND
WRIGHT-PATTERSON AIR FORCE BASE, OHIO

NOTICES

When US Government drawings, specifications, or other data are used for any purpose other than a definitely related Government procurement operation, the Government thereby incurs no responsibility nor any obligation whatsoever, and the fact that the Government may have formulated, furnished, or in any way supplied the said drawings, specifications, or other data, is not to be regarded by implication or otherwise, as in any manner licensing the holder or any other person or corporation, or conveying any rights or permission to manufacture, use, or sell any patented invention that may in any way be related thereto.

Qualified requesters may obtain copies from the Defense Documentation Center (DDC), Cameron Station, Alexandria, Virginia 22314. Orders will be expedited if placed through the librarian or other person designated to request documents from DDC (formerly ASTIA).

Stock quantities available, for sale to the public, from:

Chief, Input Section
Clearinghouse for Federal Scientific and Technical Information, CFSTI
Sills Building
5285 Port Royal Road
Springfield, Virginia 22151

Change of Address

Organizations and individuals receiving reports via the Aerospace Medical Research Laboratories' automatic mailing lists should submit the addressograph plate stamp on the report envelope or refer to the code number when corresponding about change of address or cancellation.

Do not return this copy. Retain or destroy.

800 - March 1965 - 448-30-665

BLANK PAGE

ANALYSIS OF MARKOV CHAIN MODELS OF ADAPTIVE PROCESSES

K. R. KAPLAN, PhD
J. SKLANSKY, DSc ENG

FOREWORD

This study was initiated by the Biophysics Laboratory of the Aerospace Medical Research Laboratories, Aerospace Medical Division, Wright-Patterson Air Force Base, Ohio. The research was conducted by the Radio Corporation of America, RCA Laboratories, Princeton, New Jersey, under Contract No. AF33(657)-11336. The research team consisted of K. R. Kaplan and J. Sklansky. J. Sklansky was the Project Scientist for RCA. H. L. Oestreicher, Chief, Mathematics and Analysis Branch, Biodynamics and Bionics Division, was the contract monitor for the Aerospace Medical Research Laboratories. The work was performed in support of Project No. 7233, "Biological Information Handling Systems and Their Functional Analogs," and Task No. 723305, "Theory of Information Handling." The research for most of the material in this report was performed during the contract period, May 1963 to March 1964. The results of additional work on asynchronous Markov chains, performed prior to May 1963, is also included.

A more compact version of this report appears as a doctoral dissertation submitted by K. R. Kaplan to the Polytechnic Institute of Brooklyn, where he was awarded the PhD degree in June 1964.

This technical report has been reviewed and is approved.

J. W. HEIM, PhD
Technical Director
Biophysics Laboratory

ABSTRACT

Learning and adaptation are considered to be stochastic in nature by most modern psychologists and by many engineers. Markov chains are among the simplest and best understood models of stochastic processes and, in recent years, have frequently found application as models of adaptive processes. A number of new techniques are developed for the analysis of synchronous and asynchronous Markov chains, with emphasis on the problems encountered in the use of these chains as models of adaptive processes. Signal flow analysis yields simplified computations of asymptotic success probabilities, delay times, and other indices of performance. The techniques are illustrated by several examples of adaptive processes. These examples yield further insight into the relations between adaptation and feedback.

BLANK PAGE

TABLE OF CONTENTS

LIST OF ILLUSTRATIONS

LIST OF ILLUSTRATIONS (Continued)

LIST OF SYMBOLS

The location of the definitions of the important mathematical symbols in this report is designated by the page number or figure number. In a few cases, the symbols are not defined explicitly in the text, because the usage of the symbols is well known. This list then gives the location of an implicit definition.

LIST OF SYMBOLS (Continued)

Symbol	Page or Figure	Symbol	Page or Figure
$S(s)$	17	$\alpha_{ij}(\tau)$	14
$S_j(s)$	17	$\hat{\alpha}_{ij}(\tau)$	26
$u_{ij}(n)$	20	δ_{ij}	16
$u_{-1}(\tau)$	15	ζ	63
$U(s)$	16	κ	49
$U_{ij}(s)$	11	λ	10, 49
$\hat{U}_{ij}(s)$	30	λ_j	13
v	60	ρ	60
W	51	τ	4
x	18	$\bar{\tau}$	6
$z(\tau)$	95	τ_{ij}	13
α	62, Fig. 3la	$(\cdot)^*$	77
$\hat{\alpha}(s)$	30		

BLANK PAGE

I. INTRODUCTION

We have been studying the behavioral effects of simple forms of feedback on adaptive processes in the life sciences and engineering. Our ultimate goal is the construction of a theory of adaptive processes. Our immediate goals are a) the accumulation of a fund of basic knowledge and intuitive insights into the properties of a broad class of adaptive processes that include stochastic models of animal learning [9] *, adaptive signal detection [8] , and adaptive pattern recognition [9] ; and b) the development of convenient mathematical tools for the analysis, synthesis, and modelling of these processes.

Our first models of adaptive processes were Markov chains, because Markov chains are simple and yet can represent time-varying statistics. In the course of using these models, we developed a number of techniques for analyzing a broad class of Markov chains.

In this report we discuss these techniques in detail. We also show how the techniques helped us in our studies of adaptive processes, and we describe a number of relations between feedback and adaptation that these studies brought forth.

ASYNCHRONOUS MARKOV CHAINS

In the past our models of adaptive processes were synchronous Markov chains, i.e., chains whose state transitions occur at uniformly spaced instants of time [5, 14] . In this report we discuss a wider class of models — the "asynchronous" Markov chains. In these chains the time between successive state transitions is a random variable. (Such chains have also been called "continuous-time" Markov chains [10] and "semi-Markov" chains [11] .)

The techniques we have developed for asynchronous chains have the following useful properties:

1. The convenience and intuitive appeal of signal-flow analysis [1, 2, 6] are extended to asynchronous chains. (Earlier work in signal-flow analysis was directed primarily at synchronous chains.)
2. The techniques facilitate the reduction of many-state synchronous chains to few-state asynchronous chains.
3. The techniques for asynchronous chains can easily be specialized to the synchronous case.

*Numbers in brackets are references shown on page 99.

PHILOSOPHY AND TERMINOLOGY

The philosophy underlying our study stems from classical feedback control theory. We assume that every adaptive system is describable as consisting of a "plant", a "critic", and a "controller" (Fig. 1). The plant refers to that part of the system which is to be trained; the critic, incorporated in the experimenter or system designer, is a mechanism that computes a performance index; the controller is that part of the system that adjusts the plant parameters in response to the input/output behavior of the plant. The controller may be viewed as a teacher that trains the plant during a "training phase"; during a "working phase" the plant operates without the controller.

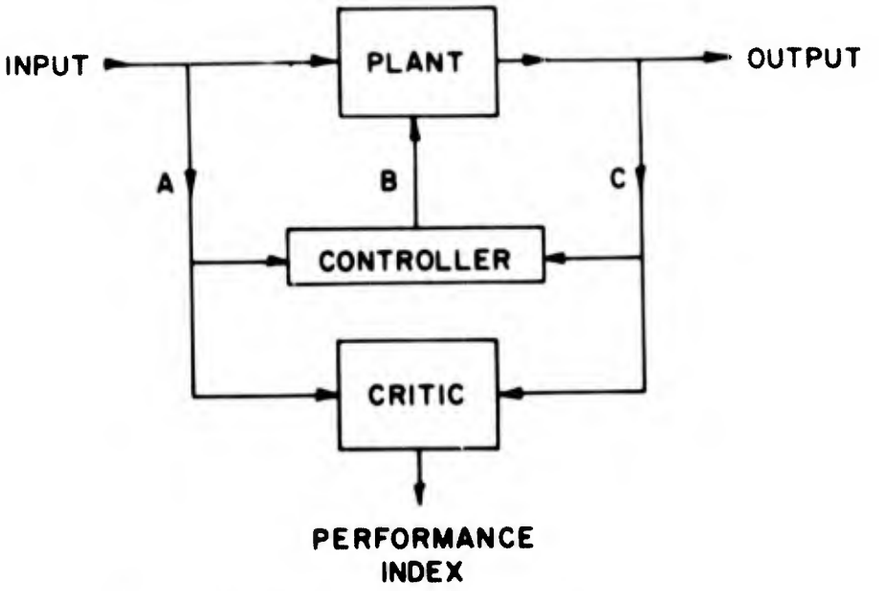

Figure 1. Block diagram of an adaptive system.

A system is viewed as *adaptive* if it exhibits one or both of the following *adaptation characteristics:*

> *Stability:* The performance index remains within prescribed bounds when the environment changes.
>
> *Reliability:* The performance index remains within prescribed bounds when the plant's internal structure changes.

Learning is viewed as a favorable time variation of the performance index in response to a step transition in the environment. Thus, we consider learning to be a particular facet of stability.

Feedback — i.e., a closed-loop training strategy — is often a means to enhance the adaptation characteristics of a plant. On the other hand, adaptive behavior may be achieved without feedback — both "open-loop" and "closed-loop" adaptive systems are possible.

The purpose of our study of adaptive processes is two-fold: a) to test the adequacy of our mathematical techniques and b) to acquire an insight into ways in which particular forms of feedback affect the adaptation characteristics of stochastic processes.

SPECIFIC ADAPTIVE PROCESSES

We report on the role of feedback in three types of adaptive processes: the adaptive random walk, the five-threshold threshold learning process, and the continuous-threshold threshold learning process.

In addition to these results, our analysis illustrates the application of the mathematical techniques.

II. ASYNCHRONOUS MARKOV CHAINS

PRELIMINARY DEFINITIONS

We are concerned with an n-state process characterized by two special properties:

1) The future of the process is (probabilistically) determined only by the present state. That is, if the process is in state i at a given instant, the subsequent behavior of the process is independent of the state sequence which occurred prior to the initiation of i.

2) The probabilities of state transition are dependent only on the state age variable τ, referenced to the time at which the state was initiated, and not on absolute time.

A representation of the process is depicted in Fig. 2. The nodes of the graph represent the process states; the directed branches signify the transition probabilities. We define $p_{ij}(\tau)\,\Delta\tau$ to be the conditional probability of making the transition from state i to state j (with *no* intervening states) in the interval $[\tau, \tau + \Delta\tau]$, given that i was initiated at $\tau = 0$. Thus $p_{ij}(\tau)$ is the first-transition density. It is convenient to restrict our analysis somewhat by imposing a condition of homogeneity on the process. We require:

$$\sum_j p_{ij}(\tau) = h(\tau), \text{ all } i$$

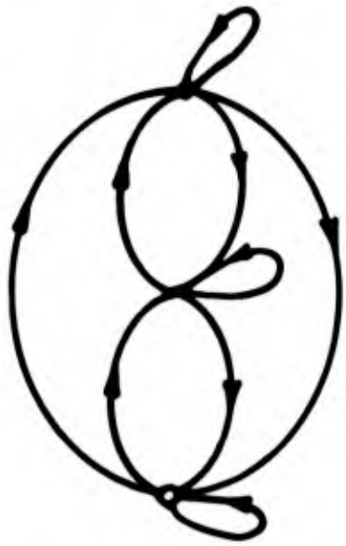

Figure 2. A three-state Markov process.

where $h(\tau)\Delta\tau$ is thus the probability that the first transition subsequent to the initiation of a state (at $\tau = 0$) occurs in the interval τ, $\tau + \Delta\tau$. Then given an arbitrary transition at $t = 0$, the probability of at least one transition within the interval $0 < t \leq \tau$ is

$$P_1(\tau) = \int_0^{\tau} h(t)\, dt$$

A further requirement on the process is the nonexistence of trapping states. The process continues to make transitions for all time. Hence

$$\int_0^{\infty} h(\tau)\, d\tau = 1 \tag{1}$$

That is, given a transition at $t = 0$, at least one subsequent transition *must* ultimately occur and hence infinitely many, since the process "renews" itself at every transition. The probability of no transitions in $0 < t \leq \tau$ is then

$$P_0(\tau) = 1 - \int_0^{\tau} h(t)\, dt \triangleq \bar{h}(\tau)$$

With

$$h(s) = \int_0^{\infty} e^{-s\tau}\, h(\tau)\, d\tau = \mathcal{L}\,(h(\tau))$$

we observe that

$$h(s)\Big|_{s=0} = 1 \tag{2}$$

and that $\bar{\tau}$, the mean time between transitions is given by:

$$\bar{\tau} = \int_0^\infty \tau\, h(\tau)\, d\tau = - h'(s) \Big|_{s=0} \tag{3}$$

where $h'(s)$ is defined as the derivative of $h(s)$ with respect to s.

It is important to make careful distinction between the notions of "transition" and "state-change". The occurrence of a state change implies a transition, but not always conversely. The quantity $p_{ii}(\tau)\,\Delta\tau$ gives the probability of the following event: Given the initiation of i at $\tau = 0$, i is "re-entered" between τ and $\tau + \Delta\tau$, with no other states having been entered in the interval $[0, \tau]$. Clearly, this event does not correspond to a state change. We must visualize an underlying (random) mechanism which "marks" transitions, some of which are associated with state changes, some are not.

Alternately, if the concept of self-transition is too unpalatable, we may phrase our problems in terms of state-change densities $q_{ij}(\tau)$. That is, let $q_{ij}(\tau)\,\Delta\tau$ be the probability of a state change $(i \to j)$ in the interval $[\tau, \tau + \Delta\tau]$, given that i was initiated at $\tau = 0$, no other states having intervened. The q_{ij}'s are related to the p_{ij}'s in the following manner, assuming $i \neq j$:

$$q_{ij}(\tau) = \underbrace{p_{ij}(\tau)}_{\text{no self-transitions}} + \underbrace{\int_0^\tau p_{ii}(t)\, p_{ij}(\tau - t)\, dt}_{\text{one self-transition}} + \underbrace{\int_0^\tau p_{ii}^{(2)}(t)\, p_{ij}(\tau - t)\, dt}_{\text{two self-transitions}} + \cdots\cdots$$

where

$$p_{ii}^{(2)}(\tau) = \int_0^\tau p_{ii}(t)\, p_{ii}(\tau - t)\, dt$$

$$p_{ii}^{(3)}(\tau) = \int_0^\tau p_{ii}^{(2)}(t)\, p_{ii}(\tau - t)\, dt$$

and so on. Thus

$$Q_{ij}(s) = P_{ij}(s) + P_{ij}(s)\left(P_{ii}(s) + \left(P_{ii}(s)\right)^2 + \left(P_{ii}(s)\right)^3 + \ldots\right)$$

$$= P_{ij}(s) \Big/ \left[1 - P_{ii}(s)\right] \quad i \neq j$$

and

$$\sum_{j \neq i} Q_{ij}(s) = \frac{h(s) - P_{ii}(s)}{1 - P_{ii}(s)}$$

and

$$\sum_{j \neq i} Q_{ij}(s) \Big|_{s=0} = \frac{1 - P_{ii}(0)}{1 - P_{ii}(0)} = 1$$

i.e., a state-change must ultimately occur.

Continuing, the probability of at least two transitions in the interval $0 < t \leq t$ is

$$P_2(\tau) = \int_0^{\tau} h^{(2)}(t)\, dt$$

where

$$h^{(2)}(\tau) = \int_0^{\tau} h(t)\, h(\tau - t)\, dt$$

i.e.

$$h^{(2)}(s) = \left[h(s)\right]^2$$

Similarly,

$$h^{(n)}(s) = [h(s)]^n$$

We note that

$$P_1(s) = h(s)/s$$

$$P_2(s) = [h(s)]^2/s$$

$$\vdots$$

$$P_n(s) = [h(s)]^n/s$$

In order to find $E(\tau)$, the expected number of transitions in an interval (given a transition at $t = 0$), we require knowledge of the $Q_n(\tau)$, defined as the probability of *exactly* n transitions in $0 \le t \le \tau$ (which includes the transition at $t = 0$). Now

$$Q_1(\tau) = \bar{h}(\tau) = 1 - P_1(\tau)$$

$$Q_2(\tau) = P_1(\tau) - P_2(\tau)$$

$$\vdots$$

$$Q_n(\tau) = P_{n-1}(\tau) - P_n(\tau)$$

and so

$$Q_n(s) = P_{n-1}(s) - P_n(s)$$

$$= [h(s)]^{n-1}\left(\frac{1-h(s)}{s}\right) = \bar{h}(s)[h(s)]^{n-1}$$

As a check, we must have

$$\sum_{n=1} Q_n(\tau) = 1, \text{ all } \tau$$

but

$$\sum_{n=1} Q_n(s) = \sum_{n=1} \bar{h}(s) \left(h(s)\right)^{n-1}$$

$$= \bar{h}(s) \left(1 + h(s) + h^2(s) + h^3(s) + \ldots.\right)$$

$$= \bar{h}(s)/1-h(s) = 1/s = \mathcal{L}\left(u_{-1}(\tau)\right)$$

Finally,

$$E(s) = \mathcal{L}\left(E(\tau)\right) = \sum_{n=1} n\, Q_n(s)$$

$$= \bar{h}(s) \left(1 + 2h(s) + 3h^2(s) + \ldots\ldots\right)$$

$$= \bar{h}(s)/\left[1-h(s)\right]^2$$

$$E(s) = \frac{1}{s\left[1-h(s)\right]} \tag{4}$$

Since $h(s)\Big|_{s=0} = 1$, $E(s)$ has a second-order pole at the origin. Expanding

$$E(s) = \frac{a}{s^2} + \frac{b}{s} + \left[\begin{array}{l}\text{terms due to left half-plane}\\ \text{poles (decaying exponentials)}\end{array}\right]$$

and

$$a = s^2 E(s)\Big|_{s=0} = \frac{s}{1-h(s)}\Big|_{s=0} = -1/h'(s)\Big|_{s=0} = 1/\bar{\tau}$$

so that

$$E(\tau) \xrightarrow[\tau \to \infty]{} \tau / \bar{\tau} = \lambda\tau$$

where $\lambda \stackrel{\Delta}{=} 1/\bar{\tau}$ is simply the mean frequency at which transitions occur.

In analogy with the 1-step transition density $p_{ij}(\tau)$, we define the "many-step" first-occurrence probability $f_{ij}(\tau)\,\Delta\tau$ to be the probability that j is initiated in the interval τ, $\tau + \Delta\tau$, for the first time subsequent to the initiation of i at $t = 0$. In similar fashion, $f_{ij}^{(n)}(\tau)\,\Delta\tau$ is defined as the probability that the n^{th} j (following the initiation of i at $t = 0$) occurs in the interval τ, $\tau + \Delta\tau$. Then

$$\mathrm{Pr}\left\{\begin{array}{l}\text{of exactly n}\\ \text{j's in } 0 \le t \le \tau\\ \text{subsequent to}\\ \text{initiation of i}\\ \text{at } t = 0\end{array}\right\} = \mathrm{Pr}\left\{\begin{array}{l}\text{of at least}\\ \text{n j's in}\\ 0 \le t \le \tau,\\ \text{etc.}\end{array}\right\} - \mathrm{Pr}\left\{\begin{array}{l}\text{of at least}\\ \text{n + 1 j's in}\\ 0 \le t \le \tau,\\ \text{etc.}\end{array}\right\}$$

$$P_n^{ij}(\tau) = \int_0^\tau f_{ij}^{(n)}(t)\,dt - \int_0^\tau f_{ij}^{(n+1)}(t)\,dt \qquad n = 1, 2, \ldots\ i \neq j$$

$$P_0^{ij}(\tau) = 1 - \int_0^\tau f_{ij}(t)\,dt$$

and

$$P_n^{ij}(s) = \frac{F_{ij(s)}^{(n)} - F_{ij}^{(n+1)}(s)}{s} \qquad n = 1, 2, \ldots; i \neq j$$

$$P_0^{ij}(s) = \frac{1 - F_{ij(s)}}{s}$$

The (transform of the) expected number of j's in an interval $0 < t \leq \tau$ at the initiation of i at $t = 0$ is

$$E_{ij}(s) = \sum_{n=0} n\, P_n^{ij}(s)$$

$$= \frac{1}{s}\left(F_{ij}(s) - F_{ij}^{(2)}(s)\right) + 2\left(F_{ij}^{(2)}(s) - F_{ij}^{(3)}(s)\right) + 3\left(F_{ij}^{(3)}(s) - F_{ij}^{(4)}(s)\right) + \cdots\cdots\Bigg) \qquad (5)$$

$$= \frac{1}{s}\left(F_{ij}(s) + F_{ij}^{(2)}(s) + F_{ij}^{(3)}(s) + \cdots\right)$$

$$= U_{ij}(s)/s \qquad i \neq j$$

where

$$U_{ij}(s) \triangleq \sum_{n=1} F_{ij}^{(n)}(s) \qquad i \neq j \qquad (6)$$

In the case $i = j$,

$$P_1^{jj}(\tau) = 1 - \int_0^{\tau} f_{jj}(t)\, dt$$

$$P_n^{jj}(\tau) = \int_0^{\tau} f_{jj}^{(n-1)}(t)\, dt - \int_0^{\tau} f_{jj}^{(n)}(t)\, dt \qquad n = 2, 3, \ldots$$

and

$$P_1^{jj}(s) = \frac{1 - F_{jj}(s)}{s}$$

$$P_n^{jj}(s) = \frac{F_{jj}^{(n-1)}(s) - F_{jj}^{(n)}(s)}{s}$$

and so

$$E_{jj}(s) = \sum_{n=0} n\, P_n^{jj}(s) = 1 + F_{jj}(s) + F_{jj}^{(2)}(s).+\ldots. = U_{jj}(s)/s \tag{7}$$

where

$$U_{jj}(s) \triangleq 1 + \sum_{n=1} F_{jj}^{(n)}(s) \tag{8}$$

Now

$$\sum_j E_{ij}(s) = E(s) = 1/s\ (1 - h(s))$$

and we have

$$\sum_j U_{ij}(s) = 1/(1 - h(s)) \tag{9}$$

Let us develop a simpler characterization of the $U_{ij}(s)$, as well as some pertinent properties. We observe that

$$f_{ij}^{(2)}(\tau) = \int_0^{\tau} f_{ij}(t)\ f_{jj}(\tau - t)\ dt$$

$$F_{ij}^{(2)}(s) = F_{ij}(s)\ F_{jj}(s)$$

and

$$F_{ij}^{(n)}(s) = F_{ij}(s) \left[F_{jj}(s)\right]^{n-1}$$

and so

$$U_{ij}(s) = F_{ij} \left(1 + F_{jj}(s) + \left[F_{jj}(s)\right]^2 + \ldots\right) = \frac{F_{ij}(s)}{1 - F_{jj}(s)}$$

while

$$U_{jj}(s) = 1 + F_{jj}(s) + \left[F_{jj}(s)\right]^2 + \cdots$$

$$= 1/1 - F_{jj}(s)$$

i.e.,

$$U_{ij}(s) = \delta_{ij} + F_{ij}(s)\ U_{jj}(s) \tag{10}$$

(The symbol δ_{ij} is defined on page 16.)

Since $F_{ij}(s)$ is the transform of a first-occurrence probability, and we implicitly assume that every state is accessible from every other stage*, we have

$$F_{ij}(s)\Big|_{s=0} = \int_0^\infty f_{ij}(\tau)\, d\tau = 1 \tag{11}$$

and further

$$F'_{ij}(s)\Big|_{s=0} = -\int_0^\infty \tau f_{ij}(\tau)\, d\tau \triangleq -\tau_{ij} \tag{12}$$

the mean time required to initiate j subsequent to the initiation of i at $\tau = 0$.

In view of [11], $U_{jj}(s)$ [and hence $U_{ij}(s)$] possesses a pole at the origin. We have

$$\operatorname*{Res}_{s=0}\left[U_{jj}(s)\right] = \lim_{s\to 0}\left(\frac{s}{1-F_{jj}}\right) = -1/F'_{jj}(s)\Big|_{s=0}$$

$$= 1/\tau_{jj} = \lambda_j$$

where λ_j is the mean frequency at which j is initiated. We wish to calculate p_j, the average (steady-state) probability of j being occupied, that is, the mean fraction of the time that j is occupied. From Fig. 3, we observe that

$$p_j = \frac{\text{mean occupancy time (in state j)}}{\text{mean time between initiations of j}}$$

$$= \overline{\tau}/\tau_{jj} = \lambda_j \overline{\tau}$$

*No transient states.

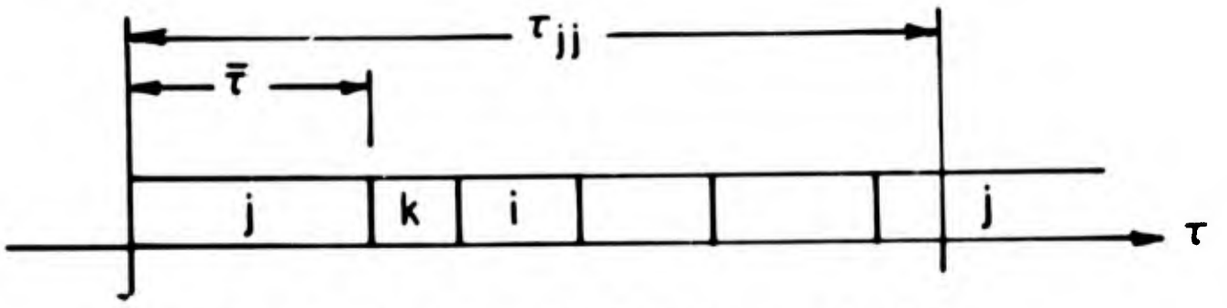

Figure 3. "Average" process behavior for computation of p_j.

Recall that

$$\sum_j U_{ij}(s) = 1/1 - h(s) \cdot \tag{9}$$

i.e.,

$$\sum_j (1 - h(s))\ U_{ij}(s) = 1 \tag{13}$$

If Eq. (13) is evaluated at $s = 0$, we find

$$\sum_j \frac{\left(-h'(s)\right)\Big|_{s=0}}{\left(-F'_{jj}(s)\right)\Big|_{s=0}} = \sum_j \frac{\bar{\tau}}{\tau_{jj}} = \sum_j p_j = 1$$

and we note for future reference that

$$\left(1 - h(s)\right)\ U_{ij}(s)\Big|_{s=0} = p_j \tag{14}$$

THE SIGNAL-FLOW ANALOG

We will see in the ensuing development that the $U_{ij}(s)$ provide the connection between the random process and an equivalent linear system. We will show how this linear system can be conveniently analyzed by signal-flow techniques.

Let $\alpha_{ij}(\tau)$ be the probability (not density) that state j is *occupied* τ seconds after i is initiated. That is, a transition to j (be it first, second, or whatever) must be the last transition in the interval $[0, \tau]$. Then

$$\alpha_{ij}(\tau) = \int_0^\tau \left[\left(f_{ij}(t) + f_{ij}^{(2)}(t) + f_{ij}^{(3)}(t) + \ldots\right)\ dt\right] \bar{h}\,(\tau - t) \tag{15}$$

The bracketed term in the integrand is the probability that j is initiated between t and t + dt after i, while h (τ - t) gives the probability of no transitions for the remainder of the interval. Hence,

$$\alpha_{ij}(\tau) = \int_0^{\tau} u_{ij}(t)\ \bar{h}(\tau - t)\ dt \tag{16}$$

and

$$\alpha_{ij}(s) = U_{ij}(s)\ \left(\frac{1 - h(s)}{s}\right) \tag{17}$$

We note that

$$\sum_j \alpha_{ij}(s) = \left(\frac{1 - h(s)}{s}\right)\sum_j U_{ij}(s) = 1/s = \mathcal{L}\left(u_{-1}(\tau)\right) \tag{17a}$$

where $u_{-1}(\tau)$ is a "unit step function," i.e., a function whose value is 0 for $\tau < 0$, 1 for $\tau \geq 0$. This result was expected, since it is certain that one of the process states is occupied at every instant of time, and further, that

$$s\alpha_{ij}(s)\Big|_{s=0} = \operatorname*{Res}_{s=0}\ \alpha_{ij}(s) = U_{ij}(s)\ (1 - h(s))\Big|_{s=0} = p_j \tag{17b}$$

i.e.,

$$\alpha_{ij}(\tau) \xrightarrow[\tau \to \infty]{} p_j$$

The definition of $\alpha_{ij}(\tau)$ suggests the following recursive relationship:

$$\alpha_{ij}(\tau) = \sum_k \int_0^{\tau} p_{ik}(t)\ \alpha_{kj}(\tau - t)\ dt + \delta_{ij}\ \bar{h}(\tau) \tag{18}$$

where the first term in Eq. (18) accounts for the probability of reaching j via one or more transitions, while the second term allows for the possibility of no transitions. Continuing

$$\alpha_{ij}(s) = \sum_k P_{ik}(s)\ \alpha_{kj}(s) + \delta_{ij}\ \frac{(1 - h(s))}{s} \tag{19}$$

and so by Eq. (17),

$$U_{ij}(s) = \sum_k P_{ik}(s)\ U_{kj}(s) + \delta_{ij} \tag{20}$$

where

$$\delta_{ij} \triangleq \begin{cases} 0 \text{ for } i \neq j \\ 1 \text{ for } i = j \end{cases}$$

In matrix notation, with $U(s) = U_{ij}(s)$, etc., we have

$$U(s) = P(s)\ U(s) + I$$

where $I = \{\delta_{ij}\}$ = identity matrix.

$$\begin{aligned} [I - P(s)]U(s) &= I \\ U(s) &= [I - P(s)]^{-1} \end{aligned} \tag{21}$$

Alternately,

$$\begin{aligned} U(s)\ (I - P(s)) &= I \\ U(s) &= U(s)\ P(s) + I \end{aligned} \tag{22}$$

that is, U and P commute. From Eq. (22), we note that

$$U_{ij}(s) = \sum_k U_{ik}(s)\ P_{kj}(s) + \delta_{ij} \tag{23}$$

Consider now the flow graph of a linear system. Let the graph be topologically identical to that of the Markov process under analysis, and let the node-to-node transfer functions be the $P_{ij}(s)$. Let $R_{ij}(s)$ be the (transformed) response at node j due to a unit impulse at node i. Then

$$R_{ij}(s) = \sum_k R_{ik}(s)\ P_{kj}(s) + \delta_{ij}$$

and so

$$R_{ij}(s) = U_{ij}(s)$$

That is, the Uij(s) may be computed as the impulse responses of an appropriate flow graph. Consequently, if the stimulus vector is S(s), the response vector R(s) will be

$$R(s) = S(s)\ U(s).$$

A word about motivation. It is the quantity $\alpha_{ij}(\tau)$ which provides a significant description of the future (probabilistic) behavior of the process. The probability transients are contained in $\alpha_{ij}(\tau)$, as well as the average probabilities, p_j. As given by Eq. (17), $\alpha_{ij}(s)$ is directly related to Uij(s), which may now be computed by applying the familiar rules of flow-graph reduction to the calculation of a source-to-sink transmission function. The first occurrence probability density $f_{ij}(\tau)$ has an equally useful "system" interpretation, which we will pursue in succeeding paragraphs. Our aim is to fully exploit the probability flow-graph analog.

The system interpretation of $F_{ij}(s)$ is made evident through an artifice that will be of continuing importance in the subsequent analysis. With reference to Fig. 4, let node "i" be driven with a unit impulse, and we wish to calculate the necessary stimulus at node j, Sj(s), which results in zero signal at node "j". Using superposition, we find

$$U_{ij}(s) - S_j(s)\ U_{jj}(s) = 0$$

and

$$S_j(s) = \frac{U_{ij}(s)}{U_{jj}(s)} = F_{ij}(s) \quad (i \neq j)$$

by Eq. (10).

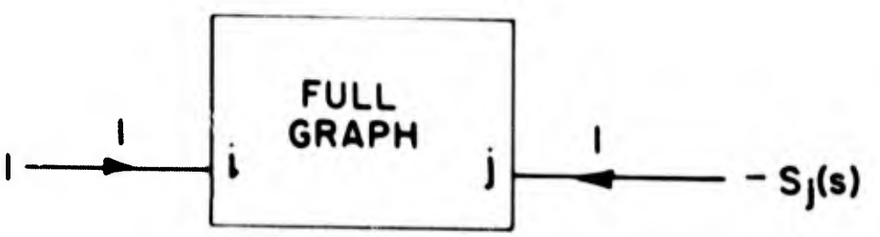

Figure 4. Configuration for achieving zero signal at node j.

Since the response at node "j" is identically zero, we can remove all branches emanating from node "j" with no alteration in the responses at the other nodes in the system. Further, the signal entering "j" must be precisely equal to $S_j(s) = F_{ij}(s)$ in order to create a null at "j". Thus, $F_{ij}(s)$ is simply the response at "j" due to an impulse drive at "i" when "j" is a sink, i.e., all branches leaving "j" are deleted.

For illustrative purposes, we consider the graph of Fig. 5, where, for simplicity, we have taken $p_{ij}(\tau) = p_{ij}\,\delta(\tau - 1)$, i.e., the process changes state every second. We note that

$$P_{ij}(s) = \int_0^\infty p_{ij}(\tau)\, e^{-s\tau}\, d\tau = p_{ij}\, e^{-s\tau} := x p_{ij};\ x \triangleq e^{-s}$$

Since

$$\sum_j P_{ij}(s)\Big|_{s=0} = h(s)\Big|_{s=0} = 1$$

we obtain the condition

$$\sum_j p_{ij} = 1, \text{ all } i$$

as in Fig. 5.

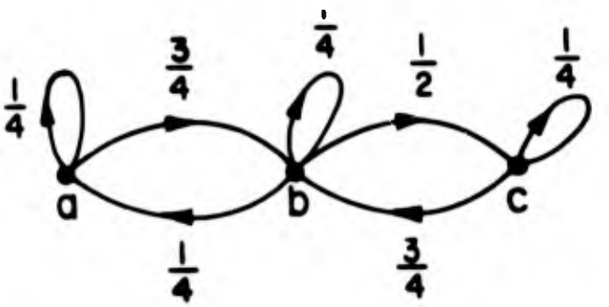

Figure 5. Illustrative example.

In order to calculate $F_{ac}(x)$ node "c" is taken as a sink, and node "a" is driven with an impulse as in Fig. 6. We have

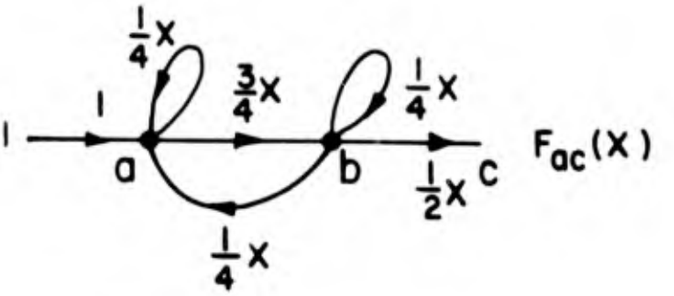

Figure 6. System for calculation of F_{ac}.

$$F_{ac}(x)^{*} = \frac{1}{\left(1 - \frac{1}{4}x\right)} \frac{\left(\frac{3}{4}x\right)\left(\frac{1}{2}\right)x}{1 - \frac{1}{4}x - \frac{\frac{3}{16}x^{2}}{1 - \frac{1}{4}x}} = \frac{\frac{3}{8}x^{2}}{1 - \frac{1}{2}x - \frac{1}{8}x^{2}}$$

Note that

$$F_{ac}(s)\Big|_{s=0} = F_{ac}(x)\Big|_{x=1} = \frac{\frac{3}{8}}{1 - \frac{1}{2} - \frac{1}{8}} = 1$$

and further

$$-F'_{ac}(s)\Big|_{s=0} = x\,F'_{ac}(x)\Big|_{x=1} = \tau_{ac}$$

Thus

$$\tau_{ac} = \frac{\left[\left(\frac{3}{8}\right)\left(\frac{3}{4}\right) + \left(\frac{3}{8}\right)\left(\frac{1}{2}\right) + \left(\frac{1}{4}\right)\right]}{\left(\frac{3}{8}\right)^{2}} = 4 \text{ sec.}$$

Using long division, we find

$$F_{ac}(x) = \frac{3}{8}x^{2} + \frac{3}{16}x^{3} + \frac{9}{64}x^{4} + \frac{3}{32}x^{5} + \cdots\cdots$$

$$f_{ac}(\tau) = \frac{3}{8}\delta(\tau - 2) + \frac{3}{16}\delta(\tau - 3) + \cdots\cdots$$

*Our terminology is loose, but standard. $F_{ac}(x)$ is not $F_{ac}(s)$ with x replacing s. Strictly, we should write $F_{ac}[-\ln(x)]$.

To calculate $U_{aa}(x)$, we refer to the configuration of Fig. 7, where we have

$$U_{aa}(x) = \frac{1}{1 - \frac{1}{4}x - \frac{\left(\frac{3}{4}\right)x\left(\frac{1}{4}\right)x}{1 - \frac{1}{4}x - \frac{\left(\frac{1}{2}\right)x\left(\frac{3}{4}\right)x}{1 - \frac{1}{4}x}}} = \frac{\left(1 - \frac{1}{2}x - \frac{5}{16}x^2\right)}{(1-x)\left(1+\frac{1}{2}x\right)\left(1-\frac{1}{4}x\right)}$$

Note the pole at $x = 1$ $(s = 0)$. Via partial fraction expansion, there results

$$U_{aa}(x) = \frac{\frac{1}{6}}{1-x} + \frac{\frac{1}{6}}{1+\frac{1}{2}x} + \frac{\frac{2}{3}}{1-\frac{1}{4}x}$$

$$u_{aa}(n) = \frac{1}{6} + \frac{1}{6}\left(-\frac{1}{2}\right)^n + \frac{2}{3}\left(\frac{1}{4}\right)^n \quad n = 0, 1, 2, \ldots$$

$$= 1, \frac{1}{4}, \frac{1}{4}, \frac{5}{32}, \frac{23}{128}, \ldots$$

where n is an integer-valued instant of time. In general, $u_{ij}(n)$ is the probability of an occurrence of state j at time n, given that state i occurred at time 0. The long-term behavior of $u_{aa}(n)$ is governed by the slowest-decaying term,

$$u_{aa}(n) \approx \frac{1}{6}\left[1 + \left(-\frac{1}{2}\right)^n\right]^*$$

which accounts for the damped oscillation about the steady-state value of 1/6 (Fig.

$U_{bb}(x)$ may be obtained in similar fashion, obtaining $p_b = 1/2$, and hence $p_c = 1/3$, since $p_a + p_b + p_c = 1$.

*For n = 4, the approximation gives 68/374, as opposed to 69/374 = 23/128, or about a 1-1/2 percent error.

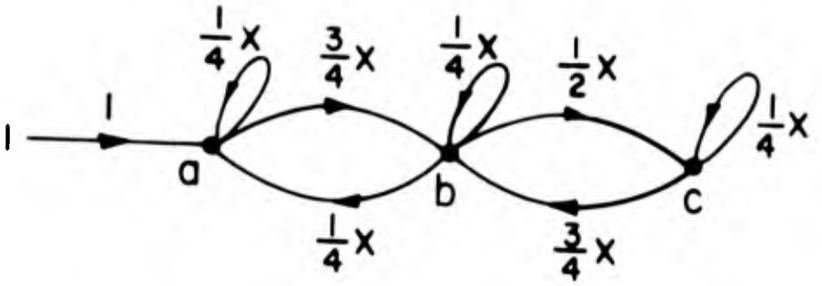

Figure 7. Calculation of U_{ac}.

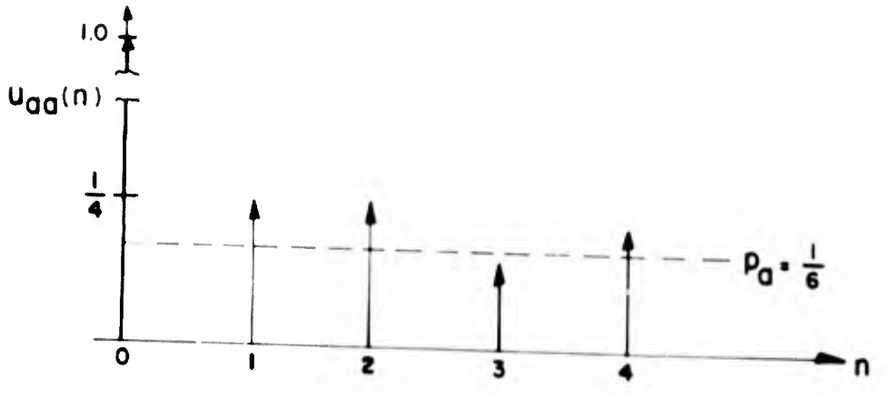

Figure 8. The distribution $U_{aa}(n)$.

ASYMPTOTIC ANALYSIS

The above techniques have allowed us to exploit the well-known properties of linear flow-graphs in order to extract pertinent features of the process dynamics. This approach can be further enhanced to a point where the asymptotic (or "steady-state") probabilities may be found in a purely routine, arithmetic manner. In order to establish this technique, an observation due to Sittler[1] will be stated, proven, and then enlarged upon.

$F_{ij}(s)$ has been previously defined as the transform of the first-occurrence probability $f_{ij}(\tau)$, or analogously, the source-to-sink transmission of an appropriate flow graph. In such a graph, and for *discrete* processes, transitions every second, Sittler states that the total signal through a node for all time is equal to the average time consumed in passing through the corresponding state of the original process, and further, that these average delays (signals) may be summed to obtain the overall delay, τ_{ij}. We generalize this theorem to say, if $R_k(s)$ is the signal at "k" with "j" a sink, and "i" driven with an impulse, then

$$\sum_k R_k(s)\Big|_{s=0} = \tau_{ij}/\overline{\tau} = \lambda\tau_{ij} \tag{24}$$

where, of course

$$R_k(s)\Big|_{s=0} = \int_0^\infty r_k(\tau)\, e^{-s\tau}\, d\tau\Big|_{s=0}$$

$$= \int_0^\infty r_k(\tau)\, d\tau$$

is precisely the total signal passing through node "k" for all time. To prove Eq. (24), it is necessary to characterize the signals R_k in terms of functions pertinent to the full graph (no deleted branches). With reference to Fig. 9, it is evident that, excepting node "j", the signals in both systems are identical. (Recall the manner in which signal-flow significance was ascribed to Fij(s).) In the full graph, superposition indicates that

$$R_k(s) = U_{ik}(s) - F_{ij}(s)\, U_{jk}(s), \qquad k \neq j$$

$$= 0 \qquad\qquad\qquad\qquad k = j$$

and

$$\sum_k R_k(0) = \lim_{s\to 0} \sum_k R_k(s) = \lim_{s\to 0} \sum_k \left(U_{ik}(s) - F_{ij}(s)\, U_{jk}(s)\right)$$

Recall that

$$\sum_k U_{ik}(s) = 1/\left[1 - h(s)\right], \text{ all } i \tag{9}$$

Hence

$$\sum_k R_k(0) = \lim_{s\to 0} \left\{\frac{1 - F_{ij}(s)}{1 - h(s)}\right\} \tag{25}$$

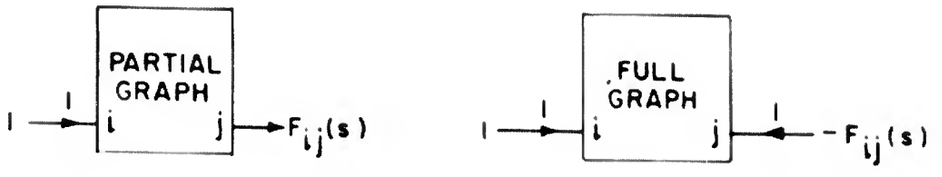

Figure 9. Equivalent systems for proof of Sittler's theorem.

The ratio in Eq. (25) is indeterminate at s = 0, and we invoke L' Hospital's rule and Eq. (12) to obtain

$$\sum_k R_k(0) = \frac{-F'_{ij}(s)\Big|_{s=0}}{-h'(s)\Big|_{s=0}} = \frac{\tau_{ij}}{\bar{\tau}} \tag{26}$$

Although the full graph of Fig. 9 is utilized to describe the $R_k(s)$, the computation $\sum_k R_k(0)$ is performed on the partial graph (node "j" a sink). Here

$$R_j(s) = F_{ij}(s); \quad R_j(0) = 1$$

since $F_{ij}(s)$ is the transform of a first-occurrence probability. Thus it is possible to compute backwards through the system using only the steady-state (s = 0) value of the node-to-node transfer functions to calculate the total signals, $R_k(0)$. Note that the sum over the nodes excludes the sink "j", since the equivalence of the systems in Fig. 9 is restricted to the interior nodes and node i.

To illustrate the use of Eq. (26) we consider the example of Fig. 6. Circumflexed quantities indicate total signals. (Recall $s = 0 \rightarrow x = 1$). In Fig. 10, we have

$$\frac{1}{2}\hat{b} = 1$$

$$\hat{b} = 2$$

$$\hat{a} = 1 + \frac{1}{4}\hat{b} + \frac{1}{4}\hat{a}$$

$$= \frac{4}{3}\left(1 + \frac{1}{2}\right) = 2$$

$$\sum_k R_k(0) = \hat{a} + \hat{b} = 4 = \tau_{ac}$$

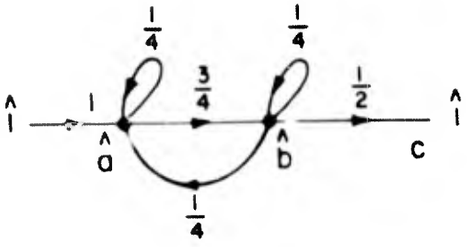

Figure 10. Calculation of τ_{ac}.

This result was obtained earlier, although the computation required somewhat more effort. The real utility of the total signal concept, however, is that it leads to an elementary algorithm for calculation of the steady-state probabilities. Since $p_j = \bar{\tau}/\tau_{jj}$, Eq. (26) may be applied to the evaluation of τ_{jj} and thus the sought-for p_j. This calculation, while representing a considerable savings in labor when contrasted with alternate procedures, is still somewhat inefficient since each node (or all but one, since $\sum_j p_j = 1$) must be considered in turn. It is possible to reduce the labor to what appears to be a bare minimum via the following observation. If the full graph is driven at node "j" with the signal $1 - F_{jj}(s) = 1/U_{jj}(s)$, the response at any node k is

$$R_k(s) = \left(1 - F_{jj}(s)\right) U_{jk}(s)$$

$$= \begin{cases} \left[\dfrac{1 - F_{jj}(s)}{1 - F_{kk}(s)}\right] F_{jk}(s) & \text{for } k \neq j \\ \\ \text{for } k = j \end{cases} \qquad (27)$$

The total signal through node "k" for all time is therefore

$$R_k(0) = \left[\frac{1 - F_{jj}(s)}{1 - F_{kk}(s)}\right] F_{jk}(s)\Big|_{s=0} = \frac{F'_{jj}(s)}{F'_{kk}(s)}\Bigg|_{s=0} = \frac{p_k}{p_j} \qquad (28)$$

where (28) is applicable for every k. Hence

$$\sum_k R_k(0) = \frac{1}{p_j} \sum_k p_k = 1/p_j \qquad (29)$$

The remaining probabilities are determined via Eq. (28). Thus

$$p_k = p_j R_k(0) = \frac{R_k(0)}{\sum_k R_k(0)} \tag{30}$$

In order to utilize Eqs. (29) and (30), we require a partial graph which, when appropriately driven, yields the same node responses as the configuration just discussed. We observe that the situation above is nothing more than that illustrated in Fig. 9, with i=j. That is, the desired graph is obtained by splitting node "j" into source and sink, and driving the source with an impulse. The total signal appearing at the sink is then unity (in fact, $F_{jj}(s)\big|_{s=0} = 1$), and we may again compute backwards through the system to determine the $R_k(0)$.

At this point, an example may be helpful. Consider the Markov chain in Fig. 5. In order to perform the computation at node "a" in this system, node a of Fig. 5 is first "split" into source a' and sink a" as in Fig. 11. We have:

$$\frac{1}{4} + \frac{1}{4}\hat{b} = 1$$

$$\hat{b} = 3$$

$$\frac{1}{2}\hat{b} + \frac{1}{4}\hat{c} = \hat{c}$$

$$\hat{c} = 2$$

Hence

$$p_a = \frac{1}{1 + 2 + 3} = 1/6$$

and

$$p_b = \hat{b}\, p_a = \frac{1}{6} \cdot 3 = 1/2$$

$$p_c = \hat{c}\, p_a = \frac{1}{6} \cdot 2 = 1/3$$

as was previously obtained. The caution regarding the exclusion of $R_{sink}(0)$ from the sum, $\sum_k R_k(0)$, still applies. In this mode of calculation, two nodes receive unit total signals, either one of which may be ignored.

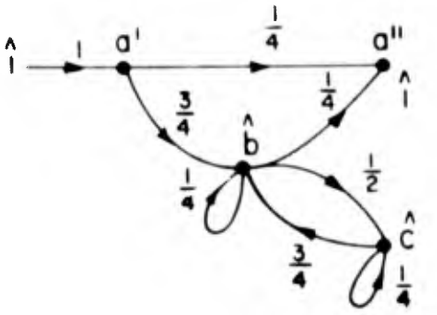

Figure 11. Calculation of steady-state probabilities illustrating "node-splitting".

STATE-REFERENCED PROBABILITIES

All of the probabilistic quantities that have so far been developed are ultimately linked to the conditional one-step densities $p_{ij}(\tau)$, and the analysis rests on the assumption that we have knowledge of these densities, i.e., we are somehow cognizant of the instants at which transitions occur. The density $f_{ij}(\tau)$ is "tied" to transition points at both ends of the interval τ. The probability $\alpha_{ij}(\tau)$ is "untied" at the "right" end (*in* state j, as opposed to the initiation of j), but is referenced to a transition at $\tau = 0$. Consider now an observer who only perceives the state of the process. The observer plots the process state versus time, and obtains a very long sample of the process behavior. Hypothesizing ergodicity, he chops his sample into many very long samples and proceeds to compute the statistics of the process. Fixing the initial state ("i", say) he examines all samples to obtain the number of times that the process is in state "j" at a fixed time τ from the starting instant. Call this number $N_{ij}(\tau)$, and let there be N samples. The ratio $N_{ij}(\tau)/N$ is thus (for very large N) an approximation to the probability $\hat{\alpha}_{ij}(\tau)$ defined as: The probability, given that the process is initially *in* state i, of being *in* state j τ seconds later. We shall investigate the relation of $\hat{\alpha}_{ij}(\tau)$ to the previously derived quantities, and develop additional relevant probabilities which are closer to observables than are the $p_{ij}(\tau)$.

As a stepping-stone to an expression for $\hat{\alpha}_{ij}(\tau)$, we first develop a "one-step" density which is untied at the left. That is, we define $\hat{p}_{ij}(\tau)\,\Delta\tau$ to be the probability, given that i is *occupied* at $t = 0$, of initiating state j in the interval τ, $\tau + \Delta\tau$, with no intervening transitions. Consider the diagram of Fig. 12. We define a set of "events" as follows:

$Q \triangleq$ j is *initiated* in $(\tau, \tau + \Delta\tau)$

$P \triangleq$ state i is *occupied* at $\tau = 0$

$R \triangleq$ i is *initiated* in $[-(t + dt), -t]$

$S \triangleq$ no transitions in $[-t, 0]$

$T \triangleq$ no transitions in $[0, \tau]$

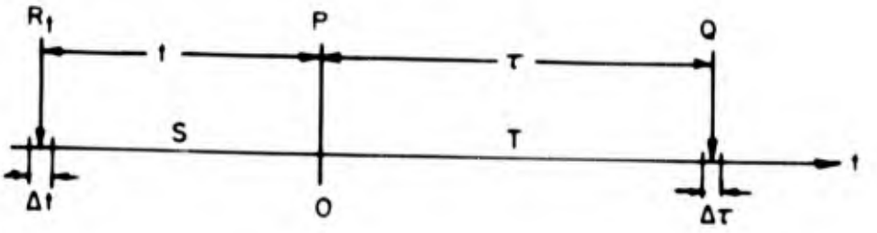

Figure 12. "Event schematic" for computation of $\hat{p}_{ij}(\tau)$.

Then

$$\hat{p}_{ij}(\tau)\,\Delta\tau = \Pr(TQ|P) = \Pr(TQP)/\Pr(P) \tag{31}$$

while

$$p_{ij}(\tau + t)\,\Delta\tau = \Pr\left(STQ|R_x\right) \tag{31a}$$

Now, Eq. (31) may be rewritten as

$$\hat{p}_{ij}(\tau)\,\Delta\tau = \lim_{\Delta t \to 0} \sum_{t} \Pr\left(R_t SPTQ\right)/\Pr(P) \tag{32}$$

and

$$\Pr\left(R_t SPTQ\right) = \Pr\left(P|R_t STQ\right)\Pr\left(R_t STQ\right)$$

But,

$$\Pr\left(P|R_t STQ\right) = 1$$

and so

$$\begin{aligned}\hat{p}_{ij}(\tau)\,\Delta\tau &= \lim_{\Delta t \to 0} \sum_{t} \Pr\left(R_t STQ\right)\Big/\Pr(P) \\ &= \lim_{\Delta t \to 0} \sum_{t} \Pr\left(STQ|R_t\right)\Pr\left(R_t\right)\Big/\Pr(P)\end{aligned} \tag{33}$$

We note that $\Pr(P) = p_i$, and $\Pr(R_t) = \lambda_i \Delta t$

$$= \frac{p_i \Delta t}{\bar{\tau}}$$

so that, recalling Eq. (31a), we obtain

$$\hat{p}_{ij}(\tau)\,\Delta\tau = \left(\int_0^\infty p_{ij}(\tau + t)\,\frac{dt}{\bar{\tau}} \right) \Delta\tau$$

Recalling that $\lambda \triangleq 1/\bar{\tau}$, we have

$$\hat{p}_{ij}(\tau) = \lambda \int_0^\infty p_{ij}(\tau + t)\,dt \qquad (34)$$

$$= \lambda \int_\tau^\infty p_{ij}(t)\,dt$$

Thus

$$\hat{P}_{ij}(s) = \lambda \left(P_{ij}(s)\Big|_{s=0} - P_{ij}(s) \right) \Big/ s \qquad (35)$$

For subsequent convenience, we shall write $\bar{P}_{ij}$ rather than $P_{ij}(s)\big|_{s=0}$. In matrix notation,

$$\hat{P}(s) = \frac{\lambda}{s} \left(\bar{P} - P(s) \right) \qquad (36)$$

We note that

$$\sum_j \hat{P}_{ij}(s) = \frac{\lambda}{s}\,[1 - h(s)] = \lambda \bar{h}(s) \triangleq \hat{h}(s) \qquad (37)$$

and, by Eq. (3), that

$$\hat{h}(s)\Big|_{s=0} = 1$$

It is now possible to compute $\hat{\alpha}_{ij}(\tau)$ as follows:

$$\hat{\alpha}_{ij}(\tau) = \sum_k \int_0^\tau \hat{p}_{ik}(t)\,\alpha_{kj}(\tau - t)\,dt + \delta_{ij} \left(1 - \int_0^\tau \hat{h}(t)\,dt \right) \qquad (38)$$

As in the similar expression for $\alpha_{ij}(\tau)$, the first term in Eq. (38) accounts for the probability of reaching j via one or more transitions, the second allows for the possibility of no subsequent transitions in $[0, \tau]$. Continuing

$$\hat{\alpha}_{ij}(s) = \sum_k \hat{P}_{ik}(s)\, \alpha_{kj}(s) + \delta_{ij} \left(\frac{1 - \hat{h}(s)}{s}\right) \tag{39}$$

and, by Eq. (17b),

$$\operatorname*{Res}_{s=0} \hat{\alpha}_{ij}(s) = \sum_k \hat{P}_{ik}(0)\, p_j = p_j$$

and

$$\sum_j \hat{\alpha}_{ij}(s) = \sum_k \hat{P}_{ik}(s) \sum_j \alpha_{kj}(s) + \left(\frac{1 - \hat{h}(s)}{s}\right)$$

Applying Eq. (17a), we get

$$\sum_j \alpha_{ij}(s) = \frac{1}{s} \sum_k \hat{P}_{ik}(s) + \left(\frac{1 - \hat{h}(s)}{s}\right)$$

$$= \frac{h(s)}{s} + \frac{1}{s} - \frac{\hat{h}(s)}{s} = 1/s = \mathcal{L}\left(u_{-1}(\tau)\right)$$

by Eq. (37).

We may also develop "careted" quantities analogous to $F_{ij}(s)$ and $U_{ij}(s)$. We define $\hat{f}_{ij}(\tau)\Delta\tau$ as the probability, given state i at $\tau = 0$, of the first subsequent occurrence of state j in the interval $[\tau, \tau + \Delta\tau]$.

Clearly,

$$\hat{f}_{ij}(\tau) = \hat{p}_{ij}(\tau) + \sum_{k \neq j} \int_0^\tau \hat{p}_{ik}(t)\, f_{kj}(\tau - t)\, dt \tag{40}$$

and

$$\hat{F}_{ij}(s) = \hat{P}_{ij}(s) + \sum_{k \neq j} \hat{P}_{ik}(s)\, F_{kj}(s) \tag{41}$$

Further

$$\hat{F}_{ij}^{(2)}(s) = \mathcal{L}\left(\hat{f}_{ij}^{(2)}(\tau)\right) = \hat{F}_{ij}(s)\ F_{jj}(s)$$

$$\vdots$$

$$F_{ij}^{(n)}(s) = \mathcal{L}\left(\hat{f}_{ij}^{(n)}(\tau)\right) = \hat{F}_{ij}(s)\ F_{jj}^{n-1}(s)$$

and so

$$\begin{aligned}\hat{U}_{ij}(s) &\triangleq \hat{F}_{ij}(s) + \hat{F}_{ij}^{(2)}(s) + \hat{F}_{ij}^{(3)}(s) + \ldots \\ &= \hat{F}_{ij}(s)\left(1 + F_{jj}(s) + \left[F_{jj}(s)\right]^2 + \ldots\right) \\ &= \hat{F}_{ij}(s)\ U_{jj}(s) \\ &= \sum_k \hat{P}_{ik}(s)\ U_{kj}(s)\end{aligned} \tag{42}$$

and

$$\sum_j \hat{U}_{ij}(s) = \sum_k \hat{P}_{ik}(s) \sum_j U_{kj}(s) = \frac{\hat{h}}{1-h} = \lambda/s \tag{43}$$

In terms of the $\hat{U}_{ij}$, $\hat{\alpha}_{ij}$ has the following form (we use matrix notation):

$$\hat{\alpha}(s) = \hat{P}(s)\ \alpha(s) + \left(\frac{1-\hat{h}(s)}{s}\right) I \tag{43a}$$

$$\begin{aligned}\hat{\alpha}(s) &= \bar{h}(s)\ \hat{P}(s)\ U(s) + \left(\frac{1-\hat{h}(s)}{s}\right) I \\ &= \bar{h}(s)\ \hat{U}(s) + \left(\frac{1-\hat{h}(s)}{s}\right) I\end{aligned} \tag{44}$$

The $\hat{\alpha}$'s and the $\hat{U}$'s have an interesting invariance property. Recall that, by Eq. (19),

$$\alpha_{ij}(s) = \sum_k \alpha_{ik}(s)\ P_{kj}(s) + \bar{k}(s)\ \delta_{ij} \tag{45}$$

and invoke the final-value theorem [4] to obtain

$$\lim_{s \to 0} s\alpha_{ij}(s) = p_j = \sum_k p_k \bar{P}_{kj} \tag{46}$$

Thus, with

$$A = \left\{a_{ij}\right\}, \quad a_{ij} = p_j$$

we have

$$A = A\bar{P} \tag{47}$$

Now

$$\begin{aligned} A\hat{U}(s) = A\hat{P}(s)\, U(s) &= \frac{\lambda}{s} A(\bar{P} - P(s))\, U(s) \\ &= \frac{\lambda}{s} AU - \frac{\lambda}{s} A(U - I) \\ &= \frac{\lambda A}{s} \end{aligned} \tag{48}$$

That is

$$\sum_i p_i \hat{U}_{ij}(s) = \frac{\lambda}{s} p_j \tag{49}$$

and so

$$\begin{aligned} A\hat{\alpha}(s) &= \bar{h} A\hat{U}(s) + A\left(\frac{1-\hat{h}}{s}\right) \\ A\hat{\alpha}(s) &= \bar{h}\frac{\lambda}{s} A + A\left(\frac{1-\hat{h}}{s}\right) \\ &= \frac{\hat{h}}{s} A + A\left(\frac{1-\hat{h}}{s}\right) = A/s \end{aligned} \tag{50}$$

$$\sum_i p_i \hat{\alpha}_{ij}(s) = p_j/s \tag{51}$$

We give an illustration of the calculation of $\hat{\alpha}$ for the discrete-time case. Consider the simple chain shown in Fig. 13. All transition probabilities have the form: $p_{ij}(\tau) = p_{ij}\,\delta(\tau - 1)$; $P_{ij}(s) = p_{ij}\,e^{-s} = xp_{ij}$. We re-work the expression for $\hat{\alpha}_{ij}(s)$ as follows:

$$\hat{\alpha}_{ij}(s) = \sum_k \hat{P}_{ik}(s)\,\alpha_{kj}(s) + \left(\frac{1-\hat{h}}{s}\right)\delta_{ij} \tag{39}$$

$$= \frac{\lambda}{s}\sum_k \left(\overline{P}_{ik} - P_{ik}(s)\right)\alpha_{kj}(s) + \left(\frac{1-\hat{h}}{s}\right)\delta_{ij}$$

$$= \frac{\lambda}{s}\left(\sum_k \overline{P}_{ik}\,\alpha_{kj}(s) - \alpha_{ij} + \bar{h}(s)\,\delta_{ij}\right) + \left(\frac{1-\hat{h}}{s}\right)\delta_{ij}$$

$$= \frac{\lambda}{s}\sum_k \left(\overline{P}_{ik} - \delta_{ik}\right)\alpha_{kj} + \frac{1}{s}\delta_{ij}$$

$$\hat{\alpha}(s) = \frac{\lambda}{s}\,(\overline{P} - I)\,\alpha(s) + \frac{1}{s}I \tag{52}$$

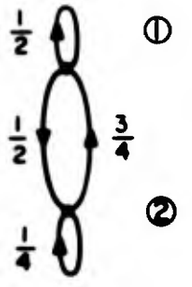

Figure 13. Two-state chain for illustrative computation of $\hat{\alpha}_{ij}(\tau)$.

Let us compute $\hat{\alpha}_{12}(s)$, in which case we require $\alpha_{12}(s)$ and $\alpha_{22}(s)$. Now

$$U_{12}(x) = \frac{1}{1-\frac{1}{2}x}\;\frac{x/2}{1-\frac{1}{4}x-\frac{3/8\,x^2}{1-1/2x}} = \frac{x/2}{(1-x)\left(1+\frac{1}{4}x\right)}$$

and

$$U_{22}(x) = \frac{1}{1 - \frac{1}{4}x - \frac{3/8\ x^2}{1 - \frac{1}{2}x}} = \frac{1 - 1/2\ x}{(1 - x)\left(1 + \frac{1}{4}x\right)}$$

Further, by Eq. (17), with $h(s) = e^{-s} = x$,

$$\alpha_{12}(x) = \frac{1-x}{s}\ U_{12}(x)$$

$$= \frac{1}{s}\left[\frac{x}{2}\ (1 - 1/4\ x + 1/16\ x^2 - \frac{1}{64}\ x^3 + \ldots)\right]$$

$$\alpha_{12}(\tau) = \int_0^{\tau} \left[\frac{\delta\ (\tau - 1)}{2} - 1/8\ \delta(\tau - 2) + 1/32\ \delta\ (\tau - 3) - \ldots.\right] d\tau$$

and

$$\alpha_{22}(\tau) = \int_0^{\tau} \left(\delta\ (\tau) - 3/4\ \delta(\tau - 1) + 3/16\ \delta(\tau - 2) + \ldots.\right)\ d\tau$$

From Eq. (52) ($\lambda = 1$)

$$\hat{\alpha}_{12}(\tau) = \left(\bar{P}_{11} - 1\right) \int_0^{\tau} \alpha_{12}(t)\ dt + \bar{P}_{12} \int_0^{\tau} \alpha_{22}(t)\ dt$$

$$= \frac{1}{2} \int_0^{\tau} \left[\alpha_{22}(t) - \alpha_{12}(t)\right]\ dt$$

We plot $\alpha_{12}(\tau)$, $\alpha_{22}(\tau)$ in Fig. 14(a), their difference in Fig. 14(b), and $\alpha_{12}(\tau)$ in Fig. 14(c).

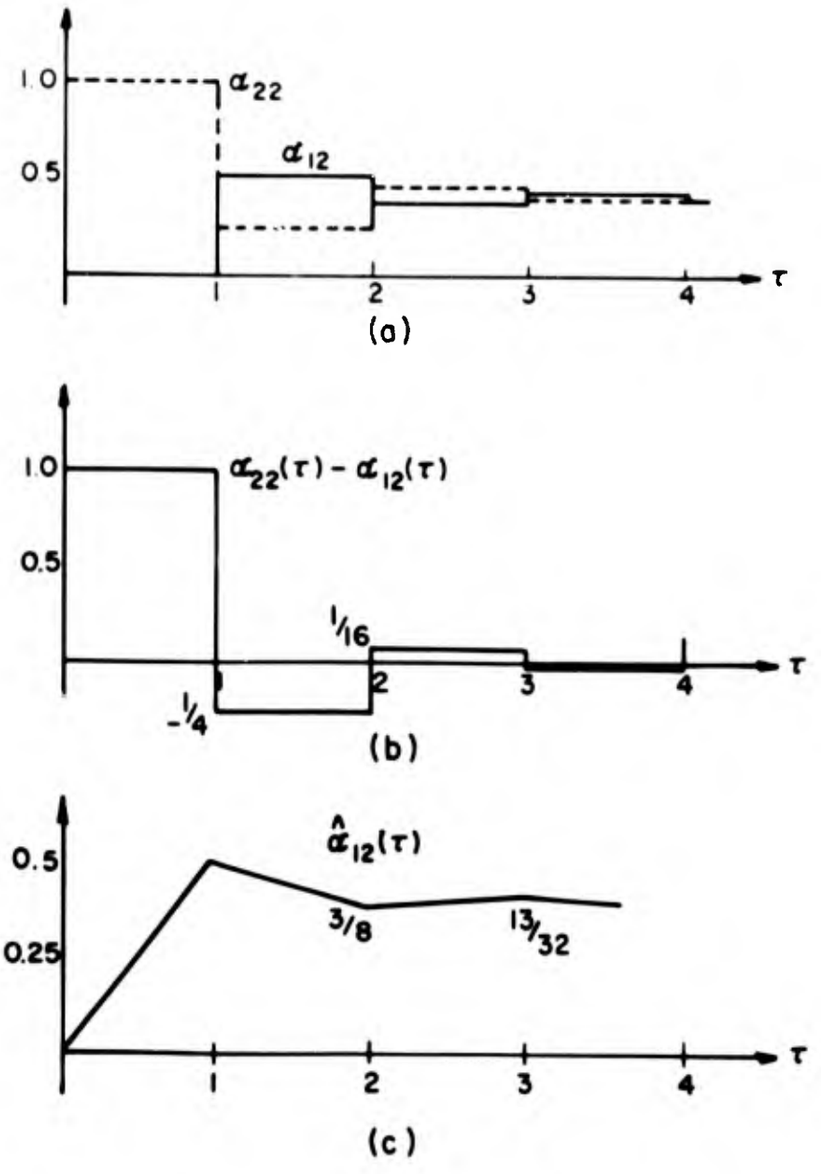

Figure 14. Successive steps in solving for $\hat{\alpha}_{12}(\tau)$.

The simple nature of the discrete-time chain permits us to compute values of $\hat{\alpha}_{12}(\tau)$ directly for particular values of τ. This gives us a means of verifying the preceding computation, as well as providing some insight into the nature of $\hat{\alpha}(\tau)$. Let us compute $\hat{\alpha}_{12}$ (1.75) directly. (See Fig. 15.) Given that the process is in state 1 initially, the probability of state 2 being occupied 1.75 seconds later is:

$$\hat{\alpha}_{12}(1.75) = \Pr\left(\begin{array}{l}\text{of reference point}\\ \text{being within 1/4}\\ \text{sec. of initiation}\\ \text{of state 1}\end{array}\right) \cdot \Pr\left(\begin{array}{l}\text{next transition}\\ \text{is to state 2}\end{array}\right)$$

$$+ \Pr\left(\begin{array}{l}\text{of reference point}\\ \text{being later than}\\ \text{1/4 sec. from in-}\\ \text{itiation of state 1}\end{array}\right) \cdot \Pr\left(\begin{array}{l}\text{arbitrary next}\\ \text{transition; tran-}\\ \text{sition following}\\ \text{is to state 2}\end{array}\right)$$

$$= \frac{1}{4}\left(\frac{1}{2}\right) + \frac{3}{4}\left(\frac{1}{2}\frac{1}{2} + \frac{1}{2}\frac{1}{4}\right)$$

$$= 1/8 + \frac{9}{32} = 13/32$$

which agrees with Fig. 14(c). Other points may be verified in the same way. We hasten to point out that the computation is this simple only in the discrete-time case.

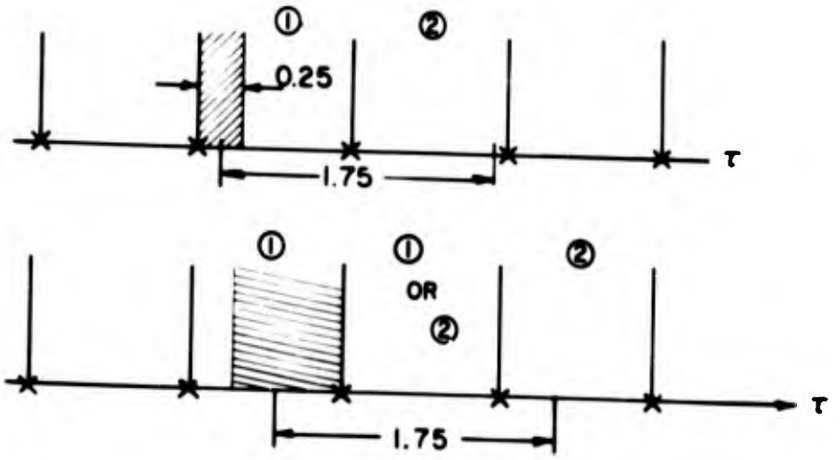

Figure 15. Computation of $\hat{\alpha}_{12}(1.75)$

CHUNG PROCESSES

As presented, the $\hat{\alpha}_{ij}(\tau)$ have the two properties that one would expect in view of their definition:

$$1)\quad \hat{\alpha}_{ij}(\tau) \geq 0, \quad \text{all } \tau$$

$$2)\quad \sum_j \hat{\alpha}_{ij}(\tau) = 1, \quad \text{all } \tau, \text{ i}$$

In his treatise on Markov chains, K. L. Chung [3] requires a third property, namely:

$$3)\quad \hat{\alpha}_{ij}(t+\tau) = \sum_k \hat{\alpha}_{ik}(t)\,\hat{\alpha}_{kj}(\tau)$$

$$= \sum_k \hat{\alpha}_{ik}(\tau)\,\hat{\alpha}_{kj}(t)$$

or in matrix form

$$\hat{\alpha}(t+\tau) = \hat{\alpha}(t)\,\hat{\alpha}(\tau) = \hat{\alpha}(\tau)\,\hat{\alpha}(t)$$

We shall show by a plausibility argument (rather than a rigorous proof) that this last is a considerable restriction on the allowable class of $p_{ij}(\tau)$,* and to pursue some of its implications. The above equation is known as the Chapman-Kolmogorov equation. We refer to processes satisfying this equation as "Chung processes".

Consider the "probability schematic" of Fig. 16. The events are defined by:

$Q \triangleq$ state j is occupied at $t + \tau$

$P \triangleq$ state i is occupied at 0

$R_k \triangleq$ state k is occupied at t

Then

$$\hat{\alpha}_{ij}(t+\tau) = \Pr(Q|P) = \Pr(PQ)/\Pr(P)$$

$$= \sum_k \Pr\left(PR_kQ\right)/\Pr(P)$$

$$= \sum_k \Pr\left(Q\middle|PR_k\right)\Pr\left(PR_k\right)/\Pr(P)$$

$$= \sum_k \Pr\left(Q\middle|PR_k\right)\Pr\left(R_k\middle|P\right)$$

*In fact, discrete-time processes do not satisfy 3), except at the transition instants.

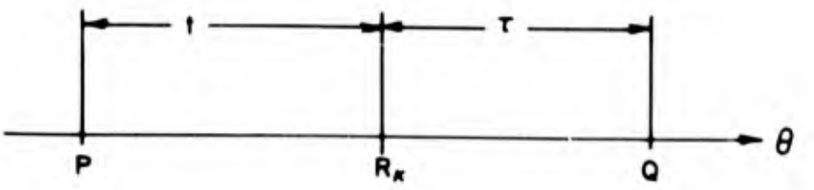

Figure 16. "Event schematic" for $\hat{\alpha}_{ij}(t + \tau)$.

Now, $\Pr(R_k|P) = \hat{\alpha}_{ik}(t)$, and hence, in general

$$\hat{\alpha}_{ij}(t+\tau) = \sum_k \hat{\alpha}_{ik}(t) \left[\Pr\left(Q|PR_k\right)\right] \tag{52a}$$

Condition 3) may be rewritten as follows:

$$\hat{\alpha}_{ij}(t+\tau) = \sum_k \hat{\alpha}_{ik}(t) \left[\Pr\left(Q|R_k\right)\right] \tag{52b}$$

since

$$\hat{\alpha}_{kj}(\tau) = \Pr\left(Q|R_k\right)$$

Comparing Eqs. (52a) and (52b), we get

$$\Pr\left(Q|PR_k\right) = \Pr\left(Q|R_k\right) \tag{52c}$$

That is, the probability of state j being occupied τ seconds after state k is occupied is independent of the behavior of the process prior to $\theta = 0$ [under condition 3)] . Now let P represent the initiation of state i at time 0. Then

$$\Pr(Q|P) = \alpha_{ij}(t + \tau)$$

and

$$\Pr\left(R_k|P\right) = \alpha_{ik}(t)$$

and so

$$\alpha_{ij}(t + \tau) = \sum_k \alpha_{ik}(t)\, \hat{\alpha}_{kj}(\tau) \tag{53}$$

We evaluate Eq. (53) at t = 0 (recall $\alpha_{ij}(0) = \delta_{ij}$) to obtain

$$\alpha_{ij}(\tau) = \sum_k \delta_{ik} \hat{\alpha}_{kj}(\tau) = \hat{\alpha}_{ij}(\tau) \tag{54}$$

and so α and $\hat{\alpha}$ are indistinguishable when 3) is invoked. It is now a simple matter to determine the nature of the $p_{ij}(\tau)$ which are implied by 3). Rewriting Eq. (43a), we have

$$\hat{\alpha}(s) = \hat{P}(s)\, \alpha(s) + \left(\frac{1-\hat{h}}{s}\right) I \tag{54a}$$

which, in view of the foregoing, is identical with

$$\alpha(s) = \bar{h}(s)\, (I - P(s))^{-1} \quad \text{(Eqs. 17, 21)} \tag{54b}$$

Equating the right members of Eqs. (54a) and (54b), we have

$$\bar{h}(s)\, [I - P(s)]^{-1} = \bar{h}(s)\, \hat{P}(s)\, (I - P(s))^{-1} + \frac{[1-\hat{h}(s)]}{s} I \tag{54c}$$

$$\bar{h}(s) = \bar{h}(s)\, \hat{P}(s) + \frac{[1-\hat{h}(s)]}{s} [I - P(s)] \tag{54d}$$

$$\hat{P}(s) = \frac{\lambda}{s} (\bar{P} - P(s)) = \frac{\hat{h}(s)}{1-h(s)} (\bar{P} - P(s)) \tag{54e}$$

Inserting Eq. (54e) into Eq. (54d), we have

$$\bar{h}(s) = \frac{\hat{h}(s)}{s} (\bar{P} - P(s)) + \left(\frac{1-\hat{h}(s)}{s}\right) (I - P(s))$$

which yields

$$P(s) = \hat{h}(s)\, \bar{P} + [h(s) - \hat{h}(s)]\, I$$

and so

$$\dot{p}_{ij}(\tau) = \hat{h}(\tau)\, \bar{P}_{ij} + [h(\tau) - \hat{h}(\tau)]\, \delta_{ij} \tag{55}$$

where, we recall, by Eq. (37),

$$\hat{h}(\tau) = \lambda \left(1 - \int_0^\tau h(t)\, dt\right) \tag{37}$$

We are not done yet. The function $h(\tau)$ (and hence $\hat{h}(\tau)$) must be restricted in such a way that $p_{ij}(\tau) \geq 0$, all τ. As a minimal condition $k(\tau) \geq 0$, so that $\hat{h}(\tau) \geq 0$, and $p_{ij}(\tau) \geq 0$ for $i \neq j$. For $i \neq j$, we require

$$p_{jj}(\tau) = \hat{h}\bar{P}_{jj} + |h(\tau) - \hat{h}(\tau)| \geq 0 \quad \text{all } j, \tau \tag{56}$$

Let $a = \min_j \bar{P}jj$, and $b = 1 - a$. Then Eq. (56) is satisfied for all j if we can find $h(\tau)$ such that

$$\hat{h}(\tau)\, a + h(\tau) - \hat{h}(\tau) = h(\tau) - b\hat{h}(\tau) \geq 0, \quad \text{all } \tau \ (0 \leq b \leq 1)$$

i.e., with $X(\tau) = \hat{h}(\tau)$. By Eq. (37), we see that $-\lambda h(\tau) = \dot{X}(\tau)$. Thus, $p_{jj}(\tau) \geq 0$ requires

$$\dot{X}(\tau) + \lambda b X(\tau) \leq 0, \quad \text{all } \tau \tag{57}$$

with the initial condition

$$X(0) = \hat{h}(0) = \lambda$$

When the equality holds in Eq. (57), it is a simple matter to show that $\lambda e^{-\lambda b \tau}$ is the required solution. Then consider the quantity,

$$Z(\tau) = \lambda e^{-\lambda b \tau} - X(\tau) \tag{58}$$

We shall show that $Z(\tau) \geq 0$, and hence in Eq. (57), $X(\tau) \leq \lambda e^{-\lambda b \tau}$. We differentiate Eq. (58):

$$\dot{Z}(\tau) = -\lambda^2 b e^{-\lambda b \tau} - \dot{X}(\tau)$$

In view of Eq. (57)

$$\dot{Z}(\tau) \geq -\lambda^2 b e^{-\lambda b \tau} + \lambda b X(\tau)$$

$$\dot{Z}(\tau) \geq -\lambda^2 b e^{-\lambda b \tau} + \lambda b \left(\lambda e^{-\lambda b \tau} - Z(\tau) \right)$$

$$\dot{Z}(\tau) + \lambda b Z(\tau) \geq 0, \ Z(0) = 0$$

Since $Z(0) = 0$, $\dot{Z}(0) \geq 0$. If $\dot{Z}(0) = 0$, $Z(\tau) \equiv 0$, all τ. If $\dot{Z}(0) > 0$, then $Z(\tau) > 0$, since $Z(\tau) < 0$ and $\dot{Z}(\tau) > -\lambda b Z(\tau)$ imply that $Z(\tau)$ is increasing whenever it is negative, and hence, could not be negative. We have thus shown that

$$X(\tau) = \hat{h}(\tau) \leq \lambda e^{-\lambda b \tau} \tag{59}$$

Since

$$\int_0^\tau h(t)\, dt = \frac{1 - \hat{h}(\tau)}{\lambda}$$

we have

$$\int_0^\tau h(t)\, dt \geq 1 - e^{-\lambda b \tau} \tag{60}$$

We find a lower bound for $\hat{h}(\tau)$ (and an upper bound for $\int_0^\tau h(t)\, dt$) as follows: For that j for which $\bar{P}_{jj} = a$, we have

$$\int_0^\tau p_{jj}(\tau)\, d\tau = \int_0^\tau |h(t) - b\hat{h}(t)|\, dt < \int_0^\infty p_{jj}(\tau)\, d\tau = \bar{P}_{jj} = a$$

Thus

$$\int_0^\tau h(t)\, dt < a + b \int_0^\tau \hat{h}(t)\, dt$$

but, by Eq. (59),

$$b \int_0^\tau \hat{h}(t)\, dt \leq 1 - e^{-\lambda b \tau}$$

and so

$$\int_0^\tau h(t)\,dt \le \min\left[1,\ a + \left(1 - e^{-\lambda b\tau}\right)\right] \tag{61}$$

Summarizing, if $p_{ij}(\tau)$ is specified by Eq. (55), as it is when 3) is required, then $p_{ij}(\tau) \ge 0$ implies

$$\max\left[0,\ \lambda\left(e^{-\lambda b\tau} - a\right)\right] \le \hat{h}(\tau) \le \lambda e^{-\lambda b\tau} \tag{62}$$

or equivalently,

$$1 - e^{-\lambda b\tau} \le \int_0^\tau h(x)\,dx \le \min\left(1,\ a + 1 - e^{-\lambda b\tau}\right) \tag{63}$$

We can also show that Eq. (62) is a sufficient condition for positive $p_{ij}(\tau)$, as well as being necessary. Assume that Eq. (62), and hence Eq. (63), are true, and that $p_{jj}(\tau) < 0$. That is

$$h(\tau) - b\,\hat{h}(\tau) < 0$$

Then

$$\int_0^\tau h(t)\,dt < b \int_0^\tau \hat{h}(t)\,dt$$

Applying Eq. (62)

$$\int_0^\tau h(t)\,dt < 1 - e^{-\lambda b\tau}$$

which contradicts Eq. (63).

The bounds on $\hat{h}(\tau)$ and $\int_0^\tau h(t)\,dt$ are sketched in Fig. 17. We note that if $a = 0$, i.e., if there is at least one state in the process for which $p_{ji}(\tau) \equiv 0$, then upper and lower bounds in Eqs. (62) and (63) coalesce, and

$$h(\tau) = \hat{h}(\tau) = \lambda e^{-\lambda\tau}$$

and

$$p_{ij}(\tau) = \bar{P}_{ij}\, \lambda e^{-\lambda\tau}$$

is the only set of transition probabilities for which condition 3) may apply. Even if $a \neq 0$, we can show that when $p_{ij}(\tau)$ has the form of Eq. (55), $\alpha = \hat{\alpha}$ may be computed as though $p_{ij}(\tau) = \bar{P}_{ij}(\lambda e^{-\lambda\tau})$. Consider

$$\hat{\alpha}(s) = \alpha(s) = \bar{h}(s)\ (I - P(s))^{-1}$$

$$= \bar{h}(s)\ \left(I - \hat{h}(s)\,\bar{P} - \left[h(s) - \hat{h}(s)\right] I\right)^{-1}$$

$$= \bar{h}(s)\ \left((1 - h + \hat{h})\ \left(I - \frac{\hat{h}\,\bar{P}}{1 - h + \hat{h}}\right)\right)^{-1}$$

$$\alpha(s) = \frac{\bar{h}}{1 - h + \hat{h}}\ \left(I - \frac{\hat{h}\,\bar{P}}{1 - h + \hat{h}}\right)^{-1}$$

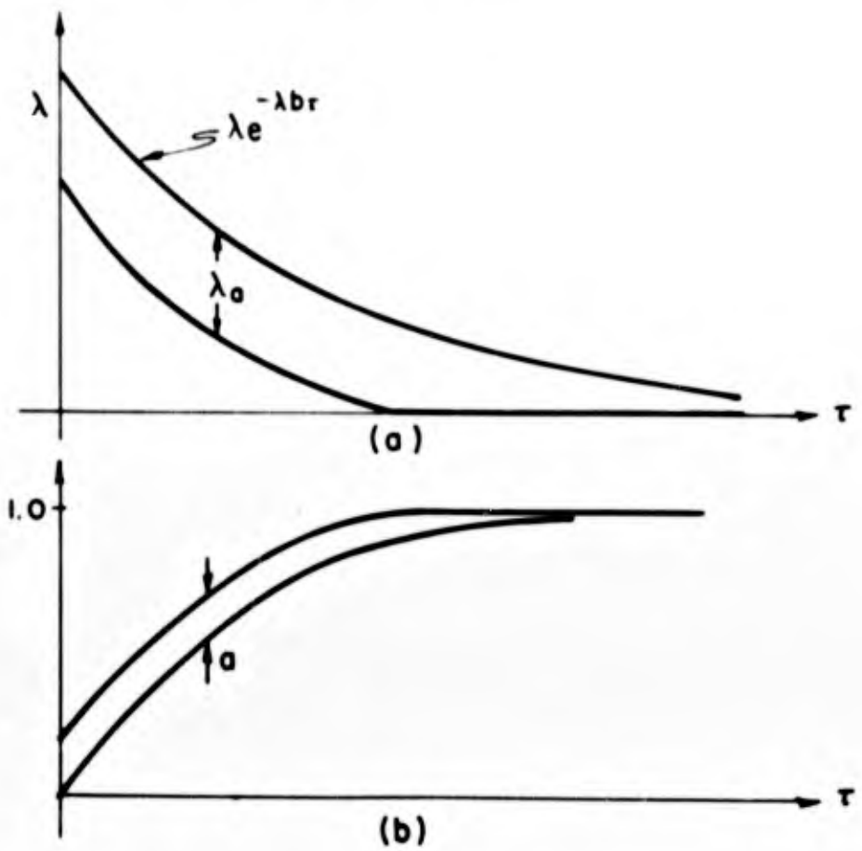

Figure 17. Bounds on $\hat{h}(\tau)$ and $\int_0^\tau h(t)dt$.

BLANK PAGE

But

$$\frac{\hat{h}(s)}{1-h(s)+\hat{h}(s)} = \frac{\lambda/s}{1+\lambda/s} = \frac{\lambda}{s+\lambda}$$

and

$$\frac{\bar{h}(s)}{1-h(s)+\hat{h}(s)} = \frac{1}{s+\lambda} = \frac{1-\lambda/s+\lambda}{s}$$

so that

$$\hat{\alpha}(s) = \alpha(s) = \left(\frac{1-\lambda/s+\lambda}{s}\right) \left(I - \left(\frac{\lambda}{s+\lambda}\right)\bar{P}\right)^{-1}$$

and the process appears, $\hat{\alpha}$ and α-wise, as if

$$h(s) = \lambda/s+\lambda$$

$$P_{ij}(s) = h(s)\ \bar{P}_{ij}$$

We may phrase this matter of the equivalence of $\hat{\alpha}$ and α in a somewhat more general manner. Consider two processes M and M_1, and let $\alpha = \alpha_1$. Then by Eq. (54b)

$$\left(1-h_1(s)\right)\ \left(I-P_1(s)\right)^{-1} = \left(1-h(s)\right)\ \left(I-P(s)\right)^{-1}$$

and so

$$P_1(s) = \left(\frac{1-h_1(s)}{1-h(s)}\right) P(s) + \left(\frac{h_1(s)-h(s)}{1-h(s)}\right) I \qquad (64)$$

Then first, if P(s) is of the form

$$P(s) = \hat{h}(s)\ \bar{P} + \left[h(s) - \hat{h}(s)\right] I \qquad (64a)$$

We insert Eq. (64a) into Eq. (64), to obtain

$$P_1(s) = \left(\frac{1-h_1(s)}{1-h(s)}\right) \lambda \left(\frac{1-h(s)}{s}\right) \bar{P} + \left[\left(\frac{1-h_1(s)}{1-h(s)}\right) \left[h(s) - \hat{h}(s)\right] + \left(\frac{h_1(s)-h(s)}{1-h(s)}\right)\right] I \qquad (64b)$$

and since

$$\bar{P}_1 = \frac{\lambda}{\lambda_1}\,\bar{P} + \left(1 - \frac{\lambda}{\lambda_1}\right) I \quad \text{(Evaluate Eq. (64) at } s = 0.\text{)} \tag{65}$$

Evaluate Eq. (65) for $\bar{P}$ and substitute the resulting expression in Eq. (64b). This yields

$$P_1(s) = \frac{\lambda}{\lambda_1}\,\hat{h}_1(s)\left(\frac{\lambda_1}{\lambda}\,\bar{P}_1 - \left(\frac{\lambda_1}{\lambda} - 1\right) I\right) + \left[h_1(s) - \frac{\lambda}{\lambda_1}\,\hat{h}_1(s)\right] I \tag{65a}$$

$$= \hat{h}_1(s)\,\bar{P}_1 + \left(h_1(s) - \hat{h}_1(s)\right) I \tag{65b}$$

Note that the right members of Eqs. (64a) and (65b) have the same form, so that $P_1(s)$ is in the same family as $P(s)$. A particularly simple member of that family is that for which $h(s) = \hat{h}(s) = \lambda/s+\lambda$, and $P(s) = \lambda/(s+\lambda)\,\bar{P}$. If we are studying the process described by $P_1(s)$, and we choose $\bar{P} = \bar{P}_1$ [which then imposes $\lambda = \lambda_1$, in view of Eq. (64)] then the simple process characterized by $P(s) = \lambda_1/(s+\lambda_1)\,\bar{P}_1$ will yield the same values of $\hat{\alpha}$ and α as the more complicated process characterized by $P_1(s)$ in Eq. (65b).

There are some additional consequences of Chung's third condition. We list them below (they are readily verified):

(1) $$U_{ij}(s) = \hat{U}_{ij}(s) + \left(\frac{1-\hat{h}}{1-h}\right)\delta_{ij} \tag{66}$$

(2) $$F_{ij}(s) = \hat{F}_{ij}(s) \qquad i \neq j \tag{67}$$

$$\frac{1-\hat{F}_{jj}(s)}{1-F_{jj}(s)} = \frac{1-\hat{h}(s)}{1-h(s)}$$

(3) $$\sum_i p_i\,p_{ij}(\tau) = p_j\,h(\tau) \tag{68}$$

REVERSIBLE CHAINS

We conclude this section by touching briefly on the question of reversible processes, where we generalize a well-known result in the theory of discrete-time chains. Consider the "probability schematic" in Fig. 18, with

$$Q \triangleq j \text{ is initiated in } \tau,\ \tau + \Delta\tau$$

$$P \triangleq i \text{ is initiated in } 0,\ 0 + \Delta\tau$$

$$S \triangleq \text{no transitions in } (0,\ \tau)$$

Using Bayes' law, we write

$$\Pr(SQ \mid P)\ \Pr(P) = \Pr(SP \mid Q)\ \Pr(Q) = \Pr(PSQ)$$

Now,

$$\Pr(SQ \mid P) = p_{ij}(\tau)\ \Delta\tau$$

and

$$\Pr(SP \mid Q) \triangleq \overleftarrow{p_{ij}}(\tau)\ \Delta\tau$$

where $\overleftarrow{p_{ij}}(\tau)\ \Delta\tau$ is the backwards probability of the event: given that j is initiated at $\tau = 0$, the most recent transition was to i and occurred in the interval $[-(\tau + \Delta\tau),\ -\tau.]$ Furthermore,

$$\Pr(P) = \lambda_i\ \Delta\tau;\quad \Pr(Q) = \lambda_j\ \Delta\tau$$

so that we find

$$\lambda_i\ p_{ij}(\tau) = \lambda_j\ \overleftarrow{p_{ij}}(\tau) \tag{69}$$

If both sides of Eq. (69) are multiplied by $\bar{\tau}$, we have

$$p_i\ p_{ij}(\tau) = p_j\ \overleftarrow{p_{ij}}(\tau) \tag{70}$$

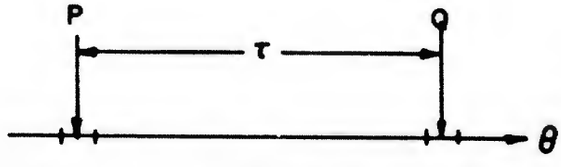

Figure 18. "Event schematic" for $p_{ij}(\tau)$.

A reversible process is one wherein the condition

$$p_{ji}(\tau) = \overleftarrow{p_{ij}}(\tau) \tag{71}$$

obtains, i.e., the process statistics are invariant under a reversal of the time axis. We define the matrix D as: $D = \text{diag}\,(p_1, p_2, \ldots, p_N)$. Then Eq. (70) means

$$D\,P(\tau) = \overleftarrow{P(\tau)}\,D$$

It is now a simple matter to show that a process is reversible if and only if

$$DP(\tau) = P^T(\tau)\,D \tag{72}$$

where

$$P^T(\tau) = \left\{p_{ji}(\tau)\right\}$$

If

$$DP(\tau) = P^T(\tau)\,D,$$

then

$$\overleftarrow{P(\tau)}\,D = P^T(\tau)\,D$$

and

$$p_{ji}(\tau) = \overleftarrow{p_{ij}}(\tau) \quad \text{(reversibility)}$$

Conversely, if the process is reversible, i.e., if,

$$P^T(\tau) = \overleftarrow{P(\tau)}$$

then

$$\begin{aligned} P(\tau) &= \left[\overleftarrow{P(\tau)}\right]^T \\ &= \left[DP(\tau)\,D^{-1}\right]^T \\ &= D^{-1}\,P^T(\tau)\,D \end{aligned}$$

where the superscript T indicates the transposed matrix.

and so

$$DP(\tau) = P^{T}(\tau)\, D$$

An interesting aspect of the Chung processes is that, although they are not of necessity reversible, the backward inter-transition density $k_j(\tau)$ is independent of j, and is, in fact, equal to $k(\tau)$, the corresponding forward density. Proof: Since

$$\overleftarrow{h}_j(\tau) = \sum_i \overleftarrow{p}_{ij}(\tau) = \frac{1}{p_j} \sum_i p_i\, p_{ij}(\tau)$$

By Eq. (68), we have

$$\sum_i p_i\, p_{ij}(\tau) = p_j\, h(\tau) \tag{68}$$

for the Chung processes. Hence

$$\overleftarrow{h}_j(\tau) = h(\tau), \quad \text{all } j.$$

III. ANALYSIS OF ADAPTIVE PROCESSES

ADAPTIVE RANDOM WALK

In this section we shall examine the effectiveness of a particular feedback policy in an adaptive random walk. A particular object of the analysis will be the comparison of closed-loop and open-loop performance. A subsidiary goal will be the determination of how ignorance of certain of the model parameters will affect the performance of the system.

We consider a three-state process containing an adjustable parameter, k, which, in turn, has three distinct values. It is assumed that adjustments in k leave the topology of the graph describing the process unchanged; the only manifestation of the k values is in the transition probabilities. In other words, to each value of k there corresponds a 3-state process. With k at its "quiescent" value (k=0), the process is taken as symmetric about its center state. With k = +1, the process is "biased" toward an end state; for k = -1 (denoted $\bar{1}$ for convenience), the bias is toward the other end state. The "unadjusted" (k=0) process is depicted in Fig. 19. Direct application of the formalism for computing the steady-state probabilities gives*

$$(p_0)_0 = \frac{a}{a+2b} \triangleq p$$

$$(p_1)_0 = (p_{\bar{1}})_0 = \frac{b}{a+2b} = \frac{b}{a}\,p \triangleq q$$

$$p + 2q = 1$$

We also require that

$$(p_1)_1 = (p_{\bar{1}})_{\bar{1}} = p$$

$$(p_0)_1 = (p_0)_{\bar{1}} = \lambda p$$

*$(p_i)_j$ refers to the steady-state probability of state i in the process corresponding to k = j. (i, j = $\bar{1}$, 0, 1).

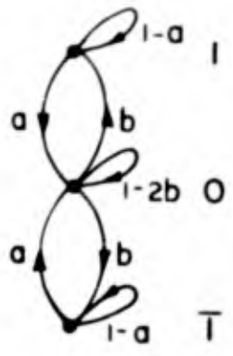

Figure 19. Process for k = 0.

where λ is a parameter ranging from q/p to 2q/p. Figure 20 illustrates the "open-loop" processes and their associated steady-state distributions. Note that all transition probabilities must be positive and less than unity. Hence

$$0 \leq a \leq 1 \qquad \text{(a)}$$

$$0 \leq b \leq 1/2 \qquad \text{(b)}$$

$$0 < 1 - \left(a + \frac{b\kappa}{\lambda}\right) < 1 \qquad \text{(c)}$$

where

$$\kappa \equiv \frac{2q}{p} - \lambda$$

Examination of this last inequality gives, for $\lambda = 2q/p$,

$$a + b \leq 1 \qquad \text{(d)}$$

One can verify that for the given range of λ, inequalities (a), (b), and (d) restrict all transition probabilities in the required manner. In the ab-plane, inequalities (a), (b), and (d) form a trapezoid enclosing all admissible pairs (a,b). We call this region the "admissible trapezoid."

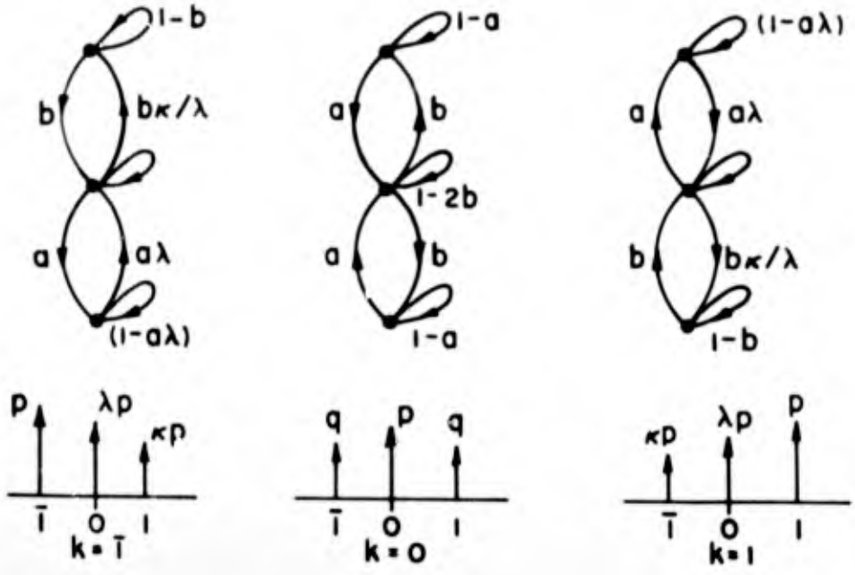

Figure 20. Open-loop configuration with associated distributions.

The feedback scheme is shown in Fig. 21. The present state of the process is monitored, and k is adjusted in accordance with the following policy: When the process reaches a $\bar{1}$ state, k is incremented by + 1 (if possible); when a 1 state is reached, k is incremented by -1 (if possible). The control "task" is to keep the process in the center state of any of the three open-loop processes as much of the time as possible. The measure of performance is the steady-state probability that a center state is occupied. In accordance with the specified control policy, the "closed-loop" structure is illustrated in Fig. 22.

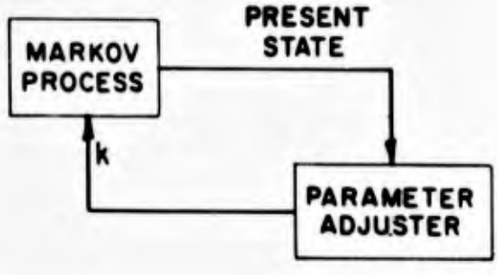

Figure 21. Feedback loop based on 3-valued adjustment.

The probability transitions from process to process are designated *feedback transitions*. The exact nature of these transitions is a matter of speculation, since we have no precise way of knowing whether or not the process will undergo an instantaneous state change when k is incremented. Since these transitions may constitute a major area of ignorance for the designer, it is desirable that the performance of the control loop be relatively insensitive to them. To obtain some insight into this matter, the control policy will be evaluated for tw seemingly dissimilar cases:

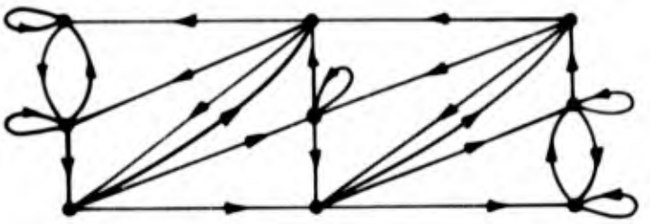

Figure 22. Closed-loop graph for "end-fired" policy.

Case I. The feedback transition values are the steady-state probabilities of the terminal states.

Case II. The feedback transition values are the transition probabilities emanating from the center state of the terminal process, i.e., the process corresponding to the new value of k.

In the analysis of Case II, the control policy will be generalized somewhat to include the effects of waiting time, W. That is, W + 1 successive occurrences of an end state are required before k is incremented.

For Case I, the "closed-loop" configuration is depicted in Fig. 23. We wish to compute the center-state probabilities, add them to obtain the probability π_0, and ultimately inquire, $\pi_0 > p$? That is, does the closed-loop performance exceed that of the open-loop? In order to take advantage of the symmetry, the 00 state is split into source and sink, as in Fig. 24.

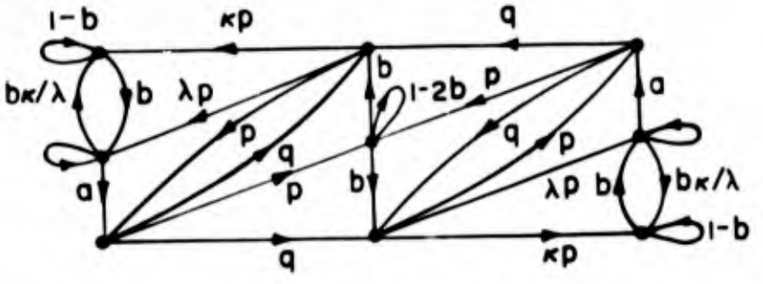

Figure 23. Closed-loop; Case I feedback transitions.

We may write

$$1 = 1 - 2b + 2p\hat{y}$$

$$\hat{y} = b/p$$

$$\hat{x} = 2q\hat{y} + b = b\left(1 + \frac{2q}{p}\right) = b/p$$

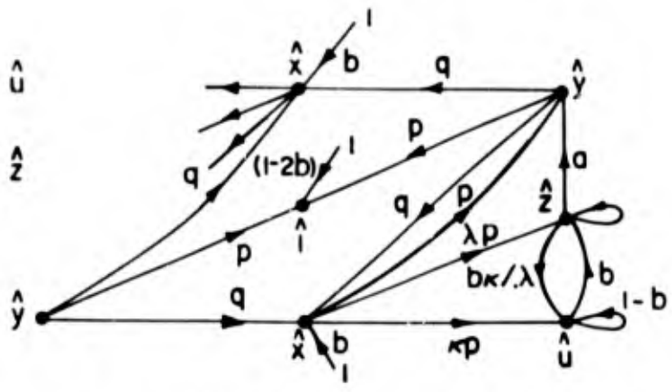

Figure 24. Splitting at OO node for steady-state computations.

Further,

$$\hat{y} = a\hat{z} + p\hat{x} = a\hat{z} + b$$

$$\hat{z} = \frac{\hat{y}-b}{a} = \frac{b}{a}\left(\frac{1}{p} - 1\right) = \frac{b}{a}\,\frac{2q}{p} = 2\left(\frac{q}{p}\right)^2$$

$$\hat{\mu} = \kappa p\hat{x} + \frac{\kappa b}{\lambda}\,\hat{z} + (1-b)\,\hat{\mu}$$

$$\hat{\mu} = \kappa\left(1 + \frac{2}{\lambda}\left(\frac{q}{p}\right)^2\right)$$

Hence,

$$\pi_0 = \frac{1 + 2\hat{z}}{1 + 2\,(\hat{\mu} + \hat{x} + \hat{y} + \hat{z})} \tag{69}$$

For $\lambda = \frac{q}{p}$, Eq. (69) becomes

$$\pi_0 = \frac{p^2 + 4q^2}{p^2 + 4q^2 + 4bp + 2q}$$

and it is readily shown that $\pi_0 > p$ if

$$a < q\left(\frac{2q}{p} - 1\right) \tag{70}$$

With $\lambda = 2\frac{q}{p}$, the required constraint is

$$a < q\left(\frac{2q}{p} - 1\right) + \frac{1}{2} \tag{71}$$

The upper bound on a in Eq. (70) is easily plotted in the ab-plane by first sketching loci of constant q (and hence p = 1-2q). The upper bound in Eq. (71) follows immediately. Figure 25 illustrates the results, with that area in the ab-plane bounded by Eq. (70) or Eq. (71) and the previous inequalities (a), (b), (d) defining the range of a, b values for which steady-state improvement is achieved. The appropriate constraint for an intermediate value of $\lambda = (3/2)(q/p)$ is also included.

The region of admissible pairs (a, b) for which the closed-loop performance, π_0, exceeds the open-loop performance, p, falls in the region bounded from above by the upper-bound curves shown in Fig. 25 and bounded from below by the admissible trapezoid.

We call this the "improvable" region. Note that the area of the improvable region is larger than one-half of the area of the admissible region when $\lambda = 2q/p$. For other values of λ, the area of the improvable region is still substantial — about 1/3 or more of the admissible region. If we are confident *a priori* that (a, b) lies inside the improvable region, we can be confident that the feedback policy will yield improved steady-state performance, even though we may be ignorant of the particular values of a and b.

For the Case II feedback transition probabilities, we consider the structure of Fig. 26. As mentioned, the "end-fired" control policy is extended to include a waiting time requirement. Figure 27 shows the "dissection" of the 00 state prior to an evaluation of the steady-state probabilities. We write

$$\hat{s}_i = b(1 + 2\hat{x})(1 - a)^{i-1}$$

and

$$\hat{y} = \hat{s}_w = b(1 + 2\hat{x})(1 - a)^{w-1}$$

At the 00 node

$$1 = (1 - 2b)(1 + 2\hat{x}) + 2a\sum_{i=1}^{w}\hat{s}_i$$

$$1 = (1 + 2\hat{x})\left(1 - 2b + 2ab\left(\frac{1 - (1 - a)^w}{1 - (1 - a)}\right)\right)$$

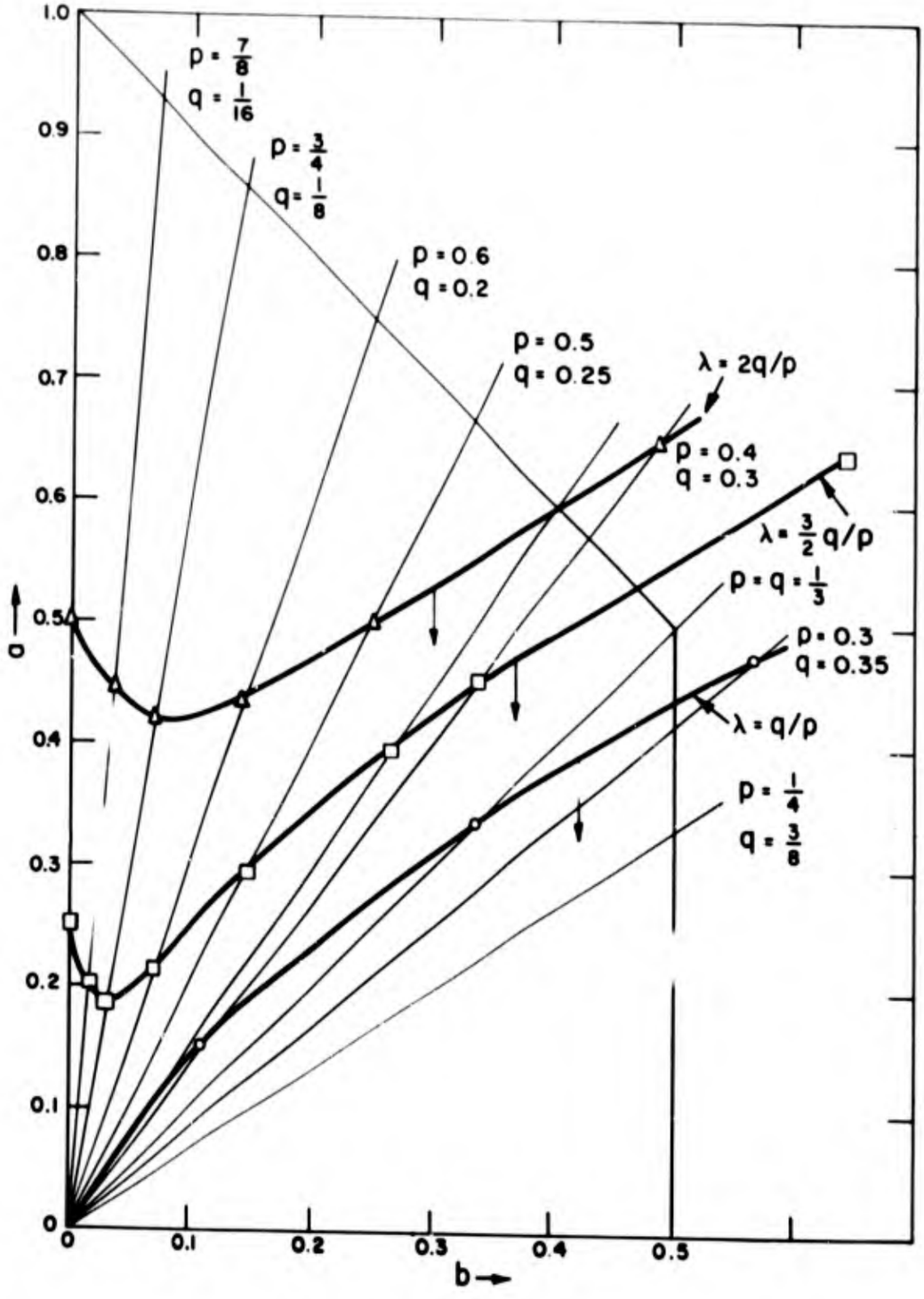

Figure 25. Areas of steady-state improvement, Case I.

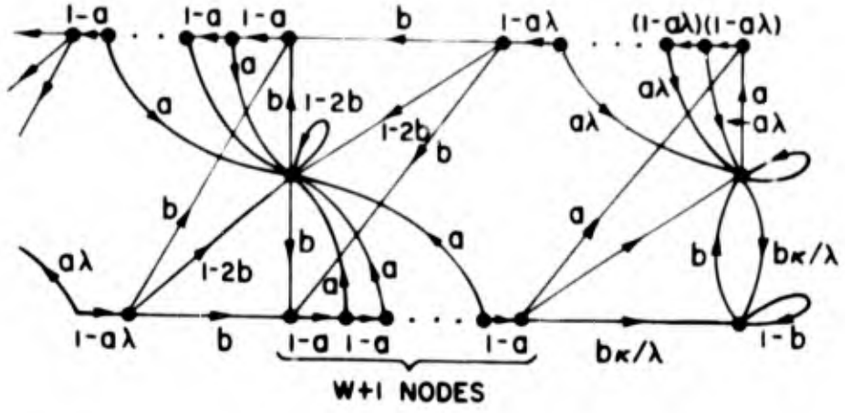

Figure 26. Case II feedback transitions, W-fired control.

$$1 = (1 + 2\hat{x})\,(1 - 2b\,(1 - a)^{W})$$

and

$$\hat{x} = \frac{1}{2}\left(\frac{1}{1 - 2b\,(1 - a)^{W}} - 1\right) = \frac{b\,(1 - a)^{W}}{1 - 2b\,(1 - a)^{W}}$$

Then

$$\hat{y} = \frac{b\,(1 - a)^{W-1}}{1 - 2b\,(1 - a)^{W}}$$

or

$$\hat{x} = (1 - a)\,\hat{y}$$

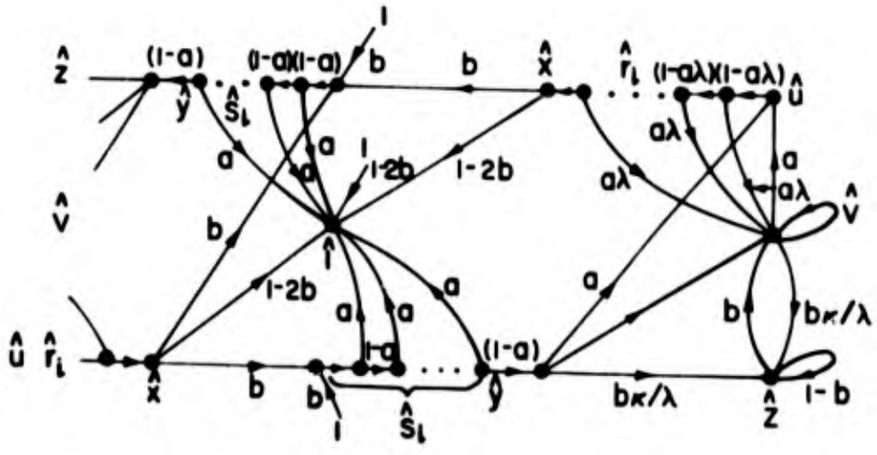

Figure 27. Graph for steady-state analysis.

Also,

$$\hat{r}_i = \frac{\hat{x}}{(1 - a\lambda)^i}$$

and

$$\hat{\mu} = \hat{r}_w = \frac{\hat{x}}{(1 - a\lambda)^w}$$

Since

$$\hat{\mu} = a(\hat{v} + (1 - a)\hat{y}) = a(\hat{v} + \hat{x})$$

$$\hat{v} = \frac{\hat{\mu}}{a} - \hat{x} = \hat{x}\left(\frac{1}{a(1 - a\lambda)^w} - 1\right)$$

and

$$\hat{z} = \frac{b\kappa}{\lambda}(\hat{v} + (1 - a)\hat{y}) + (1 - b)\hat{z}$$

$$= \frac{\kappa}{\lambda}(\hat{v} + \hat{x}) = \frac{\kappa}{\lambda}\hat{x}\,\frac{1}{a(1 - a\lambda)^w} \cdot$$

Finally,

$$\pi_0 = \frac{1 + 2\hat{v}}{1 + 2\left(\sum_i \hat{s}_i + \sum_i \hat{r}_i + \hat{v} + \hat{z} + 2\hat{x}\right)} \tag{72}$$

where

$$\sum_i \hat{r}_i = \frac{\hat{x}}{1 - a\lambda}\left(1 + \frac{1}{1 - a\lambda} + \cdots \frac{1}{(1 - a\lambda)^{w-1}}\right) = \frac{\hat{x}}{a\lambda}\left(\frac{1}{(1 - a\lambda)^w} - 1\right)$$

For w = 0 (ordinary "end-firing"), π_0 reduces to

$$\pi_0 = \frac{1 - 4aq}{p\left(1 + \frac{1}{\lambda}\left(\frac{2q}{p}\right)^2\right)} \tag{73}$$

With $\lambda = q/p$, we find that $\pi_0 > p$ if $a < q$. For the other extreme of $\lambda = 2q/p$, improvement is achieved for all $a < 1/2$.

For $w = 1$, we ultimately require that ($\lambda = q/p$):

$$b^2 + \frac{b}{2a}\left(a - \frac{1}{2}\right)(a - 2) - \frac{3a}{4} > 0 \tag{74}$$

For $\pi_0 > p$, and with $\lambda = 2q/p$, we find:

$$b^2 + \frac{b}{2a}\left(a - \frac{1}{2}\right)(a - 1) - \frac{3}{8}\left(a - \frac{1}{3}\right) > 0 \tag{75}$$

is the final constraint. The curves of constraint for Eq. (73) through Eq. (75) are plotted in Fig. 28. Again, the improvable regions are bounded from above by these curves and from below by the admissible trapezoid. We note again that the area of the improvable region is one-third or more of the area of the admissible region. If our ignorance of (a,b) is bounded by a curve lying mostly in the improvable region, then we can be confident that Case II feedback yields improved closed-loop steady-state performance.

The graphical results indicate:

(a) The policy of waiting is not significantly effective. In Case II with $\lambda = q/p$, $w = 0$ is superior to $w = 1$ for $a > b$, inferior for $a < b$. Again, with $\lambda = 2q/p$, $w = 1$ favors $a < 2b$, but "loses ground" for $a > 2b$.

(b) Superimposing Figs. 25 and 28 for the conditions $w = 0$, $\lambda = 2p/q$, $\lambda = p/q$ yields Fig. 29. We see here that changing the feedback policy from Case I to Case II has only a moderate effect on the upper boundary corresponding to any particular value of $\lambda p/q$. We also see that this change of feedback policy has virtually no effect on the area of the improvable region.

Thus, two different feedback policies — Case I and Case II — can improve the asymptotic performance of an adaptive random walk, even in the face of considerable ignorance of the open-loop parameters. Furthermore, the two policies are about equally effective in their ability to mask an ignorance of or unpredicted changes in the open-loop parameters.

THRESHOLD LEARNING PROCESS

The threshold learning process (TLP) is an adaptive version of the Neyman-Pearson observer [13]. This process provides a simple framework for the study

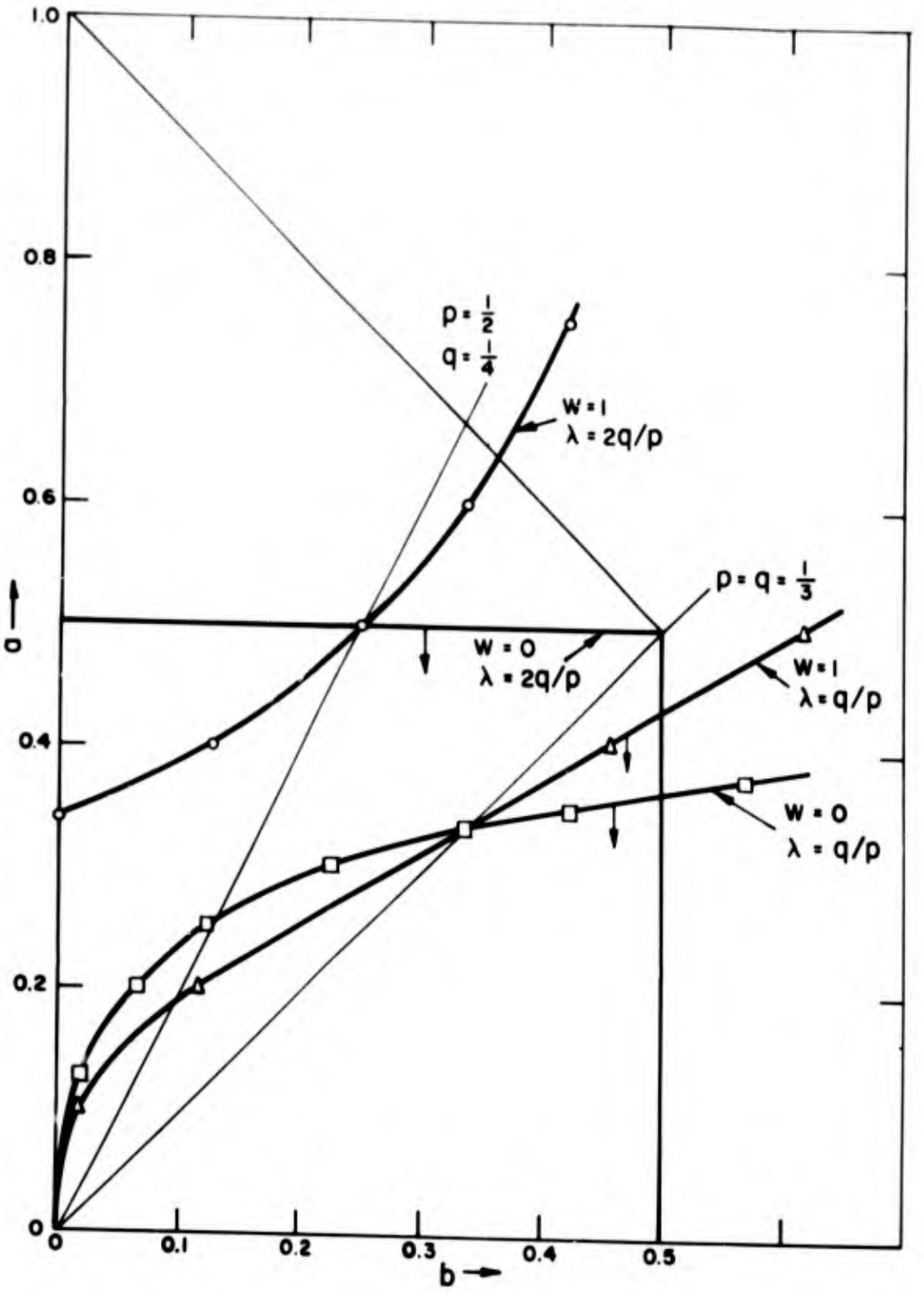

Figure 28. Areas of steady-state improvement, Case II.

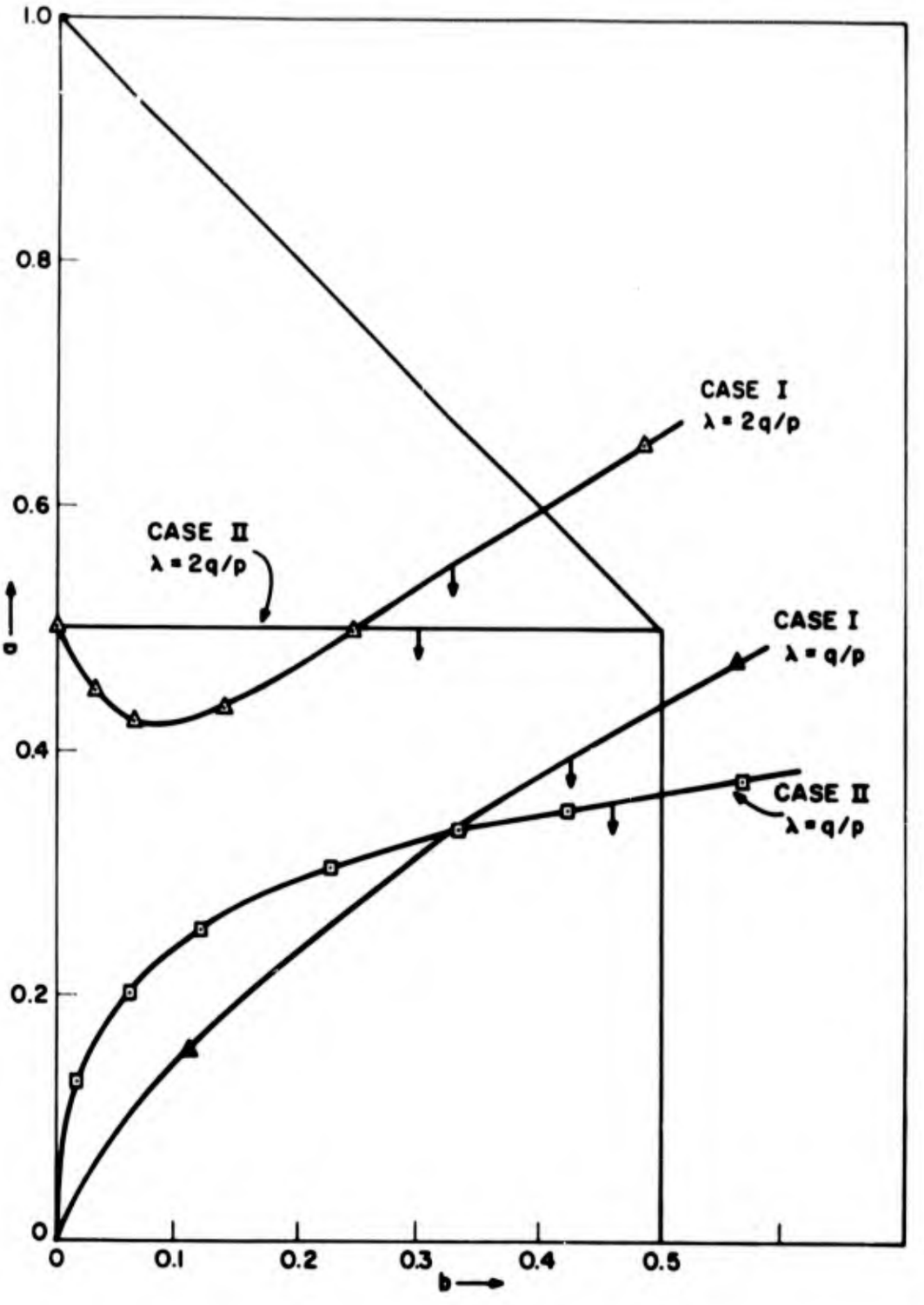

Figure 29. Comparison of Case I and Case II.

of adaptation and learning. Furthermore, it appears in a variety of applications, including signal detection, pattern recognition, discrimination learning, and information retrieval.

In earlier reports we focused our attention on three-threshold TLPs, because of the relative ease with which these TLPs can be analyzed, and because of evidence that certain qualitative properties of three-threshold TLPs extend to many-threshold TLPs.

Unfortunately, the number of meaningful feedback policies in three-threshold TLPs is severely limited. Consequently, to permit the analysis of feedback policies that are more sophisticated than simple incremental feedback, five-threshold TLPs were studied. In addition the effects of a number of feedback policies on continuous threshold TLPs were studied. In a continuous-threshold TLP the available thresholds occupy a continuum on a real line segment, and the reinforcement increments are very small, approaching zero as a limit. We have reported here the effects of several feedback policies on the asymptotic performance of five-threshold TLPs and continuous-threshold TLPs.

Definition of threshold learning process: In a threshold learning process an observer is required to distinguish between two signals, designated "0" and "1". The signals are transmitted sequentially in time (with each transmission independent of all previous) through a noisy channel. The observer makes his decisions by employing a threshold criterion; if the received signal exceeds (in amplitude) some predetermined level, the transmission is presumed to be a "1", and if the signal fails to achieve threshold, the observer interprets the transmission as a "0". In order that some form of adaptation to the environment (message and noise statistics) may take place, the observer, for a time, is provided with knowledge of the actual transmission, which he may then compare with his "guess". Corrective action, i.e., threshold adjustment is then employed, and after some time, a threshold value which is optimum, or near-optimum (for the particular environment), should be achieved. This phase of operation is the so-called "training phase". When the feedback between transmitter and receiver is interrupted (the standard training message is ended) the system operates in its "working phase", utilizing a threshold value which reflects the message statistics of the source and the noise characteristics of the channel. The way in which adjustment action is taken during the training phase is called the "feedback policy", and several such policies will be investigated in subsequent sections. The training process will have been useful, i.e., the feedback policy successful, if the observer guesses correctly with greater frequency than that prior to training.

In typical situations, the channel characteristics will give rise to the probability densities of Fig. 30. The shaded incremental area under the left-hand curve is the conditional probability $p_0(v)\Delta v$, that the received signal v, has a value between v and $v + \Delta v$, given that a "0" was transmitted. Similarly for the right-hand function $p_1(v)$, reflecting the density of received values in the presence of a "1" signal. Suppose "zeros" are transmitted with a frequency of ρ. We define, for a fixed threshold k:

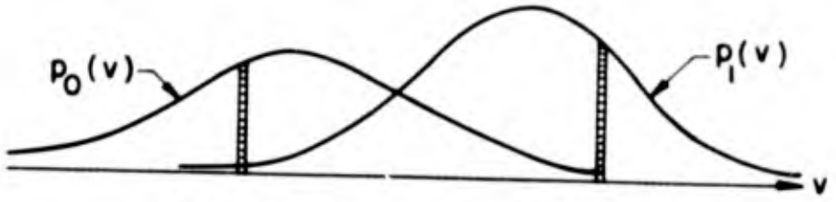

Figure 30. Densities of received signals.

$$a \triangleq \text{Prob ("1" transmitted and } v < k) = \text{"false rest probability"}$$

$$= (1 - \rho) \int_{-\infty}^{k} p_1(v)\, dv$$

$$b = 1 - (a + c) = \text{Prob ("0" transmitted and } v < k)$$

$$+ \text{Prob ("1" transmitted and } v > k) = \text{probability of correct guess}$$

$$= \rho \int_{-\infty}^{k} p_0(v)\, dv + (1 - \rho) \int_{k}^{\infty} p_1(v)\, dv$$

$$c \triangleq \text{Prob ("0" transmitted and } v > k) = \text{"False alarm probability"}$$

$$= \rho \int_{k}^{\infty} p_0(v)\, dv$$

Let

$$f_0(v) = \rho\, p_0(v);\ f_1(v) = (1 - \rho)\, p_1(v)$$

Then

$$b'(k) = f_0(k) - f_1(k)$$

and

$$b''(k) = f_0'(k) - f_1'(k)$$

so that for $k = k_0$, at which point $f_0(v)$ intersects $f_1(v)$, the probability of correct guess is highest. Of course, k_0 is not known to our observer, or else his problem would be nonexistent.

Simple Incremental Feedback

Let there be a fixed number of thresholds available to the observer, and suppose that during training, he makes his adjustments in accordance with the following policy: In case of a false-alarm, use, for the next observation, a threshold just to the right of the present value (visualize the threshold values as points on the real line). If a false-rest occurs, move left one notch, and make no adjustment if the guess is correct. Obviously, the policy has very little "memory", but we will show that it can be moderately effective. In another context, that of the psychologist interested in models of learning the policy we have described is illustrative of a simple "reinforcement" scheme.

For concreteness, we assume that the probability densities which characterize the channel are those of Fig. 31(a), where α is a parameter. Let K denote the number of available threshold values. The K threshold values shall be distributed uniformly over the range of received signals. This arrangement is illustrated in Fig. 31(b) and (c), for K = 3 and K= 5, respectively. In Fig. 30(c) the five threshold values are spaced so as to divide the interval $[0, 4]$ into six equal parts. The Markov chain which is representative of each system is also shown in Fig. 30. The states of the chain are the threshold values. The values assigned to the transition probabilities reflect the feedback policy, in this case simple incremental feedback.

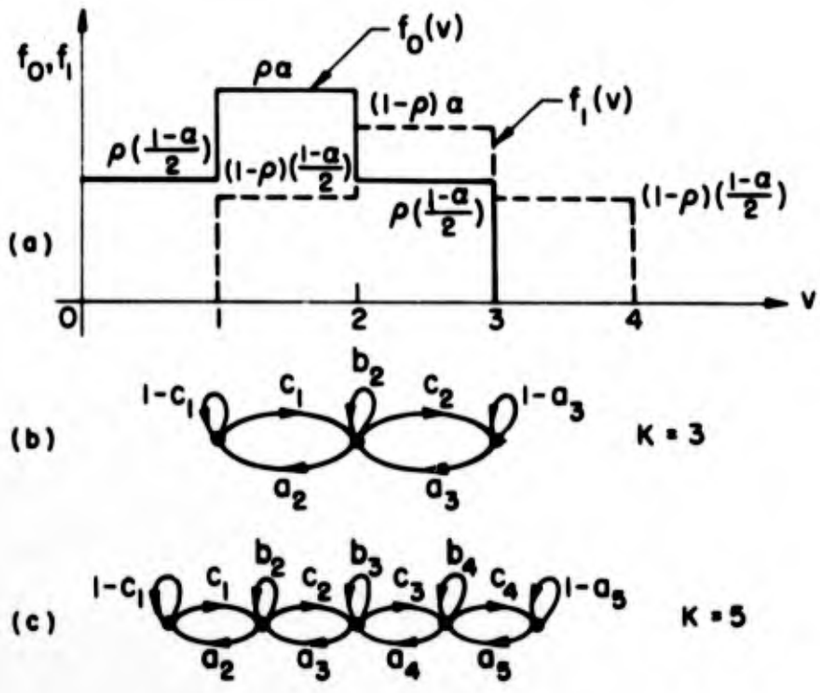

Figure 31. Assumed staircase densities.

We now define the asymptotic success index ζ, which is the probability of correct guess after an infinitely long training phase. The index is formulated as follows: Suppose we train for a very long time; then the probability of being at a particular threshold value when training ends is approximately the steady-state value, which depends on the feedback policy. That is, for each threshold, there is a probability p_{k_i} the $k = k_i$ when training is ended. With $k = k_i$, the probability of correct guess in the working phase is b_i. Hence, ζ is computed as

$$\zeta = \sum_i b_i \, p_{k_i}$$

We illustrate these notions with a numerical example. Let there be five thresholds linked by the chain of Fig. 32. Note that the rightward transition probabilities decrease, and the leftward transition probabilities increase, as the threshold moves from left to right. This monotonic relationship is in keeping with the definitions of the false-alarm and false-rest probabilities.

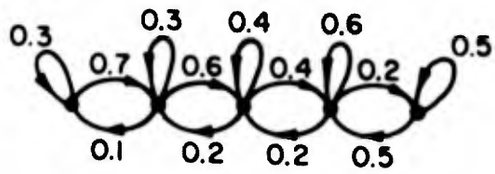

Figure 32. Illustrative 5-state chain.

Figure 33 gives a succession of distributions for the threshold states, assuming (arbitrarily) that the initial threshold is the center one. The steady-state distribution is computed by the methods that we have described earlier. We have

$$p = (.01, \; 0.08, \; 0.24, \; 0.48, \; 0.19)$$

and

$$b = (0.3, \; 0.3, \; 0.4, \; 0.6, \; 0.5)$$

so that

$$\zeta = b \cdot p = 0.506$$

This is superior to 0.42, the probability of correct guess if one (of five) thresholds is picked at random and left unchanged ($p_{random} = 1/5 \sum_i b_i$), but not as good as if the threshold with the largest b were chosen and fixed, in which case the success probability would be: $b_4 = 0.6$. Of course, this last result assumes perfect knowledge of the source and noise statistics, which is unrealistic. We hypothesize a certain form for the statistics of the system only to permit a quantitative comparison of several methods of control, i.e., feedback policies.

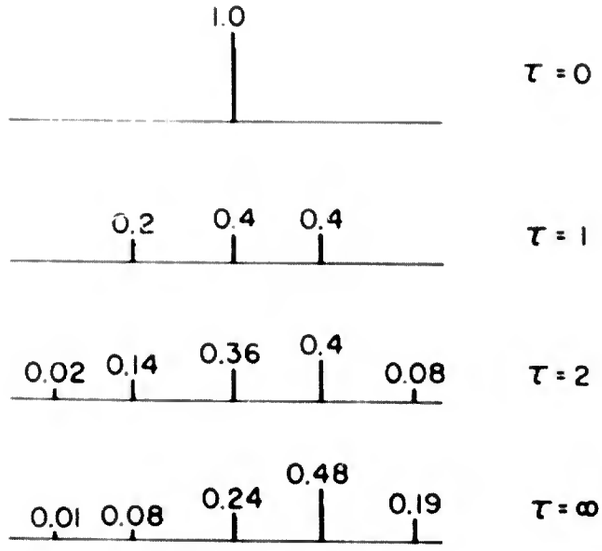

Figure 33. Successive distributions over the thresholds.

For three thresholds (referring now to Fig. 31) the parameters of the chain may be specified as indicated in the first table of Fig. 34. The second table shows the parametric relationships for K = 5. It is a straightforward matter to compute

$$\zeta_3 = \frac{b_1\left(\frac{a_2}{c_1}\right) + b_2 + b_3\left(\frac{c_2}{a_3}\right)}{\left(\frac{a_2}{c_1}\right) + 1 + \left(\frac{c_2}{a_3}\right)}$$

and

$$\zeta_5 = \frac{b_1\left(\frac{a_3}{c_2}\right)\left(\frac{a_2}{c_1}\right) + b_2\left(\frac{a_3}{c_2}\right) + b_3 + b_4\left(\frac{c_3}{a_4}\right) + b_5\left(\frac{c_3}{a_4}\right)\left(\frac{c_4}{a_5}\right)}{\left(\frac{a_3}{c_2}\right)\left(\frac{a_2}{c_1}\right) + \left(\frac{a_3}{c_2}\right) + 1 + \left(\frac{c_3}{a_4}\right) + \left(\frac{c_3}{a_4}\right)\left(\frac{c_4}{a_5}\right)}$$

In Figs. 35 and 36, contours of constant ζ are plotted in the $\alpha\rho$ square ($0 \le \alpha, \rho \le 1$). The shaded area in each case indicates the region for which $\zeta \ge 0.8$. In addition, contours of optimum performance, ζ_M, have been plotted in Fig. 37. The performance ζ_M is optimum in the sense that for a given pair (α, ρ), the threshold value yielding the largest b has been used to compute ζ. That is to say, we may partition the $\alpha\rho$ square into several regions, in each of which a particular threshold value gives highest success probability b. For example, in the 3-threshold system of Fig. 31, k = 1 is "best" when

$$b_1 \ge b_2 \text{ and } b_1 \ge b_3,$$

	1	2	3
a	0	$\frac{1}{2}(1-\rho)(1-\alpha)$	$\frac{(1-\rho)}{2}(1+\alpha)$
b	$1-c_1$	$1-(a_2+c_2)$	$1-a_3$
c	$\frac{\rho}{2}(1+\alpha)$	$\frac{\rho}{2}(1-\alpha)$	0

	1	2	3	4	5
a	0	$\frac{1}{6}(1-\rho)(1-\alpha)$	$\frac{1}{2}(1-\rho)(1-\alpha)$	$(1-\rho)\left(\frac{1-\alpha}{2}+\frac{2}{3}\alpha\right)$	$(1-\rho)\left(\frac{2}{3}+\frac{1}{3}\alpha\right)$
b	$1-c_1$	$1-(a_2+c_2)$	$\frac{1}{2}(1+\alpha)$	$1-(a_4+c_4)$	$1-a_5$
c	$\rho\left(\frac{2}{3}+\frac{1}{3}\alpha\right)$	$\frac{1}{2}\rho(1-\alpha)+\frac{2}{3}\rho\alpha$	$\frac{1}{2}\rho(1-\alpha)$	$\frac{1}{6}\rho(1-\alpha)$	0

Figure 34. Parametric relationships for three and five thresholds.

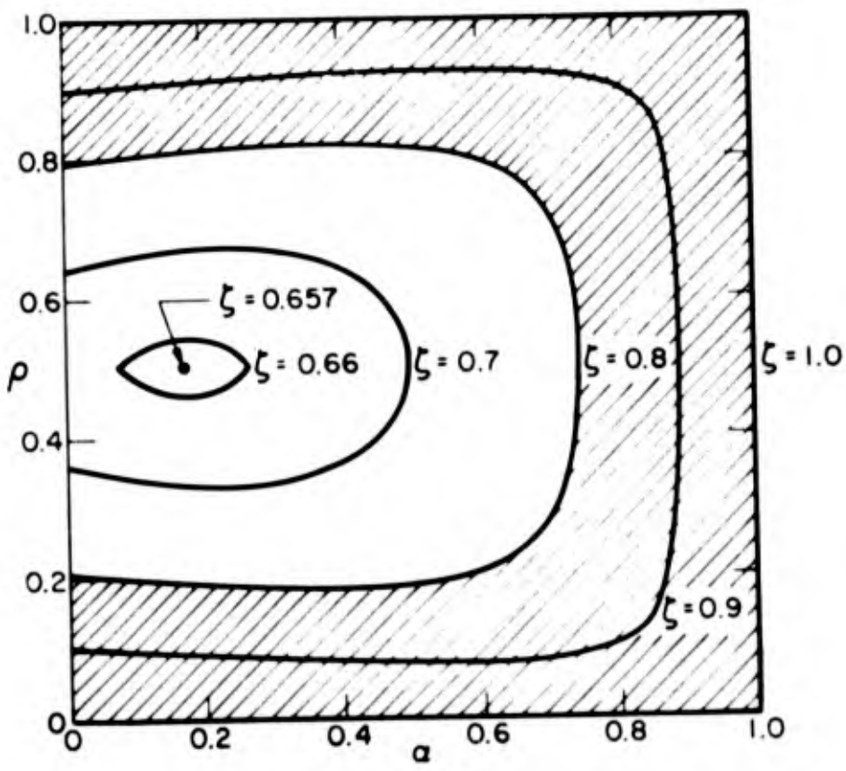

Figure 35. ζ-contours for simple incremental policy, three-threshold case.

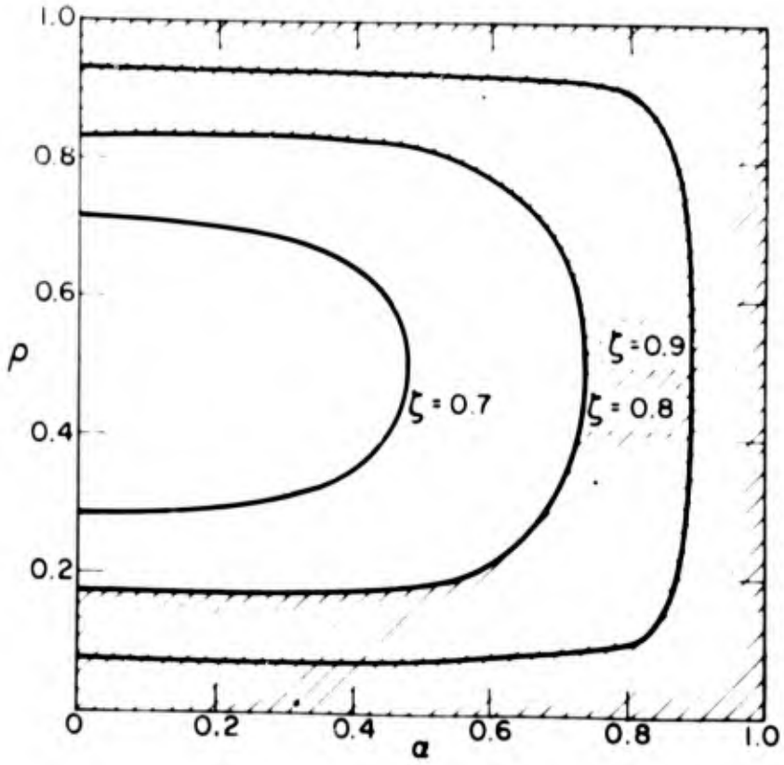

Figure 36. ζ-contours, simple incremental policy, five thresholds.

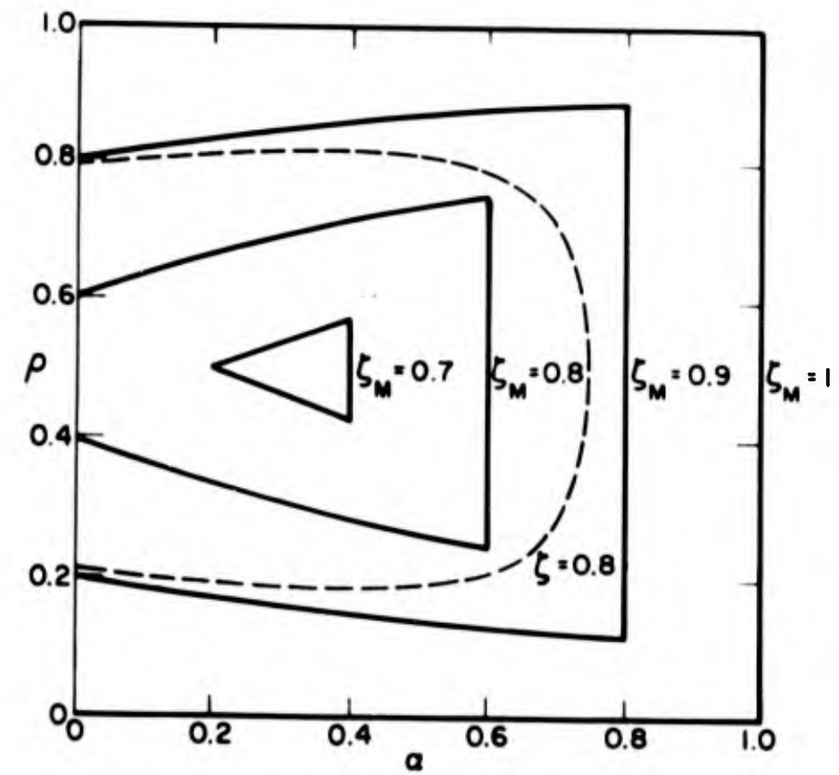

Figure 37. Optimum ζ contours

which implies

$$\rho \leq \min\left(\frac{1}{2}, \frac{1-\alpha}{1+\alpha}\right).$$

Similarly, k = 3 is "best" for

$$\rho \geq \max\left(\frac{1}{2}, \frac{2\alpha}{1+\alpha}\right)$$

and k = 2 gives highest success probability for $(1-\alpha/1+\alpha) \leq \rho \leq \alpha/1+\alpha$. These three regions are sketched in Fig. 38 (the broken-line curve is the contour for $\zeta = 0.8$). Finally, ζ contours for a continuous-threshold TLP have been plotted in Fig. 39. These are the contours of steady-state performance index under the assumption that the available threshold values occupy a continuum on a real-line segment; the partial differential equation which describes this situation is derived in Appendix I. The appendix also contains a discussion of the dynamics of the performance index, as well as the formulation of the expression which yields the contours of Fig. 39.

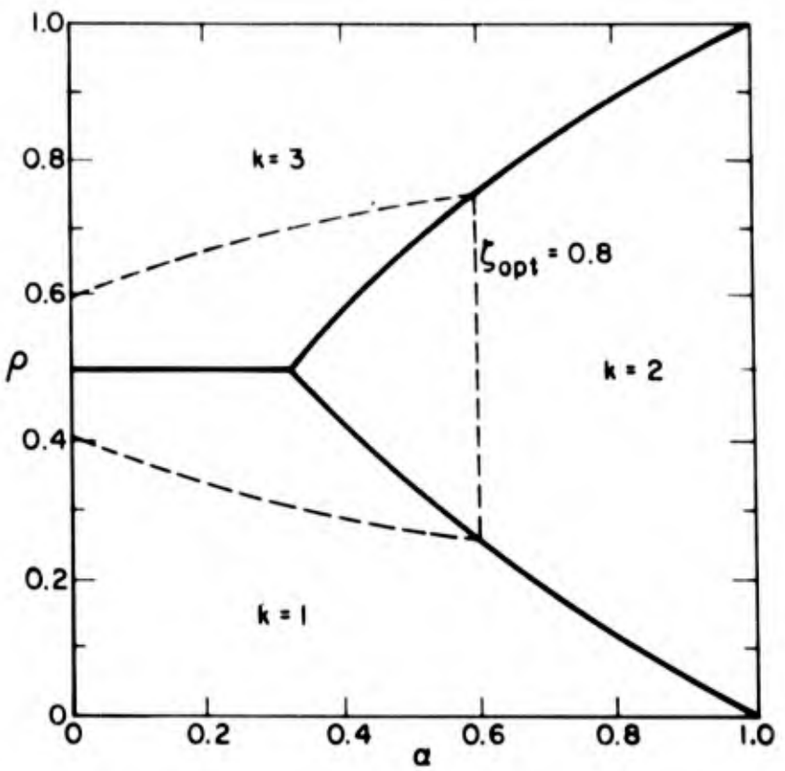

Figure 38. Partition of $\alpha\,\rho$ square into optimized regions.

The contours in Figs. 35 and 36 are almost identical. Hence increasing the number of thresholds from K = 3 to K = 5 has very little effect on the asymptotic performance, no matter what the values of α and ρ may be. This observation lends support to an earlier conjecture on the qualitative significance of the behavior of the three-threshold model [5].

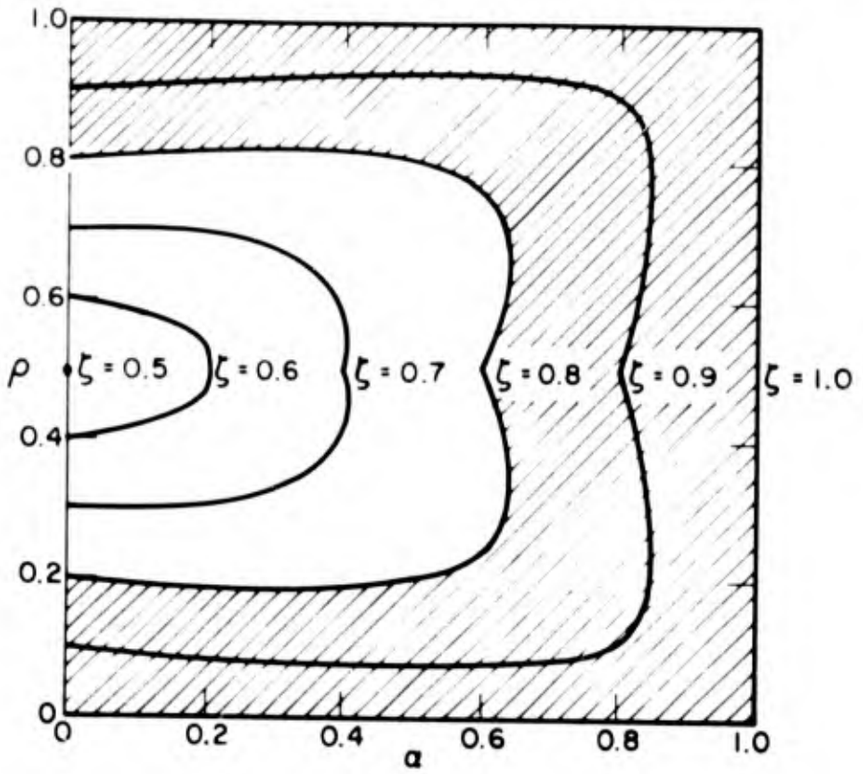

Figure 39. ζ **contours for continuous-threshold, simple incremental policy.**

Figures 35, 36 and 39 suggest that for the staircase distributions which we have assumed, the five-threshold case is a reasonable description (as regards steady-state performance index) of the results for an arbitrary number of thresholds, particularly when $|\rho - 1/2| \geq 1/4$. That is to say, we may rule out the possibility that some particular number of threshold values will give startlingly different results than any other number, particularly when $|\rho - 1/2| \geq 1/4$.

A comparison of Figs. 36 and 39 or of Figs. 36 and 37 shows that the distance of ζ from its optimum value, i.e., $\zeta_M - \zeta$, is significant when $|\rho - 1/2| < 1/4$. This weakness of the simple incremental feedback in Model I [defined by Fig. 31(a)] was also noted in [5]. Consequently, we would like to find a feedback policy that brings ζ closer to the optimum values when $|\rho - 1/2| < 1/4$. Such a policy was found: it consists simply of including inertia or "waiting time" in the laws of motion of the threshold. We shall discuss this policy in the section, "Control Policies with Memory."

Conditionally Random Feedback

The simple incremental feedback policy is probably the simplest "intelligent" training strategy. By way of contrast, we have also investigated a near-chaotic policy (dubbed conditionally random) which operates as follows: Given a successful guess, make no threshold alteration; given an error, move, with equal probability,

to *any* different threshold. Thus, given threshold k, the probability of remaining at this value is b(k), the probability of transition to any other threshold value is $1 - b(k)/K - 1$, where we have K thresholds available (Fig. 40).

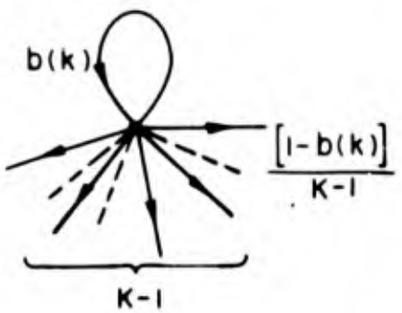

Figure 40. An arbitrary threshold in the model of the conditionally random policy.

For 5 thresholds, one readily derives the following formula for ζ:

$$\zeta = 1 - \frac{5}{\sum_{i=1}^{5} (1-b_i)^{-1}}$$

The resulting ζ-map is shown in Fig. 41. The area of the map for which $\zeta \geq 0.8$ is less than in Fig. 36 (simple incremental, 5-threshold), but not drastically so. This comparison is somewhat misleading; the conditionally random strategy does the "wrong" thing some of the time, but the sparse number of thresholds does not permit a severe deterioration of the performance index. A truer contrast is offered when one considers the infinite threshold case (Appendix II). With infinitely many thresholds to choose from, near-chaos turns into complete chaos, yielding corresponding degradation of the performance index (Fig. 42). (We also observed a reduction in ζ when K was raised from 3 to 5.) A comparison of Figs. 39 and 42 reveals that, as expected, the rational strategy is substantially superior to the random one.

Completely Random Feedback

The most unintelligent feedback policy in a TLP is completely random feedback. This policy consists of a completely random choice of threshold, without regard to the present or past performance of the observer. The value of ζ for such a feedback policy is very easy to compute: it is merely a weighted average of the open-loop success probabilities.

We evaluated the effect of raising the number of thresholds from K = 3 to K = 5 in a TLP with completely random feedback. As expected, the increase in K resulted in a substantial reduction in ζ. A similar reduction in ζ was observed in the case of conditionally random feedback for the same change in K.

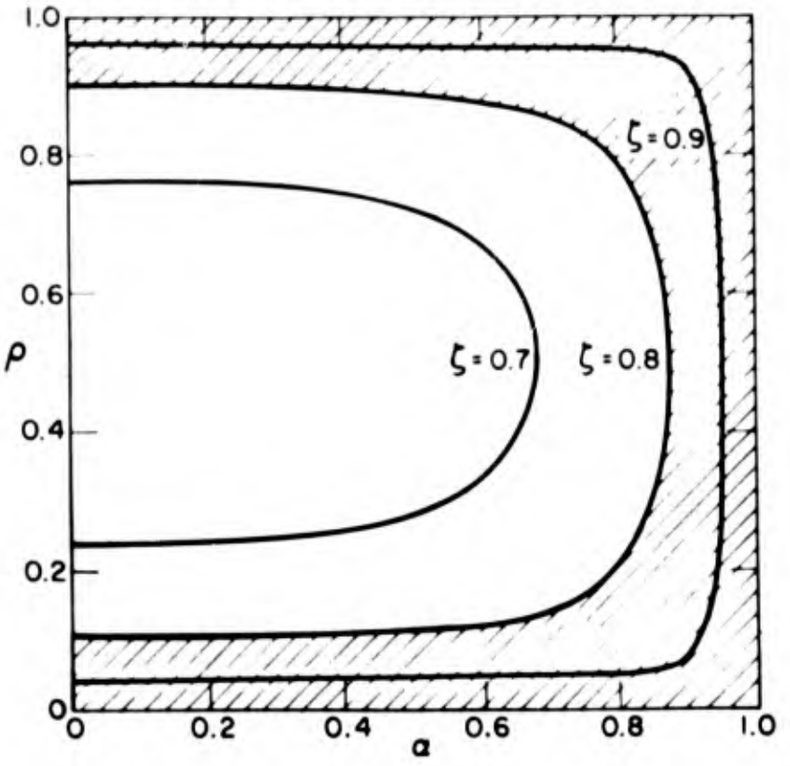

Figure 41. ζ **contours, conditionally random policy,** $K = 5$.

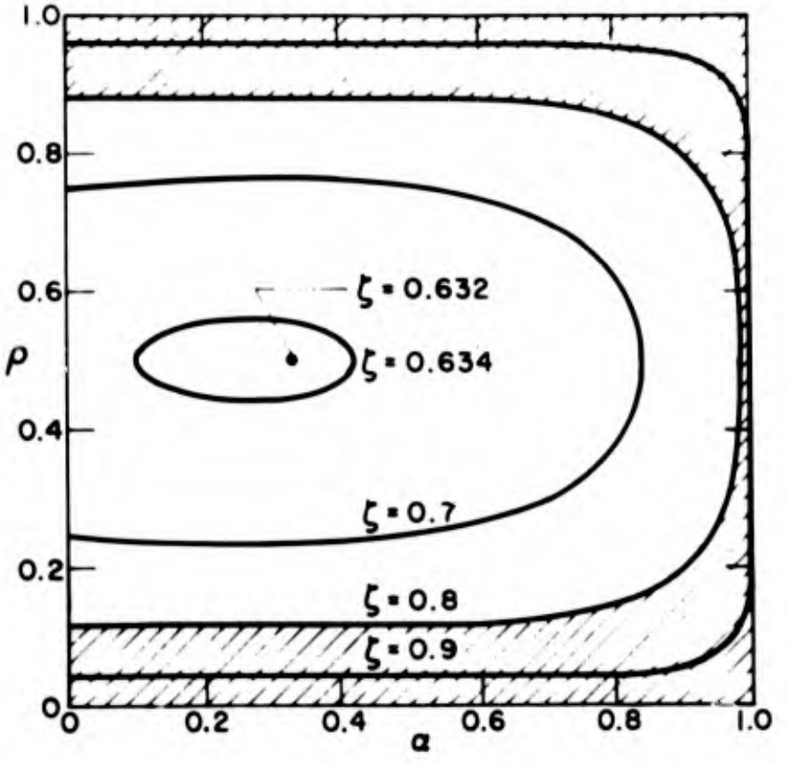

Figure 42. ζ **contours for continuous-threshold conditionally random policy.**

These results show that, regardless of the feedback policy, the choice of the set of thresholds has an important influence on ζ when K is small, but has little influence on ζ when K is large.

Feedback Policies with Memory

The effectiveness of the simple-incremental policy is chiefly limited by its memoryless nature; the impetus for threshold adjustment is provided by the most recent observation, while earlier observations are ignored. The inadequacies of the scheme are analogous to the shortcomings of a simple servomechanism with proportional feedback. In this section we shall examine a number of control policies which have modest memory capacities. The introduction of memory into the feedback policy raises the number of states, M, in the Markov chain model. The simple incremental policy is one of the few policies in which M = K. Even a small amount of memory in the feedback policy causes M to be two or more times as large as K. We will find that feedback policies with memory may be modelled in two ways: By an M-state model, M >> K, having simple delayed-impulse transition densities in the flow graph, or by a K-state model (one state for each threshold) with more complicated transition densities. By reason of its manageability, we will work with the K-state model, where the nature of the state-to-state transition densities will necessitate a slight alteration in our formalism for calculating steady-state probabilities.

The theory in Section II was developed under the mild constraint that:

$$\sum_j p_{ij}(\tau) = h(\tau), \text{ all } i$$

In other words, given that a state has just been initiated, the density governing the time of subsequent transition is the same for all states. The relaxation of this constraint, i.e.,

$$\sum_j p_{ij}(\tau) = h_i(\tau)$$

requires that some of the analytic techniques be altered. In particular, it is now the case that:

$$\bar{\tau}_j = \int_0^\infty \tau\, h_j(\tau)\, d\tau = -\, h_j'(s)\Big|_{s=0} \qquad (3)'$$

and

$$p_j = \frac{\bar{\tau}_j}{\tau_{jj}}$$

$$\frac{-h_k'(s)}{-h_j'(s)} R_k(s)\Big|_{s=0} = \frac{-h_k'(s)}{-h_j'(s)} \frac{F_{jj}'(s)}{F_{kk}'(s)}\Big|_{s=0} = \frac{p_k}{p_j} \tag{28}'$$

and

$$\sum_k \left[\frac{-h_k'(s)}{-h_j'(s)} R_k(s)\Big|_{s=0}\right] = 1/p_j \tag{29}'$$

and finally that

$$p_k = \frac{\dfrac{-h_k'(s)}{-h_j'(s)} R_k(s)\Big|_{s=0}}{\displaystyle\sum_k \left[\frac{-h_k'(s)}{-h_j'(s)} R_k(s)\Big|_{s=0}\right]} \tag{30}'$$

Our analysis of various feedback policies with memory will illustrate the nature of these modified steady-state calculations.

Two-Step Waiting With Parity — We consider a scheme wherein two successive errors of similar type are required before a threshold adjustment is made, with the provision that the first of these errors be preceded by a correct guess. That is, the concatenation of errors of opposite type is a cancelling influence as far as adjustment is concerned.

It will be expedient to denote the feedback policy in question by the kinds of error sequences which result in threshold adjustments. Toward this end, let A represent the occurrence of a false rest, B the occurrence of a correct guess, and C the occurrence of a false alarm. Then "two-step-waiting with parity" means: A threshold adjustment is caused by error sequences which terminate in the endings BAA or BCC, with no subsequence having had either ending. Of course, "left" action is taken on the BAA ending, "right" action on the BCC ending.

Consider, in a set of threshold values, three adjacent values, k_{i-1}, k_i, k_{i+1}. Figure 43(a) shows the Markov chain which links these thresholds under the feedback policy described. As is evident, there is not a one-to-one correspondence between states (nodes) and threshold values. We can bring about such a correspondence, however, by reducing the flow graph to the form in Fig. 43(b) using Mason's

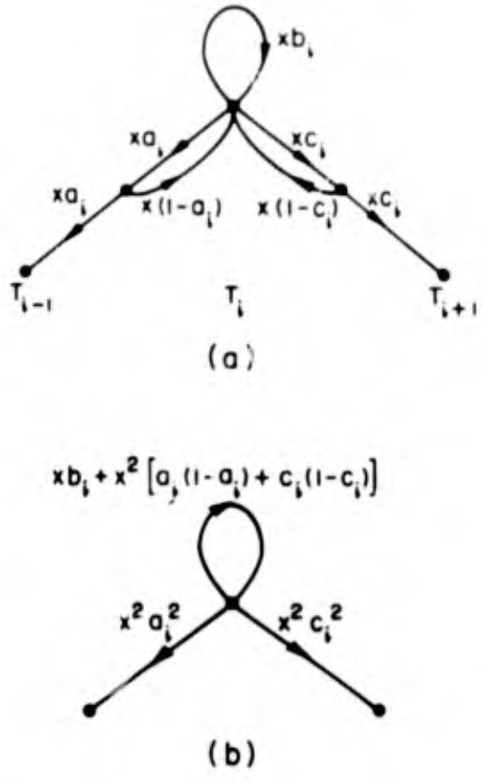

Figure 43. Graph at i^{th} threshold for "two-step waiting with parity" policy.

techniques[6]. The price for achieving this reduction in the number of states is greater complexity in the transition functions and in the "total signal" techniques which we use to obtain the steady-state probabilities. Note that in Fig. 43(a) we have at every node

$$\sum_j p_{ij} = x, \text{ all } i \ (a_i + b_i + c_i = 1)$$

$$= \mathcal{L}[\delta(\tau - 1)]$$

while in Fig. 43(b)

$$h_i = \sum_j p_{ij} = xb_i + x^2(1 - b_i) = \mathcal{L}[b_i \delta(\tau - 1) + (1 - b_i)\delta(\tau - 2)]$$

Of course, it is still the case that

$$h_i(x)\Big|_{x=1} = b_i + 1 - b_i = 1$$

We also note that

$$\bar{\tau}_i = \int_0^\infty \tau h_i(\tau)\, d\tau = h_i'(x)\Big|_{x=1} = 2 - b_i$$

Figure 44 shows the steady-state graph for five thresholds. (By "steady-state graph" we mean a signal flow graph in which the operators x and s have been replaced by 1 and 0, respectively.) The center node has been split in accordance with the total-signal algorithm. Using circumflexes to indicate total signals, we obtain:

$$\hat{x}_1 = \left(\frac{a_2}{c_1}\right)^2 \quad \left(\frac{a_3}{c_2}\right)^2 \qquad \text{(i)}$$

$$\hat{x}_2 = \left(\frac{a_3}{c_2}\right)^2 \qquad \text{(ii)}$$

$$\hat{x}_3 = 1 \qquad \text{(iii)}$$

$$\hat{x}_4 = \left(\frac{c_3}{a_4}\right)^2 \qquad \text{(iv)}$$

$$\hat{x}_5 = \left(\frac{c_3}{a_4}\right)^2 \left(\frac{c_4}{a_5}\right)^2 \qquad \text{(v)}$$

so that

$$p_i = \frac{\left(\frac{2-b_i}{2-b_3}\right)\hat{x}_i}{\sum_{i=1}^{5}\left(\frac{2-b_i}{2-b_3}\right)\hat{x}_i} \qquad i = 1, 2, 3, 4, 5$$

and finally

$$\zeta = \sum_i b_i\, p_i$$

is the usual index of success. The threshold configuration is again that of Fig. 31(c), the second table of Fig. 34 relates the a_i, b_i, c_i to the environmental parameters ρ and α, and Fig. 45 depicts the contours of constant ζ in the $\alpha\rho$-plane. Comparison of this last figure with Fig. 39 indicates that despite the sparse number of adjustment values, the memory capacity of the two-step waiting policy, though minimal,

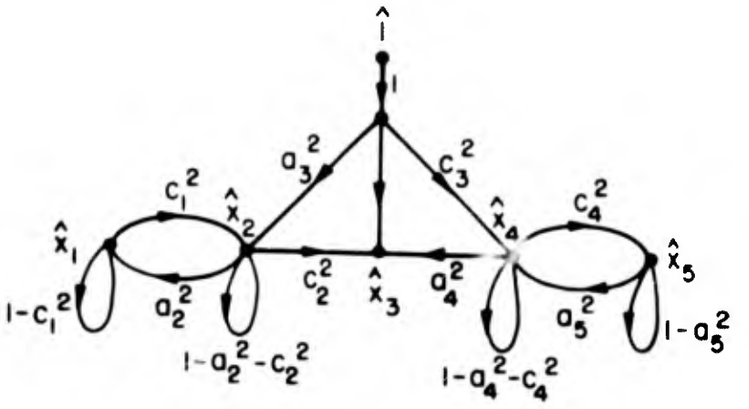

Figure 44. Total signal computation.

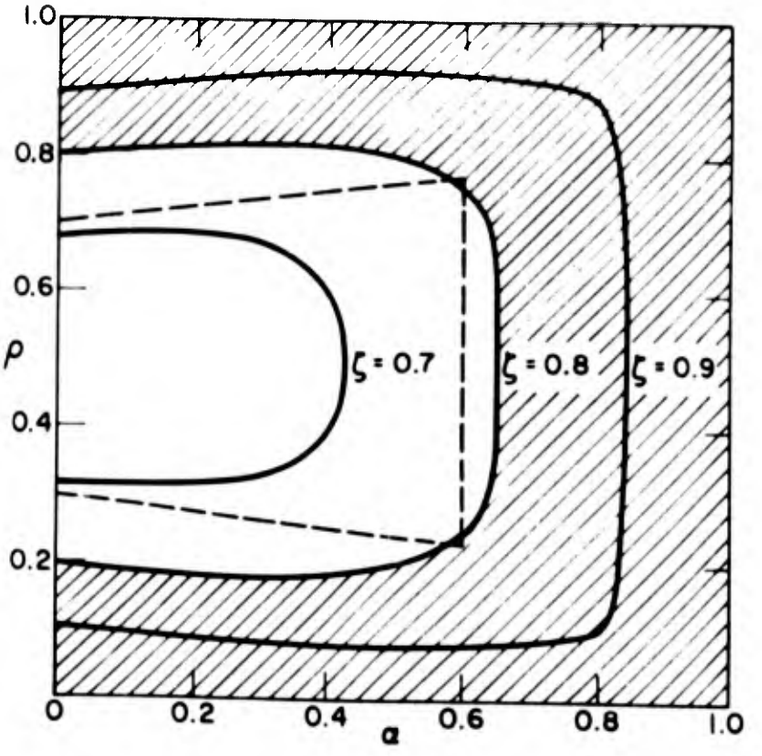

Figure 45. ζ contours, "two-step waiting with parity."

is sufficient to achieve results nearly as good as those obtained in the continuous threshold case with simple incremental feedback. We hasten to point out that this comment pertains to the asymptotic value of performance index; it is obvious that more training time is required of a policy which looks into the past for its control signals. On intuitive grounds, we suspect that as more "inertia" is built into the adjustment routine, more training observations are necessary in order that the system get a good "whiff" of the environment.

APPLICATION OF ASYNCHRONOUS THEORY

Of parallel interest to the quantitative results of our analysis is the fact that our mathematical techniques do not lose their value when faced with complex feedback policies. We are discussing policies wherein one readily constructs a "fine structure" (many states per threshold) model. Computations become very unwieldy in the case of a large number of states. Hence we convert, via signal-flow graph reduction, to a "coarse" model (one state per threshold) and exploit the extended version of the algorithm (page 72) for calculation of the steady-state probabilities. This is the application of asynchronous theory which we spoke of in the introduction; in these "coarse" models, transitions occur at integer values of time, but not at *every* integer; i.e., the spacing between transitions is a random variable.

TWO-STEP WAITING

In terms of the events A, B, C defined in the preceding section, the two-step waiting policy is defined as follows: "left" adjustment is made on AA, "right" adjustment on CC. Figure 46(a) shows the M-state model for the i^{th} threshold, Fig. 46(b) the K-state model for the i^{th} threshold, where

$$A_i(x) = (a_i x + a_i c_i x^2)\, a_i x \,/(1 - a_i c_i x^2)$$

$$B_i(x) = b_i x \left(\frac{1 + [a_i x(1 + c_i x) + c_i x(1 + a_i x)]}{1 - a_i c_i x^2} \right)$$

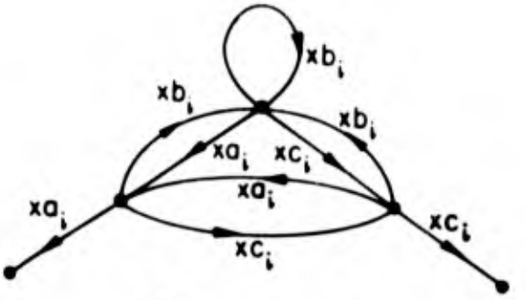

(a) Fine Structure

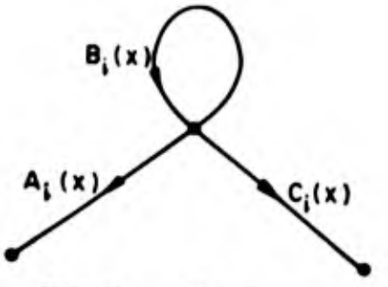

(b) "Coarse" Equivalent

Figure 46. Graph at i^{th} threshold, two-step waiting policy.

$$C_i(x) = (c_i x + a_i c_i x^2)\, c_i x \,/(1 - a_i c_i x^2)$$

$$h_i(x) = A_i(x) + B_i(x) + C_i(x)$$

$$h_i'(x)\Big|_{x=1} = (1 + a_i + c_i + a_i c_i)\,/(1 - a_i c_i)$$

We note that a completed version of Fig. 46(b) would be the same as Fig. 31(c), except for nomenclature. In fact, either will serve as the generic form for all feedback policies wherein: (a) five thresholds are available, and (b) threshold values are incremented in single increments, i.e., one to the "left", or one to the "right". The particular way in which the feedback policy manifests itself depends on the nature of the transition densities. As a result, we can produce a general formula for those situations satisfying (a) and (b) above, to wit:

$$\zeta = \frac{\sum_{i=1}^{5} b_i \dfrac{h_i'(1)}{h_3'(1)} \hat{x}_i}{\sum_{i=1}^{5} \dfrac{h_i'(1)}{h_3'(1)} \hat{x}_i}$$

where $h_i'(1) \equiv h_i'(x)\big|_{x=1}$, and the $\hat{x}$ are given by expressions (i) - (v) (p. 74), except that $A_i(1)$ replaces $(a_i)^2$ and $C_i(1)$ replaces $(c_i)^2$. This unifying form of ζ is particularly suited to digital computer calculation of the ζ contours. That is, one simply specifies the A_i, C_i, and h_i by the appropriate (for the feedback policy) functions of a_i, b_i, and c_i, which are, in turn, appropriate functions of environmental parameters (in our case, ρ and α), and lets the computer "grind out" the ζ contours. In fact, this is precisely the scheme that we have used.

Having developed some "formal machinery" with which to describe various policies and their representative parameters in the Markov model, we can streamline the discussion of other feedback policies. Consider, for example, the "two-out-of-three" feedback policy, defined as follows: "Left" (right) action is taken on error sequences ending in A (C), such that one of the preceding 2 errors was also on A (C), no earlier sequence having had such a triplet as an ending. The M-state Markov model is shown in Fig. 47, and one can derive (albeit tediously):*

$$(\cdot)^* = (1 - (\cdot))^{-1}$$

$$E_1(a, b, c) = [a(cba)^* + c(abc)^*\, ba(cba)^*]$$

$$E_2(a, b, c) = [bc(abc)^*\, ba(cba)^*]^*$$

$$A(a, b, c) = \left[E_1(a, b, c)\right]\left[E_2(a, b, c)\right](a + ba + ca) + \left[E_1(c, b, a)\right]\left[E_2(c, b, a)\right](a^2 + aba)$$

*The index i has been dropped for convenience.

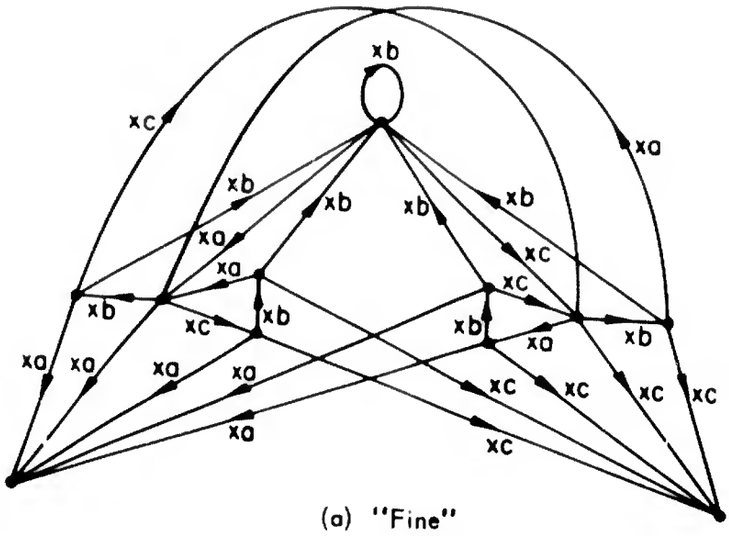

(a) "Fine"

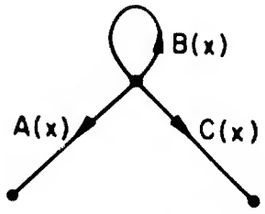

(b) "Coarse"

Figure 47. Two-out-of-three waiting.

$$C(a, b, c) = A(c, b, a)$$

$$B(a, b, c) = b + (b^2 + cb)\left[E_1(a, b, c)\right]\left[E_2(a, b, c)\right] + (b^2 + ab)\left[E_1(c, b, a)\right]\left[E_2(c, b, a)\right]$$

$$h'(1) = 1 + \left[a + (abc)(abc)^*\right]\left[abc + ab^2c\right] * (1 + b)(1 + c) + \left[c + (cba)(cba)^*\right]\left[cba + cb^2a\right] * (1 + b)(1 + a)$$

The expression for h' (1) was not obtained by summing A, B, and C, differentiating, and then setting x = 1. Rather, we made expeditious use of the total signal concept (again). After all, the h(x) of a "K-state" graph is nothing more than a particular source-to-sink transmission in the "M-state" graph. This transmission is thus the transform of a first-occurrence probability [h (1) = 1]; the mean of this probability is $h'(x)\big|_{x=1}$ and may be found by Sittler's method. We illustrate this simplification by computing $h'(x)\big|_{x=1}$ for the two-step waiting policy. Figure 48 shows the signal interpretation of h(x), first in the K-state model, then in the M-state model. The

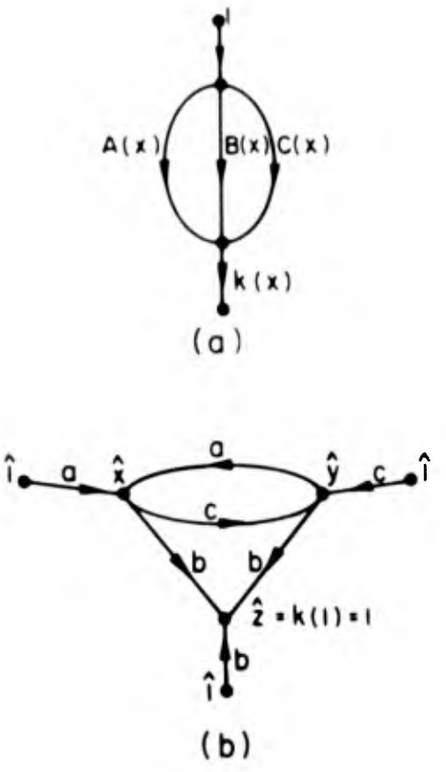

Figure 48. Computation of h '(1) for two-step waiting policy.

total signal driving the graph is 1; the total signal collected at the sink is 1. By Eq. (26) [Section II], the sum over the nodes of the total signals is simply h' (1), since $\bar{\tau}$, the mean time between transitions, is unity in the M-state graph. Hence

$$\hat{x} = a + a\hat{y}$$

$$\hat{y} = c + c\hat{x}$$

$$\hat{x} = (a + ac)(1 - ac)$$

$$\hat{y} = (c + ac)/(1 - ac)$$

$$h'(1) = 1 + \hat{x} + \hat{y} = (1 - ac + a + c + 2ac)/(1 - ac)$$

$$= (1 + a + c + ac)/(1 - ac)$$

IV. SUMMARY AND CONCLUSIONS

Two areas of accomplishment are reported:

1. The development of a body of mathematical techniques, with emphasis on signal-flow analysis, strengthens our ability to understand and analyze the dynamic behavior of synchronous and asynchronous Markov chains.

2. The application of these techniques to a study of Markov chain models of adaptive processes enhances our understanding of the relation between adaptation and feedback.

The details are summarized below.

ASYNCHRONOUS MARKOV CHAINS

Some adaptive processes are conveniently represented by "asynchronous" Markov chains, i.e., Markov chains whose state transitions occur randomly rather than periodically. We have shown how signal flow techniques, with their convenience and intuitive appeal, can be applied to the analysis of asynchronous Markov chains.

The basic reason for the feasibility of signal-flow analysis to Markov chains is the fact that the Laplace transform, $P_{ij}(s)$, of the probability transition density, $p_{ij}(\tau)$, behaves exactly as a signal in a flow graph of a linear system.

ASYMPTOTIC ANALYSIS

In most Markov chain models of adaptive processes the success probability $z(n)$ is related to the vector of state probabilities $\underline{p} = \{ p_i(n) \}$ by the inner product

$$z(n) = \underline{b} \cdot \underline{p}(n), \tag{76}$$

where $\underline{b}$ is a vector of nonnegative elements at least one of which is positive. Consequently, the computation of state probabilities is an important subgoal in the analysis of Markov chain models of adaptive processes. It turns out that the asymptotic values of these probabilities are particularly easy to compute.

Starting from the earlier work of Sittler [1], we developed a technique for computing the entire set of asymptotic state probabilities of a Markov chain with a minimum of computational labor. The technique eliminates the need for finding the roots of the characteristic equation of the Markov chain. We then extended the technique to cover asynchronous Markov chains.

The method in brief goes as follows. First find a Markov chain model of the adaptive process. This Markov chain may be synchronous or asynchronous. Then express the success probability $z(n)$ by a formula of the form of Eq. (76). If $\underline{b}$ contains any zero-valued elements, then the corresponding states of the Markov chain

may be eliminated by flow-graph reduction. Reduce the flow graph of the Markov chain so that only the states corresponding to the nonzero values of $\underline{b}$ are in the reduced graph. The reduced graph will generally represent an asynchronous chain, even if the original graph represented a synchronous chain.

Now find the expression for the sum $h_i(s)$ of the impulsive-response signals emanating from each node of the reduced flow graph:

$$h_i(s) = \sum_j P_{ij}(s)$$

Then split one of the nodes, say node j, into a source and sink. Let d_i be the negative of the first derivative of $h_i(s)$ at $s = 0$. Apply a unit signal to the source. Let r_k be the response to this signal at each node. Let q_j be

$$q_j \triangleq \sum_m \left(\frac{d_m r_m}{d_j} \right)$$

Then, by Eq. (30) the asymptotic state probability at node k is

$$p_k = \frac{d_k}{d_j} \frac{r_k}{q_j} \tag{77}$$

The value computed for p_k is, of course, independent of the choice of the split node j.

Observe in Eq. (77) that only d_k and r_k need be computed for each node. The quantities d_j and q_j are used for every p_k. In many cases, d_k is independent of k. For synchronous chains, in particular, $d_k = 1$ for every k.

This technique proved to be particularly useful in our analysis of the asymptotic effects of nonzero-memory feedback in five-threshold TLPs.

STATIONARITY AND REVERSIBILITY

We applied our techniques for analyzing asynchronous Markov chains not only to advancing a computational technique (specifically, the computation of asymptotic probabilities), but also to advancing our understanding of stationary asynchronous chains and, in particular, reversible stationary asynchronous chains.

Stationary asynchronous chains are chains whose "untied" transition probabilities $\hat{\alpha}_{ij}(t)$ satisfy the Chapman-Kolmogorov equation:

$$\hat{\alpha}_{ij}(t + \tau) = \sum_k \hat{\alpha}_{ik}(t) \hat{\alpha}_{kj}(\tau) \tag{78}$$

where $\hat{\alpha}_{ij}(t)$ is the probability that the process will occupy state j at time t, given that the process occupied state i at time 0. We found that the "untied" node sums, $\hat{h}_i(t)$, must lie within the following exponential bounds:

$$\text{Max}\left[0, \lambda\left(e^{-\lambda bt} - a\right)\right] < \hat{h}(t) < \lambda e^{-\lambda bt} \tag{79}$$

where

$$\lambda \triangleq -\frac{1}{h'(s)\Big|_{s=0}} \tag{80}$$

$$a \triangleq \text{Min}\left[P_{jj}(s)\Big|_{s=0}\right] \tag{81}$$

$$b \triangleq 1 - a \tag{82}$$

$$\hat{h}(\tau) \triangleq \lambda \int_0^{\tau} \left[\delta(t) - h(t)\right] dt \tag{83}$$

[Equation (83) is derived from Eq. (37).]

A Markov chain is reversible if and only if its transition probabilities $p_{ij}(\tau)$ and its asymptotic state probabilities p_i satisfy

$$p_i\, p_{ij}(\tau) = p_j\, p_{ji}(\tau). \tag{84}$$

We found that if an asynchronous chain is both reversible and stationary, then the following constraint must be satisfied:

$$\frac{1}{p_j}\sum_i p_i\, p_{ij}(\tau) = \sum_j p_{ij}(\tau). \tag{85}$$

We applied signal flow techniques to the study of Markov chain models of two types of adaptive processes incorporating simple forms of feedback: adaptive random walks and threshold learning processes. The goal of this study was to gain an insight into the ability of various forms of feedback to mask unpredicted environmental fluctuations and unforeseen failures of machine parts.

ADAPTIVE RANDOM WALK

We found in a simple adaptive random walk that feedback can raise the expected asymptotic performance of the process even though our ignorance of the open-loop parameters may encompass a large portion of the entire parameter space.

We found furthermore, that two feedback policies were not significantly different in their ability to overcome ignorance or environmental fluctuations. I.e., the two feedback policies yielded similar adaption characteristics. This is an indication that the adaptation characteristics of the random walk is to a certain degree insensitive to the choice of feedback policy.

THRESHOLD LEARNING PROCESSES (TLPs)

Because the number of meaningful feedback policies in three-threshold TLPs is severely limited, the effects of several feedback policies in five-threshold TLPs and continuous-threshold TLPs were studied. The emphasis of this study was on the effects of the various policies on asymptotic performance. The dynamic performance of continuous-threshold TLPs was also studied.

The following feedback policies were considered:

1. Simple incremental feedback: The threshold is moved up or down one increment in response to a false alarm or false rest, respectively; the threshold remains fixed if no error is incurred or if a boundary threshold prevents a desired adjustment.

2. Completely random feedback: each new threshold is chosen at random without regard to the observer's past or present performance.

3. Conditionally random feedback: if the observer's present guess is correct, the next threshold is the same as the present threshold; if the observer's guess is wrong, the next threshold is chosen at random.

4. Two-step waiting: if two false rests or two false alarms occur successively, the next threshold is one notch higher or lower than the present threshold, depending on whether two false rests or two false alarms occurred. Otherwise, the threshold remains unchanged.

5. Two-out-of-three waiting: if two false rests or two false alarms occur in the last three trials, the threshold is moved one notch up or down, depending on whether the two significant errors were false rests or false alarms. Otherwise, the threshold remains unchanged.

In all cases the open-loop TLP has constituent densities of the form shown in Fig. 31. In the case of the five-threshold TLPs, the values of the thresholds are spaced so as to divide the interval [0,4] into six equal parts. In the case of the continuous-threshold TLP, the thresholds occupy the entire real axis.

The following effects of the various feedback policies were observed:

1. Raising the number of thresholds, K, from three to five incurs a significant reduction in the asymptotic success probability, ζ, for both the conditionally random and the completely random feedback policies. Furthermore, raising K from 5 to ∞ incurs another significant reduction in ζ for the conditionally random feedback policy.

These results indicate that regardless of the feedback policy, the choice of the set of thresholds has an important effect on ζ when K is small, but has little influence on ζ when K is large. We still have not found, however, the size of K at which the effect on ζ changes from significant to insignificant.

2. The ζ contours of the five threshold TLP with simple incremental feedback are close to the ζ contours of the continuous-threshold TLP with simple incremental feedback, particularly when $|\rho - 1/2| > 1/4$. Furthermore, the ζ contours of the five-threshold TLP with simple incremental feedback were almost identical to those of a three-threshold TLP with simple incremental feedback. These results lend support to an earlier conjecture that gross qualitative properties of the learning waves of TLPs are insensitive to the number of thresholds [5].

3. In an earlier report we noted that with simple incremental feedback in Model I, the distance of ζ from its optimum value is significant. At that time we suggested that a new feedback policy be sought. In the present study we found that the inclusion of two-step waiting in the feedback policy brings the ζ of Model I close to the ζ contours of a continuous-threshold TLP with simple incremental feedback. In the latter contours, the performance degradation induced by threshold quantization is eliminated, and is close to the optimum contours when $|\rho - 1/2| > 1/4$. Hence, two-step waiting provides the performance improvement requested in the earlier report.

DYNAMIC BEHAVIOR

Because of mathematical convenience our analysis of dynamic behavior of adaptive processes was restricted to continuous-threshold TLPs. Two feedback policies in these TLPs were considered: simple incremental feedback and conditionally random feedback. The detailed analysis is given in Appendices I and II.

1. Simple Incremental Feedback in Continuous-Threshold TLPs

If the two constituent densities each have just a single peak - as is usually the case - then the learning wave z(t) must take on one of the following three forms: a) monotonic increasing, b) monotonic decreasing, or c) single peak. We found simple conditions under which z(t) takes on each of these forms.

If z(t) has a peak, then a) its settling time is shorter than the learning time z(t) would have if z(t) were monotonic (assuming the constituent densities and the initial threshold to be the same in both cases); and b) no single eigenfunction dominates z(t). But if z(t) has no peak, it is monotonic; hence, we may assume that z(t) is dominated by a single eigenfunction. This explains why ν, the learning time (or "settling time") of the dominating eigenfunction, is a good approximation of $\hat{N}$, the peak learning time of z(t) [5].

2. Conditionally Random Feedback in Continuous-Threshold TLPs

We obtained a closed-form expression for the x-transform of the learning wave of the continuous-threshold TLP with conditionally random feedback. We proved that the learning wave of this TLP can have only one of the following three forms, depending on the size of the initial threshold: a) monotonic increasing, b) monotonic decreasing, or c) single valley. We found simple conditions under which these three forms occur. In all three cases, the performance waves approach an asymptotic value ζ that is independent of the initial threshold. An integral expression for ζ was derived.

BLANK PAGE

APPENDIX I

CONTINUOUS TLP WITH SIMPLE INCREMENTAL FEEDBACK

DERIVATION

We give below a somewhat intuitive derivation of the partial differential equation which implicitly describes the probabilistic dynamics of simple incremental feedback when infinitely many thresholds are available. (The problem has already been treated by Kac, [8] although in a rather more abstract way.) We subsequently use the solution of the equation to obtain the performance index ζ, and finally arrive at the $\alpha\rho$ map of Fig. 39.

Refer to Fig. 49. Threshold values are distributed uniformly along the x-axis, separated by a distance of $2\Delta x$. Recall (Sec. III) that

$$a(x) = \int_{-\infty}^{x} f_1(u)\, du$$

$$c(x) = \int_{x}^{\infty} f_0(u)\, du$$

where f_0 and f_1 are the constituent densities of Sec. III. Let $X(\tau)$ be a continuous random variable (the threshold value at time τ) implicitly defining the density $p(x, \tau)$ by:

$$\Pr[X(\tau) < x] = \int_{-\infty}^{x} p(\xi, \tau)\, d\xi \tag{86}$$

Then

$$\begin{aligned} \Pr[X(\tau) < x] = {} & \Pr[X(\tau - \Delta\tau) = x + \Delta x] \cdot a(x + \Delta x) \\ & + \Pr[X(\tau - \Delta\tau) < x] \\ & - \Pr[X(\tau - \Delta\tau) = x - \Delta x] \cdot c(x - \Delta x) \end{aligned} \tag{87}$$

and

$$\Pr[X(\tau) < x] - \Pr[X(\tau - \Delta\tau) < x] = \int_{-\infty}^{x} [p(\xi, \tau) - p(\xi, \tau - \Delta\tau)]\, d\xi \tag{88}$$

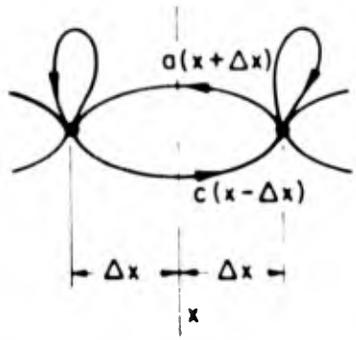

Figure 49. Threshold chain along x-axis.

so that

$$\int_{-\infty}^{x} \left[p(\xi, \tau) - p(\xi, \tau) + \frac{\partial \rho}{\partial \tau} \Delta \tau \right] d\xi$$

$$= p(x, \tau) \Delta x \, a(x) - p(x, \tau) \Delta x \, c(x)$$

I. e.,

$$\left[\int_{-\infty}^{x} \frac{\partial p}{\partial \tau} d\xi \right] \Delta \tau = -p(x, \tau) \, h(x) \Delta x \tag{89}$$

where

$$h(x) \stackrel{\Delta}{=} c(x) - a(x)$$

Some care must be exercised in taking Eq. (89) to the limit. If $\Delta x \to 0$ faster than $\Delta \tau$, then the threshold value will never change. On the other hand, if the rate of transition is increased too rapidly in comparison with the inter-threshold distance, the process will "run away". This is simply to say that Δx and $\Delta \tau$ must approach zero in a proportionate way in order that non-trivial results may obtain. We take the proportionality constant as unity in our treatment. Thus, we seek a solution $p(x, \tau)$ of the system

$$\frac{\partial p}{\partial \tau} = -\frac{\partial}{\partial x} (p(x, \tau) \, h(x))$$

$$p(x, 0) = \delta(x - x_0) \tag{90}$$

This last is obtained by differentiating the limiting form of (89) with respect to x. The initial condition is a statement of the fact that

$$\Pr [X(0) < x] = 0 \qquad x < x_0$$

$$\Pr [X(0) < x] = 1 \qquad x > x_0$$

where x_0 is the (arbitrary) initial threshold value.

There are a number of ways to solve Eq. (90), none particularly satisfying. A plausible approach, based on considerable hindsight, is as follows:

$$\frac{1}{h(x)} \frac{\partial(ph)}{\partial \tau} = - \frac{\partial}{\partial x} (ph) \tag{91}$$

With

$$w(x, \tau) = p(x, \tau)\, h(x),$$

we have

$$\frac{\partial w}{\partial \tau} = - h(x) \frac{\partial w}{\partial x} \tag{92}$$

Assume that:

$$w(x, \tau) = w(\tau - F(x)), \quad F(x) \text{ to be determined.}$$

Then

$$w'(\tau - F) = h(x)\ F'(x)\ w'[\tau - F(x)]$$

i.e.

$$F'(x) = 1/h(x)$$

$$F(x) = \int_{x_0}^{x} \frac{d\xi}{h(\xi)} \qquad x_0 \le x \le \bar{x}$$

where $\bar{x}$ is the solution of

$$h(\bar{x}) = 0$$

And so

$$p(x, 0) = \delta(x - x_0) = \frac{w[-F(x)]}{h(x)}$$

The initial condition is satisfied if w is a δ-function of the argument $\tau - F(x)$, i.e.

$$p(x, \tau) = \frac{\delta\left(\tau - \int_{x_0}^{x} \frac{d\xi}{h(\xi)}\right)}{h(x)} \tag{93}$$

We gather from Eq. (93) that the continuous-threshold process is deterministic; the density governing the threshold probabilities is a traveling "spike". That is, at time τ, the threshold value is that x for which $\tau = \int_{x_0}^{x} \frac{d\xi}{h(\xi)}$. The velocity at which the "spike" travels is not uniform, but is a function of x. In particular

$$\frac{d}{d\tau}\,(\tau - F(x)) = 0 = 1 - F'(x)\,\frac{dx}{d\tau}$$

$$v(x) = \frac{dx}{d\tau} = \frac{1}{F'(x)} = h(x) \tag{94}$$

so that the velocity of the "spike" is initially $h(x_0)$, and diminishes to zero as x approaches $\bar{x}$ (Fig. 50 is helpful; if $x_0 > \bar{x}$, v(x) is negative and the impulse travels to the left.) Thus, $\bar{x}$ is the steady-state threshold value. At $x = \bar{x}$, the false-alarm and false-rest probabilities are equal, but the probability of error $(1 - b(\bar{x}))$ is not necessarily a minimum. In [8] Kac asks if a human observer, when coping with the one-dimensional pattern recognition situation, will cause his threshold to gravitate toward $\bar{x}$, rather than that value of x for which b(x) is maximum.

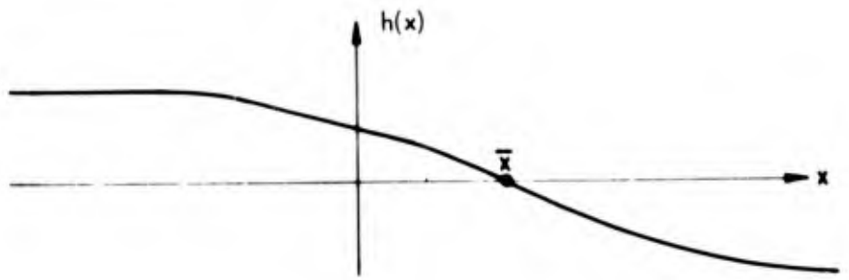

Figure 50. Typical form for h(x).

DYNAMIC BEHAVIOR

With $p(x,\tau)$ given by Eq. (93), it is a relatively direct matter to compute ζ, the steady-state performance index. In fact, we can set forth some additional qualitative information regarding the monotonicity of performance index as a function of time. Let

$$z(\tau) = \int_{-\infty}^{\infty} p(x,\tau)\, b(x)\, dx \tag{95}$$

$$z(0) = b(x_0);\ z(\tau) \longrightarrow \zeta \quad (\tau \to \infty)$$

Now

$$z(\tau) = \int_{-\infty}^{\infty} \frac{\delta(\tau - F(x))}{h(x)}\, b(x)\, dx$$

and we recall that

$$F'(x) = 1/h(x)$$

so that

$$z(\tau) = \int_{-\infty}^{\infty} \delta(\tau - F)\, b[x(F)]\, dF$$

$$= b[x(\tau)]$$

$$\zeta = b(\bar{x})$$

Figure 51 shows a typical form for b(x). Along the x-axis, to the right of x_0, we have marked points which represent successive time instants, the intervals, in time, being uniform. The associated intervals in x diminish (from left to right), however, since Eq. (94) indicates that

$$\Delta x = h(x)\,\Delta\tau$$

and h(x) decreases (Figure 50) as x moves from x_0 to $\bar{x}$. (All arguments predicated on $x_0 < \bar{x}$ are readily modified when $\bar{x} < x_0$). Successive values are $z(\tau)$ are shown on the ordinate axis. The question of monotonicity of $z(\tau)$ is then decided by whether or not $\bar{x}$ is to the right of $\hat{x}$, where $b(\hat{x})$ is the maximum value of b(x). In more generality, if $\hat{x}$ lies between x_0 and $\bar{x}$, $z(\tau)$ has a single peak. If $\bar{x}$ lies between x_0 and $\hat{x}$, $z(\tau)$ rises monotonically to its steady-state value, and if x_0 lies between $\bar{x}$ and $\hat{x}$, z decreases monotonically to steady-state. (Remember that $\bar{x}$ and $\hat{x}$ are determined by the densities f_0 and f_1; x_0 is arbitrary.)

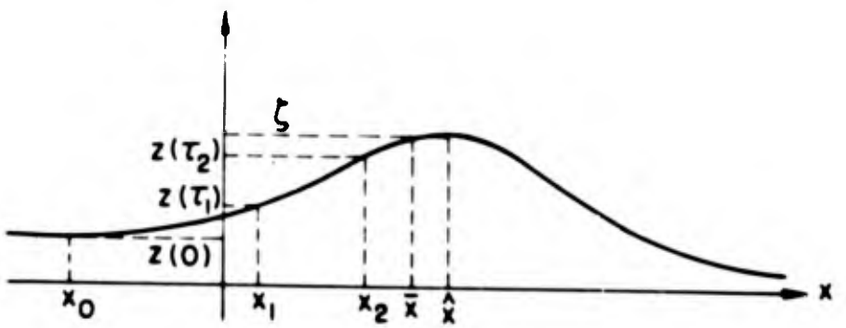

Figure 51. Typical form of b(x); successive values of z(n) plotted on ordinate axis.

Given that $\zeta = b(\bar{x})$, and the densities of Fig. 31(a), we first compute $x(\rho, \alpha)$, and finally, $\zeta(\rho, \alpha) = b(\bar{x}(\rho, \alpha))$. It is apparent that $\bar{x}$ cannot be in the intervals (0, 1) or (3, 4). In the first of these, the "false-rest" probability is zero, while ($\rho \neq 0$) the "false-alarm" probability is not. In the interval (3, 4), the converse holds, so that $\bar{x}$ may exist only in (1, 2) or (2, 3) depending on the values of ρ and α. We find, in fact that $\bar{x} \in (1, 2)$ for $\rho \leq 1/2$ and

$$\bar{x} = 1 + \frac{\rho\,(1+\alpha)}{(1-\alpha)\,(1-\rho) + 2\rho\alpha}$$

while for $\rho \geq 1/2$, $\bar{x} \in (2, 3)$, and

$$\bar{x} = 1 + \frac{(1-\alpha)\ (2\rho - 1)}{\rho\ (1-\alpha) + 2\alpha\ (1-\rho)}$$

Finally, with $b(\bar{x})$ given by

$$b(\bar{x}) = 1 - 2 \int_{\infty}^{\bar{x}} f_1(\xi)\, d\xi = 1 - 2 \int_{\bar{x}}^{\infty} f_0(\xi)\, d\xi$$

we obtain

$$\zeta = 1 - \frac{\rho\,(1-\rho)\ (1+\alpha)\ (1-\alpha)}{(1-\alpha)\ (1-\rho) + 2\rho\alpha}, \quad \rho \leq 1/2$$

$$= 1 - \frac{\rho\ (1-\rho)\ (1+\alpha)\ (1-\alpha)}{(1-\alpha)\rho + 2\ (1-\rho)\,\alpha}, \quad \rho \geq 1/2$$

which formulas are the source of Fig. 39.

APPENDIX II

CONTINUOUS TLP WITH CONDITIONALLY RANDOM FEEDBACK

DERIVATION

We wish to carry the feedback policy of Section 3.4 to the limit of zero threshold separation. We have a different problem than that presented by the simple incremental policy, where it was necessary that the product of transition rate and inter-threshold interval remain constant in the limit. In the conditionally random case, every threshold can "communicate" with every other; as the distance between thresholds is diminished the transition rate remains constant. There results, as we will show, a difference equation with variable coefficients, in contrast with the partial differential equation of Appendix I.

Let there be m + 1 thresholds uniformly distributed in the interval (a, b) such that

$$x_r = a + r\Delta x \qquad r = 0, 1, 2, \ldots m$$

$$x_m = a + m\,\frac{(b-a)}{m} = b$$

For the threshold located at x_r, there is, in the Markov model, a self-loop of weight $b(x_r)$, and m branches of weight $(1 - b(x_r))/m$ radiating to the other nodes of the model. Let x(n) represent the threshold value at the nth instant, and $P_n(x_r)$ be the probability that $X(n) = x_r$. Then we have, with $k_1 \Delta x < x - a < (k_1 + 1)\Delta x$, that

$$\Pr[X(n) < x] = \sum_{r \le k_1} P_n(x_r) \tag{96}$$

and

$$P_n(x_r) = \sum_k P_{n-1}(x_k)\, P_{kr} = \sum_{k \neq r} P_{n-1}(x_k) \left(\frac{1 - b(x_k)}{m}\right) + P_{n-1}(x_r)\, b(x_r) \tag{97}$$

Thus,

$$P_r[X(n) < x] = \left(\frac{k_1 + 1}{m}\right)\sum_r P_{n-1}(x_r)\,(1 - b(x_r)) + \sum_{r \le k_1} P_{n-1}(x_r)\, b(x_r) - \sum_{r \le k_1} P_{n-1}(x_r)\,\frac{(1 - b(x_r))}{m} \tag{98}$$

$$P_r\left[X(n) < x\right] = \frac{k_1}{m}\sum_r P_{n-1}(x_r)\ (1 - b(x_r)) + \sum_{r \le k_1} P_{n-1}(x_r)\, b(x_r) + \frac{1}{m}\sum_{r > k_1} P_{n-1}(x_r)\ (1 - b(x_r)) \tag{99}$$

Let

$$P_n(x_r) \cong p_n(x_r)\,\Delta x$$

where $p_n(x_r)$ is the continuous density we are seeking to characterize. Then

$$\sum_{r \le k_1} p_n(x_r)\,\Delta x = \left(\frac{x-a}{b-a}\right)\sum_r p_{n-1}(x_r)\ (1 - b(x_r))\ \Delta x + \sum_{r \le k_1} p_{n-1}(x_r)\, b(x_r)\,\Delta x + \frac{(\Delta x)^2}{(b-a)}\sum_{r \le k_1} p_{n-1}(x_r)\ (1 - b(x_r)) \tag{100}$$

As $\Delta x \to 0$, $m \to \infty$, and we obtain

$$\int_a^x p_n(\xi)\, d\xi = \left(\frac{x-a}{b-a}\right)\int_a^b p_{n-1}(\xi)\ (1 - b(\xi))\, d\xi + \int_a^x p_{n-1}(\xi)\, b(\xi)\, d\xi \tag{101}$$

so that, finally,

$$p_n(x) = \left(\frac{1}{b-a}\right)\left(1 - \int_a^b p_{n-1}(\xi)\, b(\xi)\, d\xi\right) + p_{n-1}(x)\, b(x) \tag{102}$$

Equation (102) is obtained by differentiating Eq. (101), and exploiting the fact that

$$\int_a^b p_n(x)\, dx = 1, \text{ all } n \tag{103}$$

Of course, we have the initial condition,

$$p_0(x) = \delta(x - x_0) \qquad a \le x_0 \le b$$

Equation (102) will be solved through the use of operational methods.

Let

$$G(x, s) = \sum_{n=0}^{\infty} p_n(x)\, s^n$$

so that Eq. (102) transforms to

$$G(x, s) - \delta(x - x_0) = s\lambda \left(\frac{1}{1 - s} - \int_a^b G(\xi, s)\, b(\xi)\, d\xi \right) + s\, G(x, s)\, b(x) \tag{104}$$

$$G(x, s) = \frac{\delta(x - x_0)}{[1 - s b(x)]} + \frac{s\lambda}{[1 - s b(x)]} \left(\frac{1}{1 - s} - \int_a^b G(\xi, s)\, b(\xi)\, d\xi \right) \tag{105}$$

where $\lambda = (b - a)^{-1}$. Equation (105) must first be solved for the integral

$$I = \int_a^b G(\xi, s)\, b(\xi)\, d\xi$$

before a formal solution may be obtained for G. If both sides of the equation are multiplied by b (x), and integrated from a to b, there results

$$I = \frac{b(x_0)}{1 - s\, b(x_0)} + s\lambda \left(\frac{1}{1 - s} - I \right) \int_a^b \frac{b(\xi)}{1 - s\, b(\xi)}\, d\xi \tag{106}$$

$$I = \left(\frac{b(x_0)}{1 - s\, b(x_0)} + \frac{s\lambda}{1 - s} \int_a^b \frac{b(\xi)}{1 - s\, b(\xi)}\, d\xi \right) \Bigg/ \left(1 + s\lambda \int_a^b \frac{b(\xi)}{1 - s\, b(\xi)}\, d\xi \right) \tag{107}$$

$$G(x, s) = \frac{\delta(x - x_0)}{1 - s\,b(x)} + \frac{s\lambda}{1 - sb(x)} \frac{\left(\frac{1}{1-s} - \frac{b(x_0)}{1 - sb(x_0)}\right)}{\left(1 + s\lambda \int_a^b \frac{b(\xi)}{1 - sb(\xi)}\, d\xi\right)} \tag{108}$$

$$G(x, s) = \frac{\delta(x - x_0)}{[1 - sb(x)]} + \frac{s}{[1 - sb(x)]} \frac{(1 - b(x_0))}{(1 - s)} \frac{1}{(1 - sb(x_0)) \left[\int_a^b \frac{d\xi}{1 - sb(\xi)}\right]} \tag{109}$$

Now, the performance index, z (n), is given by:

$$z(n) = \int_a^b p_n(x)\, b(x)\, dx \tag{110}$$

If we define the generating function, Z (s), by:

$$Z(s) = \sum_{n=0}^{\infty} z(n)\, s^n$$

we have

$$Z(s) = \int_a^b G(x, s)\, b(x)\, dx$$

$$= \frac{b(x_0)}{[1 - sb(x_0)]} + \frac{s[1 - b(x_0)]}{(1 - sb(x_0))(1 - s)} \frac{\int_a^b \frac{b(\xi)}{[1 - sb(\xi)]}\, d\xi}{\int_a^b \frac{d\xi}{[1 - sb(\xi)]}} \tag{111}$$

$$= \frac{1}{(1 - s)} - \frac{(b - a)[1 - b(x_0)]}{[1 - sb(x_0)]\ (1 - s) \left[\int_a^b \frac{d\xi}{1 - sb(\xi)}\right]} \tag{112}$$

The steady-state performance index is given by

$$\zeta = \lim_{s \to 1} \left[(1 - s)\ Z\ (s) \right] = 1 - \frac{(b - a)}{\int_a^b \frac{d\xi}{1 - b\ (\xi)}} \tag{113}$$

When (113) is evaluated for the densities of Fig. 31(a), there results

$$1 - \zeta = \frac{4}{\ln \left[\prod_{i=1}^{4} \left(\frac{x_i + y_i}{y_i} \right)^{\frac{1}{x_i}} \right]} \tag{114}$$

where:

$$x_1 = - \frac{\rho\ (1 - \alpha)}{2}\ ; \qquad y_1 = \rho$$

$$x_2 = (1 - \rho)\ \frac{(1 - \alpha)}{2} - \rho\alpha\ ;\ y_2 = \rho\ \frac{(1 + \alpha)}{2}$$

$$x_3 = (1 - \rho)\ \alpha - \rho\ \frac{(1 - \alpha)}{2}\ ;\ y_3 = \frac{(1 - \alpha)}{2}$$

$$x_4 = \frac{(1 - \rho)}{2}\ (1 - \alpha)\ ; \qquad y_4 = (1 - \rho)\ \frac{(1 + \alpha)}{2}$$

Equation (114) is graphically displayed in Fig. 42.

DYNAMIC BEHAVIOR

In Appendix I, we were able to demonstrate, in a relatively simple way, the conditions required for the performance index z (τ) to be monotonic in τ. We have an analogous result for the quasi-random policy, the outline of which we sketch below.

We define:

$$F\ (s) \triangleq (b - a)^{-1} \int_a^b \frac{d\xi}{1 - sb\ (\xi)} = \sum_{n=0}^{\infty} f_n\ s^n \tag{115}$$

$$f_n = (b - a)^{-1} \int_a^b b^n\ (\xi)\ d\xi$$

Then, from Eq. (112)

$$(1 - s)\, Z(s)\, F(s) = F(s) - (1 - b(x_0))\,(1 + b(x_0)\, s + \left[b(x_0)\right]^2 s^2 + \dots)$$

$$(z_n - z_{n-1}) * f_n = f_n - (1 - b(x_0))\left[b(x_0)\right]^n \qquad (116)$$

from which we obtain

$$\Delta_n \triangleq z_n - z_{n-1} = \left[1 - b(x_0)\right]\left[b(x_0)\,\Delta_{n-1} + g_n\right] \qquad n = 1, 2, \dots \quad (117)$$

$$\Delta_0 \triangleq -1$$

where the g_n are recursively given by

$$g_n + g_{n-1} f_1 + g_{n-2} f_2 + \dots + g_1 f_{n-1} = f_n \qquad n = 1, 2, \dots \quad (118)$$

It can be demonstrated that

$$g_{2n} = (b - a)^{-1} \int_a^b \left[b^n(\xi) + g_1\, b^{n-1}(\xi) + \dots g_n\right]^2 d\xi$$

$$g_{2n+1} = (b - a)^{-1} \int_a^b b(\xi)\left[b^n(\xi) + g_1\, b^{n-1}(\xi) + \dots g_n\right]^2 d\xi$$

i.e., all $g_n > 0$. Thus, [Eq. (117)] if $\Delta_1 > 0$, all subsequent Δ_n are positive. But $\Delta_1 > 0$ if $b(x_0) < g_1 = f_1$, so that z (n) rises monotonically whenever

$$b(x_0) < (b - a)^{-1} \int_a^b b(\xi)\, d\xi$$

If $b(x_0) = f_1$, $\Delta_1 = 0$, but all succeeding Δ_n are positive. For values of $b(x_0) > f_1$, the "zero" in Δ_n occurs for increasingly larger values of n; z (n) diminishes to a minimum, then rises monotonically to steady-state. In the limit, with

$$b(x_0) = \max_{x \in [a,b]} b(x)$$

Δ_n is negative for all n, i.e., z (n) decreases monotonically to steady-state.

REFERENCES

1. R. W. Sittler, "Systems Analysis of Discrete Markov Processes," IRE Trans. on Circuit Theory, Vol. CT-3, No. 4, December 1956, pp. 257-266.

2. W. H. Huggins, "Signal Flow Graphs and Random Signals," Proc. IRE, Vol. 45, January 1957, pp. 74-86.

3. K. L. Chung, Markov Chains with Stationary Transition Probabilities, Springer-Verlag, Berlin, 1960.

4. J. G. Truxal, Automatic Feedback Control System Synthesis, McGraw-Hill Book Co., Inc., New York, 1955.

5. J. Sklansky, "A Markov Chain Model of Adaptive Signal Detection," Contributed Paper Preprints, 1963 Bionics Symposium, Air Force Systems Command, Wright-Patterson Air Force Base, Ohio, March 1963. (AD 408 790)

6. S. J. Mason, "Feedback Theory--Some Properties of Signal Flow Graphs," Proc. IRE, Vol. 41, No. 9, September 1953, pp. 1144-1156.

7. J. Sklansky, Two-Mode Threshold Learning, AMRL Technical Documentary Report 64-39, Aerospace Medical Research Laboratories, Wright-Patterson Air Force Base, Ohio, May 1964.

8. M. Kac, "A Note on Learning Signal Detection," IRE Trans. on Information Theory, Vol. IT-8, No. 2, February 1962, pp. 126-128.

9. R. R. Bush and F. Mosteller, Stochastic Models of Learning, John Wiley and Sons, New York, 1955.

10. R. A. Howard, Dynamic Programming and Markov Processes, John Wiley and Sons, New York, 1960.

11. G. H. Weiss, A Semi-Markov Model for Clinical Trials, Technical Note BN-312, March 1963, Mathematics Research Center, U. S. Army, Madison, Wisconsin.

12. D. Braverman and N. Abramson, "Learning to Recognize Patterns in a Random Environment," IRE Trans. on Information Theory, Vol. IT-8, September 1962, pp. 58-63.

13. J. L. Lawson and G. E. Uhlenbeck, Threshold Signals, McGraw-Hill Book Co., Inc., New York, 1950, Chapter 7.

14. W. Feller, An Introduction to Probability Theory and Its Applications, Vol. 1, Second Edition, John Wiley and Sons, New York, 1957.

BLANK PAGE

UNCLASSIFIED
Security Classification

DOCUMENT CONTROL DATA - R&D
(Security classification of title, body of abstract and indexing annotation must be entered when the overall report is classified)

1 ORIGINATING ACTIVITY (Corporate author) Radio Corporation of America RCA Laboratories Princeton, New Jersey	2a REPORT SECURITY CLASSIFICATION UNCLASSIFIED 2b GROUP N/A

3 REPORT TITLE

ANALYSIS OF MARKOV CHAIN MODELS OF ADAPTIVE PROCESSES

4 DESCRIPTIVE NOTES (Type of report and inclusive dates)

Final report, May 1963 - March 1964

5 AUTHOR(S) (Last name, first name, initial)

Kaplan, K. R., PhD
Sklansky, J., DSc Eng

6 REPORT DATE January 1965	7a TOTAL NO OF PAGES 99	7b NO OF REFS 14
8a CONTRACT OR GRANT NO AF 33(657)-11336 b PROJECT NO 7233 c Task No. 723305 d	9a ORIGINATOR'S REPORT NUMBER(S) 9b OTHER REPORT NO(S) (Any other numbers that may be assigned this report) AMRL-TR-65-3	

10 AVAILABILITY/LIMITATION NOTICES

Qualified requesters may obtain copies of this report from DDC.
Available, for sale to the public, from the Clearinghouse for Federal Scientific and Technical Information, CFSTI (formerly OTS), Sills Bldg, Springfield, Virginia 22151.

11 SUPPLEMENTARY NOTES	12 SPONSORING MILITARY ACTIVITY Aerospace Medical Research Laboratories, Aerospace Medical Division, Air Force Systems Command, Wright-Patterson AFB, Ohio

13 ABSTRACT

Learning and adaptation are considered to be stochastic in nature by most modern psychologists and by many engineers. Markov chains are among the simplest and best understood models of stochastic processes and, in recent years, have frequently found application as models of adaptive processes. A number of new techniques are developed for the analysis of synchronous and asynchronous Markov chains, with emphasis on the problems encountered in the use of these chains as models of adaptive processes. Signal flow analysis yields simplified computations of asymptotic success probabilities, delay times, and other indices of performance. The techniques are illustrated by several examples of adaptive processes. These examples yield further insight into the relations between adaptation and feedback.

DD FORM 1 JAN 64 1473

UNCLASSIFIED
Security Classification

14 KEY WORDS	LINK A		LINK B		LINK C	
	ROLE	WT	ROLE	WT	ROLE	WT
Mathematical modes, bionics Stochastic processes, feedback Adaptation (physiology) Threshold learning processes Cybrenetics Adjustment (physiology) Sensory preception Environment Artificial intelligence						

INSTRUCTIONS

1. ORIGINATING ACTIVITY: Enter the name and address of the contractor, subcontractor, grantee, Department of Defense activity or other organization *(corporate author)* issuing the report.

2*a*. REPORT SECURITY CLASSIFICATION: Enter the overall security classification of the report. Indicate whether "Restricted Data" is included. Marking is to be in accordance with appropriate security regulations.

2*b*. GROUP: Automatic downgrading is specified in DoD Directive 5200.10 and Armed Forces Industrial Manual. Enter the group number. Also, when applicable, show that optional markings have been used for Group 3 and Group 4 as authorized.

3. REPORT TITLE: Enter the complete report title in all capital letters. Titles in all cases should be unclassified. If a meaningful title cannot be selected without classification, show title classification in all capitals in parenthesis immediately following the title.

4. DESCRIPTIVE NOTES: If appropriate, enter the type of report, e.g., interim, progress, summary, annual, or final. Give the inclusive dates when a specific reporting period is covered.

5. AUTHOR(S): Enter the name(s) of author(s) as shown on or in the report. Enter last name, first name, middle initial. If military, show rank and branch of service. The name of the principal author is an absolute minimum requirement.

6. REPORT DATE: Enter the date of the report as day, month, year; or month, year. If more than one date appears on the report, use date of publication.

7*a*. TOTAL NUMBER OF PAGES: The total page count should follow normal pagination procedures, i.e., enter the number of pages containing information.

7*b*. NUMBER OF REFERENCES: Enter the total number of references cited in the report.

8*a*. CONTRACT OR GRANT NUMBER: If appropriate, enter the applicable number of the contract or grant under which the report was written.

8*b*, 8*c*, & 8*d*. PROJECT NUMBER: Enter the appropriate military department identification, such as project number, subproject number, system numbers, task number, etc.

9*a*. ORIGINATOR'S REPORT NUMBER(S): Enter the official report number by which the document will be identified and controlled by the originating activity. This number must be unique to this report.

9*b*. OTHER REPORT NUMBER(S): If the report has been assigned any other report numbers *(either by the originator or by the sponsor)*, also enter this number(s).

10. AVAILABILITY/LIMITATION NOTICES: Enter any limitations on further dissemination of the report, other than those imposed by security classification, using standard statements such as:

(1) "Qualified requesters may obtain copies of this report from DDC."

(2) "Foreign announcement and dissemination of this report by DDC is not authorized."

(3) "U. S. Government agencies may obtain copies of this report directly from DDC. Other qualified DDC users shall request through

_____."

(4) "U. S. military agencies may obtain copies of this report directly from DDC. Other qualified users shall request through

_____."

(5) "All distribution of this report is controlled. Qualified DDC users shall request through

_____."

If the report has been furnished to the Office of Technical Services, Department of Commerce, for sale to the public, indicate this fact and enter the price, if known.

11. SUPPLEMENTARY NOTES: Use for additional explanatory notes.

12. SPONSORING MILITARY ACTIVITY: Enter the name of the departmental project office or laboratory sponsoring *(paying for)* the research and development. Include address.

13. ABSTRACT: Enter an abstract giving a brief and factual summary of the document indicative of the report, even though it may also appear elsewhere in the body of the technical report. If additional space is required, a continuation sheet shall be attached.

It is highly desirable that the abstract of classified reports be unclassified. Each paragraph of the abstract shall end with an indication of the military security classification of the information in the paragraph, represented as *(TS)*, *(S)*, *(C)*, or *(U)*

There is no limitation on the length of the abstract. However, the suggested length is from 150 to 225 words.

14. KEY WORDS: Key words are technically meaningful terms or short phrases that characterize a report and may be used as index entries for cataloging the report. Key words must be selected so that no security classification is required. Identifiers, such as equipment model designation, trade name, military project code name, geographic location, may be used as key words but will be followed by an indication of technical context. The assignment of links, rules, and weights is optional.

BLANK PAGE